JPRS L/10523

18 May 1982

USSR Report

SPACE

(FOUO 2/82)

FBIS FOREIGN BROADCAST INFORMATION SERVICE

NOTE

JPRS publications contain information primarily from foreign newspapers, periodicals and books, but also from news agency transmissions and broadcasts. Materials from foreign-language sources are translated; those from English-language sources are transcribed or reprinted, with the original phrasing and other characteristics retained.

Headlines, editorial reports, and material enclosed in brackets [] are supplied by JPRS. Processing indicators such as [Text] or [Excerpt] in the first line of each item, or following the last line of a brief, indicate how the original information was processed. Where no processing indicator is given, the information was summarized or extracted.

Unfamiliar names rendered phonetically or transliterated are enclosed in parentheses. Words or names preceded by a question mark and enclosed in parentheses were not clear in the original but have been supplied as appropriate in context. Other unattributed parenthetical notes within the body of an item originate with the source. Times within items are as given by source.

The contents of this publication in no way represent the policies, views or attitudes of the U.S. Government.

APPROVED FOR RELEASE: 2007/02/09: CIA-RDP82-00850R000500060036-1

JPRS L/10523

18 May 1982

USSR REPORT

SPACE

(FOUO 2/82)

CONTENTS

MANNED MISSION HIGHLIGHTS

'AIR & COSMOS' ON 'COSMOS 1267' AS PRECURSOR OF MODULAR VESSELS

Paris AIR ET COSMOS in French 31 Oct 81 p 39

[Article by Pierre Langereux, special correspondent sent by AIR ET COSMOS to Star City as guest of Soviets]

[Text] The Cosmos-1267 automatic satellite, which has been moored to the Salyut-6 orbital station since June 1981, is the precursor of new modular transport spacecraft that will enable the USSR to build a large new third-generation orbital station.

This major new objective of Soviet astronautics was officially disclosed on 17 June 1981, just 2 days before the docking of Cosmos-1267 with Salyut-6, by the Soviet number one in person.[1] Leonid Brezhnev revealed on that date that "The USSR will be putting into service permanent orbital scientific complexes whose crews will be renewed!"

A little more is known today about what Cosmos-1267 actually is and what the future Soviet orbital stations will be like, thanks especially to the facts given us at Star City by Gen Vladimir Shatalov, commander of the Soviet cosmonauts.

Cosmos-1267 is an experimental satellite of the Cosmos series designed to test new space systems in orbit and to fine-tune assembly methods for large-scale space complexes. Cosmos-1267 is not a new piloted craft but a "prototype of a modular transport vessel" that will make it possible to build permanently orbited space stations of a larger size and better equipped than the present Salyut.

These future stations will be able to accommodate three-person crews, thanks to the new three-place Soyuz T transport vessel. This will make it possible to lodge up to six cosmonauts aboard future Salyuts in cases where a "visiting" crew is sent up in addition to the "main" crew.

Cosmos-1267 is a 15-ton vessel, twice as heavy as the Soyuz T (7 tons) and almost as heavy as a Salyut station (19 tons). It will be able to carry

1) See AIR ET COSMOS No 852, 866, 867 and 875.

around 8-10 tons of cargo[2], although this characteristic does not appear to have been defined as yet. Devoid of a solar generator, Cosmos-1267 consists mainly of three elements: A propulsion module, a habitation module with air lock, and a cargo module, possibly with a recoverable compartment to bring back to earth the products manufactured under microgravity in future "space-industry workshops," as explained by Shatalov. The Cosmos-1267 habitation module resembles that of the Soyuz T, but the cargo compartment is cylindrical and the propulsion system is different, as is the docking system. This new transport vessel can be built in several variants, with different special-purpose modules, according to needs: habitational, microgravity laboratory, astronomy, geophysics, etc. The habitational module will enable crews to live and work aboard, but cosmonauts will not be launched aboard this future transport vessel, which will actually be a kind of "Super Progress."

The present Salyut will be the generative basis of these future large orbital complexes, which will consist of many habitational modules of the size of a Salyut station. The future third-generation orbital station[3], will be equipped with several docking ports that will accommodate different special-purpose modules. The facilities required for different missions will be installed in the station and in the special-purpose modules that can be added one by one as needed. This new concept of a modular orbital station is judged by the Soviet experts to be "more flexible and more economically viable" from the standpoint of a permanent establishment in space.

"The time is not far away when the USSR will put such a complex in orbit," said Soviet cosmonaut Konstantin Feoktistov on 24 June, adding that "The recent docking of Cosmos-1267 with Salyut-6 was the prototype of such an actualization."

The Soviets are now bullding the facility at Star City to house the flight simulator designed for the new modular stations. Vladimir Shatalov pointed out that: "This new facility will be in service within 3 to 4 years, by 1984-1985, that is. This means the USSR will be ready by that time to orbit a permanent modular station, based on the experimence it will have acuqired with Cosmos-1267 and its probable successors. This will provide confirmation of the capacity of these orbital complexes for flights of long duration."

The mission of Cosmos-1267, launched on 25 April 1981 and moored to Salyut since 19 June, will terminate in a few weeks or a few months

2) See AIR ET COSMOS No 866.

3) The Soviets regard the first five Salyuts as first-generation orbital stations, and Salyut 6 as the first second-generation station, capable, that is, of docking two vessels (Soyuz and Progress) simultaneously, by means of its two docking ports.

at the latest. The satellite, which carried no cargo for this test flight, is in fact scheduled to be detached prior to the possible sending of another "principal crew" to occupy the Salyut-6 station, assuming the Soviets will decide to send new crews, including the first Franco-Soviet crew, aboard Salyut 6. More probably, however, these crews will use the new Salyut-7 station, and in this case Salyut-6 will be abandoned.

9399
CSO: 8119/0700-A

BLAGOV COMMENTS ON FLIGHT OF 'SALYUT-6'--'COSMOS-1267'

Paris AIR & COSMOS in French 28 Nov 81 p 42

[Article by Pierre Langereux: "Soviet Station 'Salyut-6' in Orbit Fifty Months"]

[Text] The Soviet orbital station "Salyut-6" has been in orbit more than four years. The station, which was launched on 29 September 1977, has completed over 24,000 revolutions of the earth and covered some 10 billion kilometers. "Cosmos-1267", which the Soviets term a "heavy satellite", has been docked to the station since June 1981. "Cosmos-1267" is a precursor of new modular transport vessels which in the future will permit the Soviets to construct large third-generation orbital stations announced for 1984-85 (See AIR & COSMOS No 879).

"In the future, such complexes composed of satellites of comparable mass will be widely used," Viktor Blagov, assistant director of the "Salyut" program, declared recently to the Soviet Press Agency APN. "It is envisaged that specialised modules (astronomy laboratories, remote sensing, technological, etc.) will be joined to them. They will have a weight comparable to that of the station which will thus become a comfortable space apartment." These future third-generation orbital stations will be more optimised. "The cosmonauts will be able to live in the crew compartment with maximum comfort and work in better conditions aboard the specialised modules," explained Blagov.

For the present, "Salyut-6" remains in orbit with the "Cosmos-1267" satellite docked to one of its ends, thus forming the largest orbital complex realized to date by the USSR. The orbit of this complex has already been raised on two occasions by the engines of "Cosmos-1267". Blagov recalled this fact in announcing that the orbit of "Salyut-6"--"Cosmos-1267" will be corrected once again in the near future. According to the assistant director of the program, "the tests will require a certain additional amount of time."

"The operation of "Salyut-6" has already enabled the USSR to acquire useful experience in coordinating work in space and on the ground," declared Blagov. He added that "the new operations have led the Soviets to add a

third hall to the Flight Control Center for better simultaneous command of several spacecraft." This had been announced to us at the time of our recent visit to Moscow (See AIR & COSMOS Nos 877-882).

"Experience has shown that operation of a manned orbital station can be extended for three to five years," said Blagov. "The 'Salyut-6' station, conceived for a service period of 18 months, has actually operated for 50 months in orbit without major failure. No serious trouble has been noted apart from the natural deterioration of the solar panels and batteries," declared Blagov. But Blagov acknowledged that "the station owes a large measure of its longevity to the repairs performed on board by the cosmonauts. During these four years, 27 cosmonauts, of which 19 were Soviet and 8 citizens of eastern member countries of Intercosmos, have worked aboard 'Salyut-6' and have performed more than 1,600 scientific and technical experiments." "The cosmonauts live according to Moscow time," explained Blagov, "with days of work and days of rest, remaining in permanent contact with the Control Center and with their relatives and friends. But this does not prevent them from being overburdened with work at certain times."

In the future, the Soviets are going to remedy this problem "by further developing automation of certain command and function processes." The "Delta" autonomous navigation system tested on "Salyut-6" already handles a large part of the operations of orientation and stabilization of the station during performance of experiments. In addition, Blagov revealed that it is possible to equip the telescopes or cameras with a mini-computer connected with the "Delta" system to program the daily observations. The crew would have only to monitor the functioning of the systems and intervene only if necessary.

CSO: 1853/4-P

'AIR & COSMOS' ON TRAINING, MISSION OF SOVIET-FRENCH JOINT FLIGHT

Paris AIR ET COSMOS in French 31 Oct 81 pp 37-38

[Article by Pierre Langereux: "First French Astronaut to Fly at End of June 1982"]

[Text] The first French astronaut will fly aboard a Soviet spacecraft about the middle of next year, between June and August, most probably toward the end of June 1982. He will be launched together with two Soviets, aboard a Soyuz T spacecraft which will rendezvous with the orbital station in which they will stay for 1 week in orbit at about 250 km above the earth. The station will be either the Salyut-6 now in orbit, or more probably a new Salyut-7 which is scheduled to be launched at the start of 1982.

The station will be manned initially by a "primary crew" who are tentatively scheduled to be launched around February 1982. This crew will consist of two Soviet cosmonauts who will effect a flight of long duration, but of less than 6 months, according to Vladimir Shatalov, head of the cosmonauts. The duration of the flight will be set before their departure by officials of the USSR Academy of Sciences, as is customary, V. Shatalov disclosed. But in the case of flights of long duration, it is only after 1 month in orbit that the actual duration of the mission is finally decided, with a lead time of 5 to 10 days approximately.

This primary crew will be joined near the end of June 1982 by a "visiting crew" consisting of two Soviet cosmonauts and the first French astronaut. At this point and for the first time, there will be five persons aboard a Salyut spacecraft. Until now, the Soviet Salyut-6 station has been occupied by no more than four persons at any one time.

The two Franco-Soviet crews, who have been in training since 6 September 1981, are now training at City of the Stars, where we met them at the official introduction on 19 October organized by the CNES [National Center for Space Studies] and Intercosmos (see AIR ET COSMOS No 878).

The "titular crew," who have been designated as the first to lift off, consists of Aviation Commander Yuriy Malyshev, 4 [as published], flight commander; Engineer Alexandre Ivanchenkov, 41, flight engineer; and Jean-Loup Chretien,

43, astronaut-experimenter. We recall that Yu. Malyshev piloted Soyuz T2, the first of the new spacecraft to be launched with crew, and that A. Ivanchenkov, passenger aboard Soyuz 29, flew aboard Salyut 6 for a period of 140 days.

The "standby crew," who will replace the titular crew in case of failure of the latter, consists of Col Leonid Kizim, 40, flight commander; Vladimir Solov'e, 35, flight engineer; and Patrick Baudry, 35, astronaut-experimenter. L. Kizim took part aboard Soyuz T3 in the new spacecraft's first three-man flight. V. Solov'e is a new astronaut selected in 1977. Upon graduation in 1970 from the Bauman Advanced Technical School in Moscow, he worked first in the Space Studies Bureau Advanced Technical School in Moscow, he worked first in the Space Studies Bureau headed by Academician Sergey Korolev, then returned to the Space Operations Center as a rocket propulsion specialist. He is married and the father of two children. His father was an aeronautical test engineer.

The detailed mission plan will be set up tentatively at the end of November 1981. The two Franco-Soviet crews will undergo an initial flight-readiness examination at the end of January 1982 administered by the Control Committee of the USSR Academy of Sciences. A second examination will take place 1 month before the flight to designate the crew to be sent into space.

The present designation of one as the titular crew and the other as the standby crew notwithstanding, the chances of flying of each of the Franco-Soviet crews are about equal. In case of failure or accident on the part of one of the members of the titular crew, the entire crew would, in principle, be changed. But, according to Gen Georgiy Beregovoy, commander of City of the Stars, it is entirely possible that only one of the members may be replaced. It has already happened once that an entire crew has had to be replaced, and several times that one of the members of a primary crew has had to be, because of illness or accident. Thus, Soviet Cosmonaut Valeriy Ryumin, holder of the world's space flight record (362 days) had to be sent into space a second time in the place of Valentin Lebedev, who had suffered a knee injury.

For the moment, the two Franco-Soviet crews are pursuing their practical training which began 1 and 1/2 months ago with a 1-week survival exercise in the North Sea off the coast of Feodossia, to familiarize themselves with the procedure for a forced landing at sea. Unlike previous Soyuz's, the new Soyuz spacecraft is designed to be able to put down on land as well as at sea. The landing point can thus be displaced by some 1,000 km from the planned one in case of necessity.

The two French astronauts have also taken part in weightless-simulation exercises aboard the new IL76 laboratory plane, which enables the effecting of some 15 simulations (by way of power dives followed by climbs), whereas the previous Tu-104 provided only up to five simulations and for shorter durations. During these flights, the astronauts train to move about inside a full-scale model of the Soyuz T cabin installed in the fuselage of the plane. Further such flights are scheduled for the spring of 1982.

This training was supplemented by other exercises in survival on land, simulating landings in swamps and on lakes, with recovery by helicopter. The crews will also undergo winter training near Moscow, and not in Siberia as is customary. Actually, the flight of the Franco-Soviet crew is scheduled to take place in summer and, theoretically, survival training under mountain or extreme cold conditions is not necessary. Throughout their training, the French astronauts are monitored by an appointed military physician, Dr Sergey Ponomarev, a specialist in the training of astronauts, who has worked at the City of the Stars over the past 11 years.

But to date, the training of the French astronauts has been highly satisfactory. Chretien and Baudry are very good candidates, self-disciplined, meticulous, punctual and hard-working, according to the officials of City of the Stars. Moreover, their qualification as military pilots and their training as test pilots enable them to rapidly assimilate knowledge of the Soyuz T spacecraft and its handling. In principle, however, the French astronaut will not be called upon to pilot the Soyuz T; that is the function of the flight commander. Nevertheless, in case of difficulties, each of the passengers aboard the Soyuz T must be capable of manually piloting the spacecraft, designed, though it is, to be flown normally in the automatic mode with the help of the on-board computer.

9238
CSO: 3100/297

'AIR & COSMOS' ON FUTURE OF FRENCH-SOVIET FLIGHTS

Paris AIR ET COSMOS in French 31 Oct 81 p 39

[Article by Pierre Langereux, special correspondent sent by AIR ET COSMOS to Star City as guest of Soviets]

[Text] French officials are desirous of looking forward to further flights by French cosmonauts, following the first one scheduled for mid-1982 by, in principle, Jean-Loup Chretien. This would provide an opportunity for "backup" cosmonaut Patric Baudry to fly, and above all a means of continuing Franco-Soviet space cooperation at a very interesting level. The head of the CNES [National Center for Space Studies] expressed officially his interest in continuing joint space flights, on the occasion of the recent Franco-Soviet talks held in Rodez (France).

The Soviet officials have not yet replied officially to this French proposal. It is moreover probable they will not do so prior to completion of the first joint flight. However, those with whom we talked during our visit to Moscow are rather favorable to the idea. Gen Georgiy Beregovoy, commander of Star City, thinks that "The cooperation begun in this domain cannot be stopped." Professor Eugene Choulgenko, director of biomedicine in the Ministry of Public Health, also considers that "future joint flights would represent a consolidation of Franco-Soviet cooperation." France can actually contribute much to the USSR effort, with respect to biomedical instrumentation for manned space flights. This is already the case with the blood-echography equipment that is to be used for the first time in space on the occasion of the first Franco-Soviet flight. This equipment has greatly impressed Soviet officials, who would like to use it for further experimental work during flights of long duration.

9399
CSO: 8119/0700-A

UDC 551.593:629.198.3

SPACE RESEARCH ON ATMOSPHERIC-OPTICAL PHENOMENA FROM 'SALYUT-6'

Leningrad ATMOSFERA ZEMLI S "SALYUTA-6" in Russian 1981 (signed to press 25 Mar 81) pp 2-8, 206-207

[Annotation, introduction and table of contents from book "Earth's Atmosphere--The View From Salyut-6" by Aleksandr Ivanovich Lazarev, Vladimir Vasil'yevich Kovalenok, Aleksandr Sergeyevich Ivanchenkov and Sergey Vazgenovich Avakyan, edited by L. I. Shtannikova, Gidrometeoizdat, 2300 copies, 208 pages]

[Text] This book presents the results of research on atmospheric-optical phenomena accomplished by the main crew of the second expedition on board the Salyut-6 orbital scientific station from June through October 1978. Peculiarities of optics research in space are noted. The results of observations of the space and time distribution of night atmosphere emanation and aurora are described. Analysis of the foregoing is presented taking into consideration activity in the sphere of geophysics and solar physics. Also presented are the results of observations of such atmospheric-optical phenomena as the "mustache effect," mirror reflection of the sun from the earth's atmosphere, luminescence of zodiacal light, luminescence from the stars, planets and luminous particles.

This book is intended for a wide circle of specialists in physics of the upper atmosphere and near-earth space, astrophysics and meteorology.

Introduction

April 12th 1981 marks the 20th anniversary of the first space flight--the flight of Yuriy Alekseyevich Gagarin in the spacecraft Vostok. Since that time, many Soviet cosmonauts and cosmonauts of the socialist countries have flown missions on the Vostok, Voskhod and Soyuz Soviet manned space vehicles and on the Salyut orbital space stations. Scientific research and experimentation has been conducted on all of the manned space vehicles.

Beginning with Yu. A. Gagarin's first flight in space, extremely important studies have been conducted related to the atmosphere and atmospheric-optical phenomena. These include studies of the colored daylight and twilight halos, night emissive layers, aurora, silver clouds, glimmering stars and planets in the earth's night horizon, etc. The results of these studies have enabled us to define significantly more precisely our concept of many physical processes and phenomena observed in the earth's atmosphere. Success is achieved in this regard on almost every flight in

space--we obtain new data on optical phenomena in the earth's atmosphere. This is related to the fact that a certain set of research conditions arises for each individual space flight allowing us to study certain or other optical phenomena, and to the fact that the earth's atmosphere itself is changing, and, correspondingly, atmospheric-optical phenomena.

The main crew for the second expedition of the Salyut-6 orbital scientific station--USSR pilot-cosmonauts V. V. Kovalenok and A. S. Ivanchenkov--completed an extensive series of experiments related to the study of the atmosphere and atmospheric-optical phenomena. This crew was transported to Salyut-6 by the Soyuz-29 space vehicle, launched 15 Jun 1978. It returned to earth 2 Nov 1978 on the Soyuz-31 spacecraft. Two visiting crews of international composition were transported to Salyut-6 during the flight of this second-expedition main crew.

The first visiting international crew--USSR pilot-cosmonaut P. I. Klimuk and pilot-cosmonaut M. Hermashevskiy of the Polish People's Republic--was transported to Salyut-6 on the Soyuz-30 spacecraft launched 27 Jun 1978. The crew returned to earth on this same spacecraft on 5 Jul 1978. The second visiting crew--USSR pilot-cosmonaut V. F. Bykovskiy and GDR pilot-cosmonaut S. Jaehn--was transported to Salyut-6 on the Soyuz-31 spacecraft launched 27 Aug 1978. It returned to earth 4 Sep 1978 on board the Soyuz-29 spacecraft.

The long 140-day flight of V. V. Kovalenok and A. S. Ivanchenkov enabled systematic observations of the atmosphere and atmospheric-optical phenomena to be conducted. As a result, success was achieved in ascertaining new natural laws governing certain physical processes and phenomena observed in the earth's atmosphere. The cosmonauts' advance training for prolonged space flight enables them to conduct certain visual observations of atmospheric-optical phenomena from the very first days they are on board--chiefly response to inquiries from earth. At the beginning of a flight, however, emotional factors exert significant influence on one's perception of the surrounding environment. Cosmonauts become enraptured at the bright, colorful scenes of daylight and twilight halos, sunrises and sunsets, the beauty of the earth's cloud cover, its surface and oceans, the bright scenes of aurora, silver clouds and night emissive layers.

Later on, the cosmonauts gradually become accustomed to the scenes they are observing and focus their attention on certain processes of great significance that play a substantive role in studying the natural environment from space.

Undergoing a prolonged space flight, the cosmonauts begin to classify and analyze the phenomena they observe. Consultation with experts that takes place during periods of communication aids the cosmonauts in executing independently certain experiments of considerable importance in the study of the natural environment. The "Program For Visual Observations From Manned Space Vehicles" developed by A. I. Lazarev for the first expedition provided great assistance in conducting space experiments on board the Salyut-6 orbital station. USSR pilot-cosmonauts V. A. Dzhanibekov and O. G. Makarov delivered this program to Salyut-6 on 11 Jan 1978.

Crews of the Salyut-6 orbital station's second expedition continued the research on atmospheric-optical phenomena according to this program. They conducted visual observations and photographed emissions of the night atmosphere, aurora, silver clouds,

zodiacal light, rising and setting of the sun, planets and stars, etc. Naturally, most of the experiments were accomplished by the main crew that spent 140 days in orbit. The contents of this book are devoted chiefly to classification, analysis and interpretation of the results of these experiments.

We will make note of a number of interesting experiments conducted by the crews of Salyut-6's second expedition and note the most important results of this research. One of the most interesting observations is related to the second emissive layer on the earth's night side. The second emissive layer was observed for the first time from outer space by cosmonauts V. G. Lazarev and O. G. Makarov aboard the Soyuz-12 spacecraft in September 1973. Cosmonauts P. I. Klimuk and V. I. Sevast'yanov continued these observations on board Salyut-4 from May through July 1975. Cosmonauts Yu. V. Romanenko and G. M. Grechko frequently observed the second emissive layer from the Salyut-6 orbital station. They even obtained photographs of the first and second emissive layers of the night atmosphere. Results of the research of Yu. V. Romanenko and G. M. Grechko confirmed the notion that it was possible to observe the second emissive layer continuously in the equatorial zone.

The second emissive layer in the equatorial zone was also observed by V. V. Kovalenok and A. S. Ivanchenkov. In addition, they were the first to observe from space luminescence on a planetary scale from the second emissive layer. Later, based on the results of systematic observations, the cosmonauts turned their attention to the phenomenon where a planetary-scale outburst of the second emissive layer turns out to be a precursor of an intense aurora manifestation. A planetary luminescence of the second emissive layer was often observed as well upon completion of such an aurora. Observations of the second emissive layer have allowed us to corroborate certain well-known geophysical phenomena, and have brought to light new concepts regarding the link between upper atmosphere emissions and activity in the sphere of geophysics and solar physics.

A number of interesting results are related to aurora observations. Several of the observations of V. V. Kovalenok and A. S. Ivanchenkov are special in that these cosmonauts were the first to see areas of aurora luminescence from space not only in the region of the aurora oval, but in the middle latitudes and subtropics as well. Sometimes Salyut-6 flew over areas of aurora at latitudes of about 25 degrees. Particularly interesting were observation results with respect to the color vision in areas of aurora luminescence, which enable us to qualitatively evaluate the energy of electron flows whose excitation causes the luminescence. During the course of 49 days of flight, the cosmonauts made systematic, daily observations of the aurora. This corroborated the conjecture mentioned earlier as to the possibility of observing aurora from space continuously in the region of the aurora oval.

During the mission of Salyut-6's second expedition, information was relayed to the orbital station for the first time with regard to a magnetic storm expected on 25 Sep 1978, along with a request to conduct aurora observations south of Australia and southeast of Canada. The prediction was entirely justified, and the cosmonauts observed an aurora measuring three [degree of intensity]. V. V. Kovalenok and A. S. Ivanchenkov observed the most powerful aurora (a four) on 29 Sep 1978 in parts of the northern and southern hemispheres up to latitudes of about 25 degrees.

Observations of the "mustache effect" appeared as somewhat of a surprise--upper-atmosphere twilight luminescence overhanging the emanation from dense layers of the earth's

night atmosphere. V. V. Kovalenok and A. S. Ivanchenkov noticed that this phenomenon can look different. According to the cosmonauts, on certain occasions a single layer was seen; on others--two stretched-out areas of luminescence. Sometimes the phenomenon was not observed at all. These results can be explained both by differences in the structure of the emissive layers and by differences in the conditions of observation.

Unusual results were obtained upon observing silver clouds on the earth's twilight horizon during the initial period of flight from 25 Jun through 5 Jul 1978, when Salyut-6 was in solar orbit. P. I. Klimuk and M. Hermashevskiy, members of a visiting international crew, participated in these observations. Clearly and constantly visible at all latitudes above the atmospheric halo was a thin strip, silver in color, approximately one-fourth the thickness of the first emissive layer. This strip was quite clearly defined (more so than the ordinary silver clouds one observes). In a discussion of these results with V. I. Sevast'yanov, it became apparent that he and P. I. Klimuk had observed this strip at various latitudes during their flight on board the Salyut-4 orbital station in summer of 1975.

At the request of A. S. Ivanchenkov, observations of silver clouds were conducted in the summer of 1979 by the main crew of Salyut-6's third expedition. Cosmonauts V. A. Lyakhov and V. V. Ryumin obtained new data on the latitudinal distribution of silver clouds and other dissipating layers in the mesopause. These data define considerably more precisely our concept of the mesopause structure in the lower and equatorial latitudes.

V. V. Kovalenok and A. S. Ivanchenkov devoted a great deal of attention to observations of cloud cover structure over seas and oceans. They repeatedly observed the generation of cyclones and typhoons, and the formation of families of cyclone disturbances. The data from systematic observations of the cloud cover enabled them to express certain views on the interrelationship between large-scale cloud cover structure and the structure of sea and ocean currents.

The crew of Salyut-6's second expedition is apparently the first to observe from space such atmospheric-optical phenomena as rainbow clouds and gloria. V. F. Bykovskiy and S. Jaehn, members of a visiting international crew, participated in observing the rainbow clouds. Both of these phenomena arise as a result of solar radiation interference in clouds made up of ice crystals.

As long ago as the occasion of his first flight on the Soyuz-25 spacecraft, V. V. Kovalenok observed the phenomenon of apparent magnification of objects and formations on the ocean surface when haze appeared. During his Salyut-6 mission, Kovalenok got the impression several times within a short period that he was observing objects and formations on the earth's surface through a magnifying glass. A. A. Leonov, V. I. Sevast'yanov and other Soviet cosmonauts also mentioned observing earth objects from space as a magnified representation. This phenomenon is linked to peculiarities in the frequency-contrast response of the cosmonauts' system of optics, and to sharp change in the atmosphere's transfer function in certain regions of the globe.

Zodiacal light was often observed by P. I. Klimuk and V. I. Sevast'yanov from on board the Salyut-4 station in June and July of 1975--also by G. M. Grechko and

Yu. V. Romanenko from Salyut-6, January through March 1978. There are significant differences, however, between the observational data from Salyut-4 and Salyut-6. Klimuk and Sevast'yanov could isolate the beam structure in zodiacal light with confidence. They estimated that the beam contrast reached about 10 percent. However, Grechko and Romanenko were unable to find beam structure in zodiacal light.

V. V. Kovalenok and A. S. Ivanchenkov also conducted observations of zodiacal light. In half of the instances, Kovalenok could distinguish in it a weakly defined beam structure; Ivanchenko could not distinguish one at all.

Differences in these observations of zodiacal light are evidently related to space and time differences in the distribution of meteor showers and associations observed at various times of the year, and to variance in the contrast sensitivity of the cosmonauts' system of optics for low brightness levels.

The optics research conducted by the cosmonauts comprises a highly significant portion of a broad program for studying our natural environment from space. Extensive information has already been obtained from space with regard to the atmosphere's diverse properties and the earth's surface and ocean areas. Hitherto unknown atmospheric-optical phenomena have been discovered, and new data on radiation of the sun, planets, stars and interstellar medium have been recorded. This material is being widely utilized both for accomplishing numerous national economy-oriented tasks and for studying the natural environment. The results of optics research completed by crews of the Salyut-6 orbital station's second expedition are contributing significantly to the accomplishment of these tasks.

Contents

9768
CSO: 1866/22

LIFE SCIENCES

UDC 539.104

COMPARATIVE ANALYSIS OF BIOLOGICAL EFFECTS OF ELECTROMAGNETIC RADIATION: 1. NERVOUS SYSTEM

Moscow KOSMICHESKIYE ISSLEDOVANIYA in Russian Vol 19, No 4, Jul-Aug 81 (manuscript received 14 Aug 80) pp 649-653

[Article by V. V. Antipov, B. I. Davydov and V. S. Tikhonchuk]

[Text] Electromagnetic radiation (EMR) of non-ionizing nature has in recent years become an ecologically meaningful factor in human activity, and the field of astronautics is, of course, no exception. Hence, one must regard as normal the new surge of interest among the medical people, biologists and engineer-physicists, during the last few years, in studying the mechanisms of the biological effects of EMR, determining permissible levels of activity, matters of dosimetry and so on.

The last 15 years have witnessed the publication of many exhaustive surveys [1] and monographs [2-5] devoted to the generalization and analysis of experimental data on the mechanisms of EMR's biological effects, to matters of standards, to means and measures for protection from radiation etc., and attention has been given primarily to radio-frequency EMR. There has also been a sharp increase in the number of periodical items concerned with the problem. There are, however, at least two circumstances which make it advisable to do a comparative analysis of the biological effects of EMR. First of all, even in such monographs as the work of Baranski and Czerski [4] the basic literature is comprised of publications up to 1970 only. Secondly, in the analysis of the literature there has been insufficient emphasis on reaction of the critical systems of the organism to EMR.

This series of articles will attempt to analyze the data published up to 1979 on the effects of EMR on the central nervous system, gonads and crystalline lens, and on lethal effects.

First, a few general remarks. In this series of reports we have analyzed only those works in which the parameters of a physical factor have been specified: power density, frequency or wavelength of electromagnetic field, the irradiation conditions, biological object parameters, kind of animal, size of groups, number of tests etc. Works in which no characteristic was specified have not been analyzed.

1. Clinical-Physiological Studies

During the last 20 years clinical-physiological investigations have been conducted to detect disturbances in functional activity of the nervous, cardiovascular and digestive systems, and studies have been made of changes in the blood and metabolic indexes and in certain endocrine gland functions in a production environment, which have been called "production experiments". We attempted to evaluate the advantages and the shortcomings of the "production experiment" using the study of the functional activity of the nervous system as the most informative index of an EMR "injury" (in accordance with the opinion of many of the authors cited).

The effect of EMR on the function of the human central nervous system in a production environment has been studied by many authors [3-6]. The majority of them note that as production experience increases the frequency of the complaints about state of health increases.

According to the data from most of the clinical-physiological surveys, one gains the impression of an earlier and more pronounced reaction of the nervous system in the case of chronic irradiation [5, 7-9].

This is manifested subjectively in the form of constant headache, increased fatigability, disturbance and shortening of sleep, heightened irritability, impairment of memory and other symptoms. It is easy to discern the polymorphism of the complaints and the low recurrence of them in the investigations of the various authors.

In an objective study, vegetative disturbances were observed: tremor of hands and eyelids, heightened tendon reflexes, sweating of palms, inhibited dermographia and hyperhydrosis. According to the data [6], distortions of Shcherbak's reflex and skin temperature asymmetry were found and paroxysmal headache was sometimes observed, blanching of the skin and adynamia, often terminating in syncopic states with prolonged poor health thereafter. Such disorders were qualified as diencephalic. Some of these symptoms were found by other authors also [5, 8].

The changes in the vegetative nervous system were often accompanied by shifts in the electrical activity of the cerebral cortex [5, 6]. The clinical and experimental findings are typically polymorphic. The appearance of bilaterally synchronous slow theta and delta discharges are characteristic for persons with 6 to 10 years' work experience. The changes in the biopotentials are associated with a change in the reactivity and excitability of the nerve cells. Analogous results were obtained by other authors.

In the opinion of most of the researchers, the polymorphic change in nervous system functions with a predominance of visceral-vegetative modifications and a vaguely manifested diencephalic syndrome suggests both a direct and a mediated effect of microwaves on the central nervous system. Some [8, 10] have found a correlation between the studied indexes and the intensity of microwave irradiation and duration of production experience.

One has to view as an important aspect of the study of EMR the phenomena of human adaptation to it. The presence of this phenomenon and the effectiveness of the adaptation mechanisms in man are noted in most of the works [10]. Actually, notwithstanding man's protracted contact (over 20 years) with electromagnetic fields,

cases of serious illness from chronic exposure to low-intensity SHF fields are unknown in the scientific literature. A majority of the scientists, moreover, have formed no definite impression as to the need or justification for allotting the illness a separate nosological identity [2-5].

Analysis of production-environment clinical-physiological studies (manned spacecraft are no exception) is a very difficult task. For quantitative analysis of the bioldogical effects one must consider a number of conditions: availability of exact characteristics of the physical parameters of the factor in question and concomitant factors; establishment of the active factor dosage; selection of a method of analysis adequate for the data obtained and determination of the data's reliability; and, finally, making the optimum decision: "hazardous--non-hazardous".

Most of the clinical-physiological studies, however, do not contain the exact characteristic of the physical parameter in question: power density, wavelength, exposure time.

A frequency range (cm, dm, mm), power range (non-thermal, low intensity, weak, thermal) and exposure range (short-term, prolonged, chronic) are usually given. It must be emphasized that final dosimetric evaluation is influenced by a subject's location, its size, the presence or absence of shielding, the ability of the electromagnetic waves to reflect off of nearby objects etc. It can be agreed that any body situated in an SHF field is going to distort the field pattern in an almost unpredictable way [11]. By virtue of this fact, one faces the impossibility of getting an exact appraisal of the power density under real conditions, or the possibility of using extremely rough data based on theoretical calculations. All of this poses distinct obstacles to the analysis and comparability of the published results and, in some cases, makes it fundamentally impossible. The complexity of the real situation requires a complex method of treating the results for purposes of analysis.

2. Experimental Investigations

The effect of EMR on the functional state of the central nervous system was studied on people and monkeys, and on dogs, rabbits, female cats, rats and mice [1-5, 12].

For the purpose of studying human higher nervous activity, visual and motor analyzers, use was made of thermometry, and blind spot and peripheral vision perimetry; variation in the parameters of the preciseness of movement, simple and complex reaction rates, and the critical frequency at which light flashes tend to run together were evaluated. The results of these investigations can be summarized as follows: In the case of EMR exposure at densities of 0.3-3 mW/cm^2 in the meter, dm and cm bands, the findings were intensified hand tremor [13] and heightened excitability of the dark-adapted eye [14]; the threshold of change in the lability of the retina was found to be 0.3-0.4 mW/cm^2 for the cm band and 0.8-1 mW/cm^2 for the dm band [15], with a narrowing of the field of vision at 1 mW/cm^2.

The method of conditioned reflexes was shown to have a high sensitivity in experiments with dogs and rabbits: positive conditioned reflexes to food increase and the latent period is shortened. Under repeated exposures to 5 mW/cm^2 there was an initial intensification of the reflexes with subsequent normalization. This was regarded as adaptation to the EMR [16]. Rats were found to exhibit at first height-

ened then, later, lowered central nervous system excitability, an increase in the latent period of reaction (109 mW/cm^2 for 15-30 minutes twice a day), a decline in conditioned reflexes and disturbances in differentiation (400 mW/cm^2) [17]. Stimulation--by means of electric current--of the preganglionic nerve of the upper cervical ganglion in rabbits under 50 mW/cm^2 irradiation caused an elevation of the nerve temperature and a lessening of the latent reaction period.

A study of EEG's revealed the following general characteristics: intensified synchronization (latent period from tenths to hundredths of seconds), long desynchronization (latent period of same duration), momentary desynchronization (at moment of source activation and deactivation), aftereffects in the form of intensified desynchronization; appearance of epileptoid discharges [4, 18].

The character of the changes in the electrical activity of the cortex observed in association with EMR is maintained in the case of a disorder of the analyzer centers, hypothalamus, thalamus or a reticular formation; the directivity of the reactions is maintained when the cortex is isolated from the mesencephalon. The introduction of caffeine or adrenalin intensifies convulsive discharges in the EEG. In analyzing the experiments it is first of all necessary to answer the following question: Is it basically possible to employ the method of electroencephalography in studying the biological effects of an SHF field. Unfortunately, this question can be answered neither positively nor negatively at the present time. In the first place, the use of implanted metal electrodes in the EEG method leads to a redistribution of the SHF field and a considerable increase in its intensity [19]. The actual distortion of the exposure density is so great that it is practically impossible to predict any kind of solid figure for the density. In the second place, the implanted electrodes lead to the occurrence of standing waves [20, 21, 2]. To determine the threshold of central nervous system changes by the EEG method we used the data of Gordon [10]. The following relationships were obtained for cm and dm waves, respectively: $y = 1.33 \cdot 10^3 \cdot x^{-2.43}$ and $y = 1.36 \cdot 10^2 \cdot x^{-3.39}$, where y is $\mu W/cm^2$ and x is the exposure time in minutes.

In the investigation of biological sensitivity most of the experiments were run with rabbits and guinea pigs. Studies were made of the activity of cholinesterase, acetylcholinesterase, dehydrogenase, succinic acid and cytochrome oxidase of brain tissues, the blood and other organs.

It was revealed that the degree of cholinesterase reduction is not uniform in different parts of the brain: cerebral cortex, subcortex, cerebellar trunk. Changes in tissue cholinesterase are preceded by a reduction in blood cholinesterase.

The relationship between the observed effects and the EMR intensity and duration was clarified. The absence of any effects at all at 1 mW/cm^2 and a lowering of activity at 10, 20 and 40 mW/cm^2 were revealed. The observed decline in cholinesterase activity (tissue and blood) is associated by most of the authors with accumulation of acetylcholine in the organs studied.

There is a general conclusion as to the unquestionable involvement of certain enzymatic systems of the divisions of the brain under the effect of EMR and the need for research to obtain more reliable results [4].

On the basis of an analysis of the data in the literature on biochemical indicators the following relationship was obtained: $y = 4.33 \cdot 10^6 \cdot x^{-1.69}$, where y is $\mu W/cm^2$ and x is exposure time in minutes. An analysis of experimental data on the study of human and animal higher nervous activity suggests first of all high sensitivity of and variability of functional changes in the central nervous system under the effect of EMR. For example, according to the data of G. F. Plekhanov et al. [22], fluctuations in the sensitivity of the central nervous system are found in the range of 10^{10} to 10^1 $\mu W/cm^2$.

A second, no less important characteristic is the polymorphicity of observed changes. Practically none of the researchers found that there was no effect in response to EMR. The central nervous system evidently reacted to EMR as to any other stimulus.

A third characteristic is the presence of gradually diminishing changes proportionate to the reduction in intensity, duration and recurrence of the irradiation sessions, evaluated by most of the authors as a manifestation of the organism's adaptation. The appearance of phase variations and the increase in changes and symptoms proportionate to the increase of exposure time and experiment duration, leading to the appearance of experimental neuroses, is considered to be a phenomenon of functional cumulation.

A fourth characteristic is the caution that is well known to be exercised in evaluating the pathological significance of changes which are observed. In the overwhelming majority of the published experimental works there is no evaluation of the degree of risk associated with the effects in question.

All of this makes it difficult to analyze the data in the literature, of course. However, if we adhere to the point of view of B. M. Savin, A. G. Subbota and Ye. A. Yermolayev [23, 16], Z. V. Gordon [10] and others in evaluating the pathological significance of the observed effects as applied to the cited works, then the following relationship can be regarded as the threshold for a hazardous effect as far as changes in the central nervous system are concerned: $y = 9.8 \cdot 10^7 \cdot x^{-2.24}$, where y is $\mu W/cm^2$ and x is the exposure time in minutes

In conclusion, it must be pointed out that, notwithstanding the relatively large number of publications in which the reaction of man's or animal's central nervous system to EMR was studied, there is a need for works which would bring into play the relationship of EMR's effects to power density and exposure time, and to its frequency characteristic, and which would employ more adequate procedures (from biophysical reactions at the cell level to behavioral reactions of the entire organism), making it possible to evaluate in evolutionary aspect the pathological significance of the changes being observed.

As applied to aerospace medicine, the problem of the biological action of non-ionizing EMR has to be looked at mostly from the standpoint of the combined action of a variety of factors. There are in the literature works in which the combined effect of microwave EMR and gamma radiation has been studied [24-26]. However, evaluation of the biological effects in these investigations was made with reference to such indexes as survival rate, body weight dynamics and the peripheral blood leukocyte

count, and from certain biochemical tests characterizing the condition of the endocrine system and others. But the state of the central nervous system under conditions of the combined action of EMR and other factors--in particular, this refers to flight factors of the non-radiation kind--was not studied.

Of theoretical and practical interest are investigations of the biological effect of EMR and dynamic factors of flight, the gaseous environment, EMR and magnetic fields and so on.

More and more data are being published now suggesting that constant magnetic fields are a biologically active environmental factor.

During space flight, man and biological objects may be in a hypogeomagnetic environment for a long time or may be subjected to the effect of strong magnetic fields which are produced on spacecraft by special apparatus for protection from cosmic radiation [27]. This factor may alter the organism's reactivity, in particular, the reactivity of the central nervous system to non-ionizing EMR. One of the immediate tasks of space radiobiology may also be the study of biophysical mechanisms of the interaction of EMR with constant magnetic fields.

BIBLIOGRAPHY

1. Petrov, I. P. and Subbota, A. G., "On the Effect of SHF Electromagnetic Radiation on the Organism," VOYENNO-MED. ZH., No 2, 1966, p 2.

2. Presman, A. S., "Elektromagnitnoye pole i zhivaya priroda" [The Electromagnetic Field and Living Nature], Moscow, Nauka, 1968.

3. Petrov, I. P., "Vliyaniye SVCh-izlucheniy na organizm cheloveka i zhivotnykh" [The Effect of SHF Radiation on the Human and Animal Organism], Moscow, Meditsina, 1970.

4. Baranski, S. and Czerski P., "Biological Effects of Microwaves," Dowden, Hutchinson, Ross, Stroudsburg, Pa., USA, 1976.

5. Tyagin, N. V., "Klinicheskiye aspekty oblucheniy SVCh-diapazona" [Clinical Aspects of SHF Exposure], Moscow, Meditsina, 1971.

6. Uspenskaya, N. V., "Dynamic Observations of Workers Under Conditions of Exposure to CM-Band Electromagnetic Waves," VRACHEBNOYE DELO, No 3, 1961, p 124.

7. Drogichina, E. A. and Sadchikova, M. N., "Clinical Syndrome in the Case of Exposure to Various RF Bands," GIGIYENA TRUDA I PROFZABOLEVANIY, No 1, 1965, p 17.

8. Sadchikova, M. N. and Orlova, A. A., "On the Clinical Picture in Chronic Exposure to Centimeter Waves," Ibid., No 1, 1960, p 32.

9. Klimkiva-Deutschova, E., "The Effect of Radiation on the Nervous System," ARCH. GEWEBEPATHOL. UND GEWEBEHYG., Vol 16, 1957, p 72.

10. Gordon, Z. V., "Voprosy gigiyena truda i biologicheskogo deystviya elektromagnitnykh poley sverkhvysokikh chastot" [Problems of Work Hygiene and the Biological Effect of SHF Electromagnetic Fields], Moscow, Meditsina, 1966.

11. Michaelson, S. M., "Human Exposure to Non-ionizing Radiant Energy Potential Hazards and Safety Standards," PROC. IEEE, Vol 60, No 4, 1972, p 389.

12. Michaelson, S. M., "Radio-Frequency and Microwave Energies, Magnetic and Electric Fields," Found. of Space Biol. and Med., NASA, Washington, DC, 1975, p 409.

13. Pivovarov, M. A., The Effect on Humans of Microwave Irradiation Under Laboratory Conditions," in book "Mediko-biologicheskiye problemy SVCh-izlucheniy" [Medical-Biological Problems of SHF Radiation], Leningrad, Nauka, 1966, pp 130-140.

14. Matuzov, N. I., "Variation of Visual Analyzer Excitability in Persons Exposed to Microwaves," BYUL. EKSPER. BIOL. I MED., Vol 48, No 7, 1959, p 27.

15. Libikh, S. F., "Functional Lability of the Retina," in book "Voprosy biologicheskogo deystviya sverkhvysokochastotnogo (SVCh) elektromagnitnogo polya" [Problems of the Biological Effect of an SHF Electromagnetic Field], Leningrad, Institute of Labor Hygiene and Occupational Diseases, 1962, pp 30-31.

16. Subbota, A. G., "Criteria for Evaluating Functional Changes in an Organism Exposed to Microwaves," in book "Printsipy i kriterii otsenki biologicheskogo deystviya radiovoln" [Principles and Criteria for Evaluating the Biological Effect of Radio Waves], Leningrad, Military Medical Academy imeni S. M. Kirov, 1973, p 19.

17. Gorodetskaya, S. F., "The Effect of an SHF Field and Convection Heat on the Estrual Cycle in Mice," FIZIOL. ZH. AN SSSR, No 10, 1964, p 494.

18. Kholodov, Yu. A., "Vliyaniye elektromagnitnykh i magnitnykh poley na tsentral'nuyu nervnuyu sistemu" [Effect of Electromagnetic and Magnetic Fields on the Central Nervous System], Moscow, Meditsina, 1966, p 59.

19. Sevast'yanov, V. V., "Principles for Systematizing Investigations of the Biological Effect of RF Fields," in book "Printsipy i kriterii otsenki biologicheskogo deystviya radiovoln," Leningrad, Military Medical Academy imeni S. M. Kirov, 1973, pp 53-56.

20. Hines, H. and Randall, J., "Possible Industrial Hazards in the Use of Microwave Radiation," ELECT. ENG., Vol 71, No 10, 1952, p 879.

21. Schliephake, E., "Functional Testing of the Endocrine Glands, the Pituitary in Particular, Using Shortwave Stimulation," ELEKTROMEDIZINE, No 2, 1960, p 80.

22. Plekhanov, G. F., "Discrepancy and Error Criteria in Studying the Radiosensitivity and Radiovulnerability of Living Systems," in book "Printsipy i kriterii otsenki biologicheskogo deystviya radiovoln," Leningrad, Military Medical Academy imeni S. M. Kirov, 1973, pp 14-16.

23. Savin, B. M., Yermolayev, Ye. A. and Subbota, A. G., "Printsipy issledovaniya i kriterii otsenki biologicheskogo deystviya radiovoln" [Priciples for Studying and Criteria for Evaluating the Biological Effect of Radio Waves], Leningrad, Military Medical Academy imeni S. M. Kirov, 1973, p 83.

24. Davydov, B. I., Antipov, V. V. and Tikhonchuk, V. S. "Biological Interaction of RF Electromagnetic Waves and Ionizing Radiation," KOSMICHESKIYE ISSLEDOVANIYA, Vol 12, No 1, 1974, p 129.

25. Antipov, V. V. and Davydov, B. I., "The Combined Effect of Flight Factors," Ibid., Vol 15, No 2, 1977, p 286.

26. Davydov, B. I., Antipov, V. V. and Tikhonchuk, V. S., "Time Parameters in Microwave Exposure," Ibid., Vol 17, No 1, 1979, p 151.

27. Grigor'yev, Yu. G., "Radiatsionnaya bezopasnost' kosmicheskikh poletov" [Radiation Safety of Space Flights], Moscow, Atomizdat, 1976.

5454
CSO: 1866/8

SPACE ENGINEERING

UDC 621:396.965

TECHNIQUE AND EQUIPMENT FOR RADIOMETRIC CALIBRATION OF 'FRAGMENT' MULTISPECTRAL SCANNING SYSTEM IN ABSOLUTE ENERGY UNITS

Moscow ISSLEDOVANIYE ZEMLI IZ KOSMOSA in Russian No 6, Nov-Dec 81 (manuscript received 12 Jun 81) pp 79-88

[Article by G.A. Avanesov, A.A. Bogdanov, A.P. Naumov, A.G. Sychev, V.I. Tarnopol'skiy and G.N. Tolstykh, Institute of Space Research, USSR Academy of Sciences, Moscow, and All-Union Scientific Research Institute of Opticophysical Measurements, Moscow]

[Text] In [1-4] the authors show that for the representation of the results of remote measurements of the Earth's brightness fields made by different surveying systems (SS) operating in the optical band, particularly the "Fragment" multispectral scanning system, the latter should be given spectral energy brightness density (SPEYa) values from the "State Special Standard" [5]. However, the special features of the optical systems in SS's makes their direct comparison with the standard measuring equipment (OSI) certified by the "State Standard" impossible: special calibrating stands are needed for the geometric matching of an SS and an OSI.

The complex of demands made on calibrating stands and the specific calibration technique used are stipulated by the following considerations.

In order to determine the SPEYa of radiation entering an SS's input, it is necessary to know its sensitivity in each channel:

$$S_j = \frac{g_j}{B(\lambda_e)}, \tag{1}$$

where S_j = absolute sensitivity of the j-th channel, for which wavelength λ_e [6,7] is effective; $B(\lambda_e)$ = SPEYa of the radiation taken as the model for observations in nature; the radiation has surface and angular uniformity; g_j = the SS's output signal in the j-th channel for the model radiation.

Let $S(\lambda)$ be the SS's relative spectral sensitivity in the channel under discussion; it is then the case that

$$g_j = c\int_0^\infty B(\lambda)S_j(\lambda)\,d\lambda, \tag{2}$$

where c = a factor depending on the normalization of the relative spectral sensitivity and the geometric parameters of the SS's optical system.

When calibrating an SS from a source, the SPEYa of the radiation of which has the form $B_{st}(\lambda)$, while the geometric parameters are the same as for the model radiation, we obtain signal $g_{j\,st}$, which can be represented as

$$g_{j\,st}=c\int_0^\infty B_{st}(\lambda)S_j(\lambda)d\lambda. \qquad (3)$$

Substituting (2) and (3) into (1), we finally obtain

$$S_j=\frac{g_{j\,st}}{B(\lambda_e)}\frac{\int_0^\infty B(\lambda)S_j(\lambda)d\lambda}{\int_0^\infty B_{st}(\lambda)S_j(\lambda)d\lambda}. \qquad (4)$$

Thus, SS calibration must be done with a source having a known spectral SPEYa distribution and, moreover, the source's radiation must fill (as is the case under operational conditions) the space angle of the SS's viewing field.

It is obvious that ribbon-filament lamps without additional optics do not satisfy the second requirement. In order to calibrate the "Fragment" system, therefore, we used a working source consisting of a large-diameter integrating sphere illuminated by halogen lamps. The source is tested periodically with an OSO; that is, by (in the final account) by the State standard for SPEYa.

As follows from [4], one of the parameters needed in order to determine S_j is the SS's relative spectral ~~sensit~~ivity. In order to determine it experimentally, it is necessary to have a monochromatic source, the radiation of which fills the SS's input pupil within the limits of its viewing field's space angle.

Thus, the calibrating stand must contain three sources and a system for testing two of them on the basis of the third (an OSI). This determined the optical layout and structure of the "Poisk" stand, which was developed especially in order to calibrate the "Fragment" multispectral scanning system and is used at the present time for calibrating SS's (spectroradiometer-brightness meters) with input pupils up to 240 mm in diameter in the 0.25-2.5 μm spectral band.

A functional diagram of the "Poisk" calibration stand is shown in the figure on the next page. It consists of the following assemblies: elongated, diffuse, continuous-spectrum emitter 1, monochromatic emitter 2, OSI 3, comparator 4, calibrated diaphragm 5 and flat rotating mirror 6.

The diffuse emitter is an integrating sphere 600 mm in diameter. The sphere's inner surface is covered with barium sulfate and is illuminated by four KGM12-100 halogen lamps that are distributed uniformly over its external surface. In order to insure uniformity of the distribution of the brightness in the plane of the sphere's output opening, the radiation from the lamps enters it through MS13 milk glass. Investigations showed that the nonuniformity of the brightness in the output opening's plane does not exceed 0.5 percent.

For the monochromatic emitter we use a system consisting of an SI8-200u ribbon-filament light-measuring lamp (chosen for its stability) with a stabilized MTKS-35M

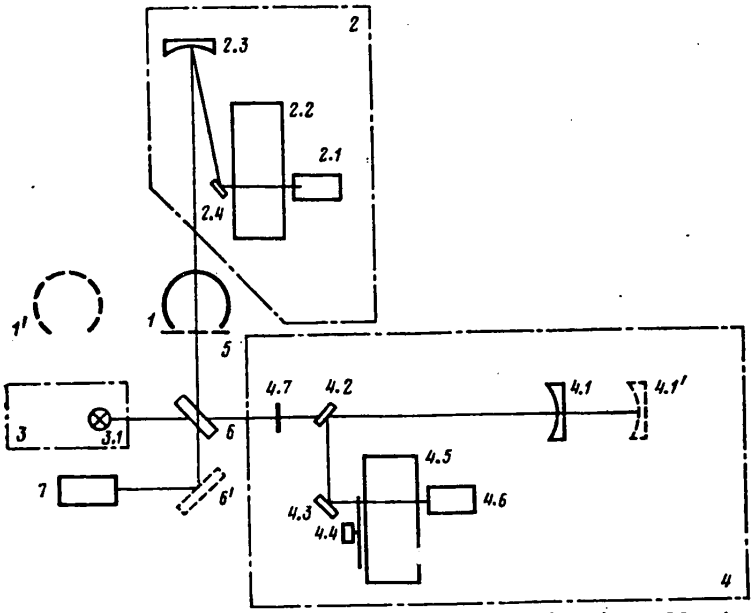

Functional diagram of the "Poisk" measuring installation.

power unit. The lamp's emissions are broken down into the spectrum by monochromator 2.2. Its exit slit is in the focal plane of spherical collimator mirror 2.3 (the mirror's light diameter is 255 mm and its focal length is 800 mm). Depending on the position of rotating mirror 6, the parallel beam formed by the collimator mirror enters either collimator 4 or the instrument being calibrated (in connection with this, the diffuse emitter is in position 1').

Standard emitter 3 is an SI10-300u light-measuring lamp that is contained in a water-cooled, lightproof housing. The lamp was first annealed, then selected for stability and uniformity of the channel body's brightness and calibrated in SPEYa units according to the "State Special Standard," so that it is a standard means for making measurements according to the All-Union testing system [5].

The operating modes of the standard lamp and those of the monochromatic and diffuse emitters are controlled by precise measurements of the voltage (with the help of V7-23 voltmeters in the lamp bases) and amount of current in their circuits. The current is determined from the results of measurements of the voltage drop in an R-310 standard resistor with the help of an R361-1 precision potentiometer. In addition to this, the stability of the sources' emissions is monitored with the help of two silicon photoreceivers that are periodically introduced into the appropriate optical channels. The signals from these receivers are measured by a Sh1513 digital voltmeter.

Comparator 4 is used to determine the SPEYa of the diffuse emitter and the relative spectral distribution of the monochromatic emitter's energy by comparing these sources with the OSI's radiation. The comparator consists of spherical mirror 4.1 (light diameter = 255 mm, focal length = 1,600 mm), calibrated screen 4.7, flat mirrors 4.2 and 4.3, modulator 4.4, monochromator 4.5 and photoreceiver block 4.6. Photomultipliers of the 28 ELUF15-00 type, which have multislit or oxygen-silver-cesium photocathodes, are used as photoreceivers in the near-ultraviolet, visible and near-infrared bands of the spectrum to 1.1 μm. In the 1.2-2.5 μm band, a

photoresistor of the FS-11AN type is used. A special unit consisting of a highly stable incandescent TRSh-2840 lamp operating on reduced voltage and an FD-24K photodiode is used to monitor the stability of the comparator's sensitivity. The lamp is powered by a B5-21 power unit. The signals corresponding to the emissions of this source are registered simultaneously by the compartor's receiver and the photodiode. Since identical deviations of the parameters of such an interconnected system is not very probable, the possible instability of the comparator's receivers can be evaluated with a high degree of accuracy.

The emissions of diffuse illuminator 1 enter the comparator when the flat rotating mirror is in position 6, while those of the monochromatic source do so when the mirror is in the same position but the diffuse illuminator is in position 1'. When the flat mirror is drawn back into position 6', the OSI's emissions enter the comparator.

The shape and size of screen 4.7, which is in the path of the light, are chosen so that, on the one hand, mirror 4.2 is in the screen's shadow and, on the other, the bundle of rays passing through diaphragm 5 is not screened.

Thus, the space angle of the shaded part of the beam from the OSI is determined completely by the dimensions of screen 4.7, while the geometric parameters of the diffuse emitter's radiation, which passes through the comparator's optical system, do not depend on the screen since they are formed by diaphragm 5. It is also obvious that the screen has no effect on the monochromatic emitter's spectral characteristics.

As has already been mentioned, the calibration technique is based on the separate determination of the relative spectral sensitivity of each measuring channel in the instrument being calibrated and the channel's absolute sensitivity to SPEYa on the effective wavelength.

During measurements, the comparator is considered to be a complex radiation receiver, while the measurement of the OSI's emissions is its calibration. The feasibility of such an approach is determined by the following facts. Because of the bulk of the flat mirror, moving it from position 6 to position 6' on each wavelength is inconvenient. Therefore, instrument readings are first made in one position (that is, for one of the sources) and then in the other (for the other source). These series of measurements can be separated by a considerable time interval. From this it follows that the parameters of the lamps' emissions and the sensitivity of the comparator's receivers must be stable, which is achieved by using highly stable power units, monitoring receivers for the illuminators, and reference sources for the receivers.

Thus, instrument calibration is preceded by calibration of the comparator with respect to the OSI, determination of the monochromatic illuminator's relative spectral characteristic, and measurement of the diffuse emitter's SPEYa.

During the measurement of the relative spectral distribution of the monochromatic illuminator's energy for each wavelength of the monochromatic radiation, the wavelength in monochromator 4.5 is set so that the receiver's signals are maximal. Since dispersion does not depend on wavelength for a monochromator with a diffraction grating, while the SPEYa of lamp 2.1 changes only slightly within the limits of

the spectral interval delineated by the slits, it can be assumed that the form of the SPEYa's spectral dependence in the plane of the exit slit of monochromator 2.2 differs little from the slit spread function. From this it follows that this dependence is identical for different wavelengths set in the monochromator. During duplicate calibration, therefore, the wavelengths set in the scales of monochromators 2.2 and 4.5 must coincide. For this same reason, during calibration with respect to source 3 and measurement of source 2, the relationship of the values of the output signal from each of receivers 4.6 will be proportional to the relationship of the absolute values of the SPEYa of the sources being compared, which means it is equal to the ratio of the relative values; that is,

$$B_2(\lambda)=B_3(\lambda)\frac{g_{k2}}{g_{k3}}, \tag{5}$$

where $B_2(\lambda)$, $B_3(\lambda)$ = relative spectral distributions of the energy of the monochromatic illuminator and the OSI, respectively; g_{k2}, g_{k3} = output signals of the comparator during irradiation of it by the monochromatic illuminator and the OSI, respectively.

In practice, however, some difference in the calibration of the monochromators (on the order of 2-3 Å) is possible. Therefore, in order to achieve precise coincidence of the maximums of the spectral intervals delineated by the monochromators, scanning is carried out in the comparator's monochromator close to the wavelength set in monochromator 2.2 until the maximum value of the signal from the receiver is obtained.

The spectral characteristic of the "Poisk" device's monochromatic illuminator, calculated in accordance with expression (5), is given in Table 1.

Table 1. Relative Spectral Characteristic of Monochromatic Emitter

Длина волны λ, мкм (1)	Относительные значения спектральной характеристики (2)	Длина волны λ, мкм (1)	Относительные значения спектральной характеристики (2)	Длина волны λ, мкм (1)	Относительные значения спектральной характеристики (2)
0,4004	0,001	0,8870	0,455	1,6665	0,369
0,4516	0,011	0,9414	0,687	1,7755	0,266
0,5060	0,045	0,9959	0,758	1,8844	0,195
0,5604	0,128	1,0503	0,968	1,9933	0,232
0,6148	0,238	1,1047	1,000	2,1023	0,144
0,6693	0,345	1,2308	1,000	2,2112	0,021
0,7237	0,393	1,3398	0,915	2,3201	0,037
0,7721	0,369	1,4487	0,761	2,4291	0,018
0,8326	0,322	1,5576	0,566		

Key:
1. Wavelength λ, μm
2. Relative values of spectral characteristic

The relative spectral characteristic $s_j(\lambda)$ of the instrument channel being calibrated is determined from the ratio

$$s_j(\lambda)=\frac{g_{j2}}{B_2(\lambda)},$$

where g_{j2} = relative value of the output signal of the instrument being calibrated during irradiation by the monochromatic illuminator on wavelength λ.

From this, by using relationship (5) we obtain the final formula for determining the relative spectral characteristic:

$$s_j(\lambda) = \frac{g_{j_2}}{B_2(\lambda)} \frac{g_{n_2}}{g_{n_3}}. \tag{6}$$

Further, from ratio

$$\lambda_e = \frac{\int_0^\infty \lambda s_j(\lambda)\, d\lambda}{\int_0^\infty s_j(\lambda)\, d\lambda} \tag{7}$$

we find the effective wavelength λ_e [6,7] for the given channel on which absolute sensitivity S_j is determined. Absolute sensitivity is determined according to the reaction of the channel being calibrated to the emissions of the diffuse source, according to the expression

$$S_j = \frac{g_{j_1}}{B_1(\lambda_e)}, \tag{8}$$

where g_{j1} = output signal of the instrument being calibrated during irradiation by the diffuse emitter; $B_1(\lambda_e)$ = SPEYa of the diffuse emitter on wavelength λ_e.

During calibration, the emissions of the diffuse illuminator can be regarded as a set of beams. When in position 4.1, the comparator's spherical mirror selects from this set the beams propagating within the limits of the space angle determined by the monochromator's entrance slit and the focal length of spherical mirror 4.1. The emissions pass through monochromator 4.5 into set of receivers 4.6.

When measuring the OSI's emissions, the comparator's spherical mirror is shifted into position 4.1'. In connection with this, an image of the lamp is created in the plane of the entrance slit of the comparator's monochromator. The emissions then pass through the monochromator into one of the interchangeable receivers.

The ratio of the values of the diffuse emitter's and OSI's SPEYa is proportional to the ratio of the receiver's corresponding signals. It is important to note here that geometric factors enter the proportionality factor (since they are different for the sources being compared), although neither the mirrors' reflection coefficients nor the characteristics of monochromator 4.5 does, since the light from the diffuse emitter and the OSI pass through the same optical channel 4.1-4.5 (from the viewpoint of its reflection coefficient, mirror 6 should be regarded as part of illuminator 1 or 2).

When calibrating the diffuse illuminator on wavelengths where the spectral sensitivity of receivers 4.6 is low, the signal-to-noise ratio turns out to be unfavorable for precise measurements. Therefore, the absolute value of the diffuse illuminator's SPEYa is determined only for several wavelengths where the signal-to-noise ratio is quite high and the relative energy distribution is measured for the rest of the wavelengths. When measuring the absolute value of the diffuse radiation's SPEYa, the monochromator's entrance slit has the same dimensions as when calibrating the comparator with respect to the OSI. However, when measuring the relative

distribution of the diffuse emitter's brightness with respect to the spectrum, the entrance slit's dimensions are increased for the purpose of improving the signal-to-noise ratios on the edges of the spectral band.

The diffuse illuminator's SPEYa is determined with due consideration for the geometric factors. In the calculation, the illuminator can be replaced by an equally bright luminous plane that coincides with diaphragm 5. The radiation that passes through diaphragm 5 and enters the monochromator is limited by space angle Ω_1, which is determined from the ratio

$$\Omega_1 = \frac{Q_к}{f_{4.1}^2}, \tag{9}$$

where $Q_к$ = area of the comparator's entrance slit; $f_{4.1}$ = focal length of mirror 4.1.

Space angle Ω_3, within the limits of which the emissions of the SI10-300u lamp enter the interior of monochromator 4.5, is determined by the relationship

$$\Omega_3 = \frac{Q_{4.1}}{l_2^2} - \frac{Q_{4.7}}{l_3^2}, \tag{10}$$

where $Q_{4.1}$ = area of the entrance pupil of mirror 4.1; $Q_{4.7}$ = area of screen 4.7; ℓ_2, ℓ_3 = distance from the ribbon of lamp 3.1 to the entrance pupil of the mirror in position 4.1' and to screen 4.7, respectively.

The comparator's output signal is proportional to the spectral density of the flow of radiation that enters the receiver. From this,

$$\frac{g_{к1}}{g_{к3}} = \frac{F_1(\lambda)}{F_3(\lambda)} = \frac{B_1(\lambda) Q_5 \Omega_1}{B_3(\lambda) Q_{3.1} \Omega_3}, \tag{11}$$

where g_{k1} = input signal of the comparator during irradiation by the diffuse illuminator; $F_1(\lambda)$, $F_3(\lambda)$ = spectral density of the flow of radiation from the diffuse illuminator and the OSI, respectively; Q_5 = area of diaphragm 5; $Q_{3.1}$ = area of the part of the SI10-300u lamp, the emissions of which enter the entrance slit of monochromator 4.5.

The lamp's ribbon is projected onto the comparator's entrance slit with a magnification equal to the ratio of the distance from mirror 4.1 to the entrance slit to the distance from the ribbon to this mirror:

$$\beta = \frac{l_1}{l_2}, \tag{12}$$

where ℓ_1 = distance from the mirror to the slit.

It is then the case that

$$Q_{3.1} = \frac{Q_к}{\beta^2}, \tag{13}$$

where $Q_{3.1}$ = area of the comparator's entrance slit.

From expressions (5)-(10) we derive the final formula for determining the diffuse illuminator's SPEYa:

$$B_1(\lambda) = B_3(\lambda) \frac{g_{к1}}{g_{к3}} \cdot \frac{l_2^2 f_{4.1}^2}{l_1^2 Q_5} \left(\frac{Q_{4.1}}{l_2^2} - \frac{Q_{4.7}}{l_3^2} \right). \tag{14}$$

Table 2. Spectral Characteristic of Diffuse Emitter

Длина волны λ, мкм (1)	Абсолютная спектральная яркость, Вт/ср·м³×10⁷ (2)	Длина волны λ, мкм (1)	Абсолютная спектральная яркость, Вт/ср·м³×10⁷ (2)	Длина волны λ, мкм (1)	Абсолютная спектральная яркость, Вт/ср·м³×10⁷ (2)
0,4004	0,235	0,8870	5,317	1,6665	3,696
0,4516	0,785	0,9414	5,991	1,7755	3,124
0,5060	1,745	0,9959	6,879	1,8844	2,699
0,5604	2,677	1,0503	7,289	1,9933	2,339
0,6148	3,469	1,1047	7,333	2,1023	1,921
0,6693	3,879	1,2308	6,871	2,2112	1,687
0,7237	4,319	1,3398	6,167	2,3201	0,733
0,7781	4,642	1,4487	4,745	2,4291	0,770
0,8326	4,899	1,5576	4,583		

Key:
1. Wavelength λ, μm
2. Absolute spectral brightness, $W/sr \cdot m^3 \times 10^7$

The values of the SPEYa of the diffuse emitter in the "Poisk" installation, as calculated with formula (14), are presented in Table 2.

Substituting (14) into (8), we obtain the final formula for determining absolute sensitivity:

$$S_j = \frac{g_j g_\omega l_1^2 Q_s}{B_s(\lambda_e)\, g_\kappa l_2^2 f_{4.1}^2 \left(\frac{Q_{4.1}}{l_2^2} - \frac{Q_{4.7}}{l_3^2}\right)}. \qquad (15)$$

Accuracy Characteristics of the "Poisk" Installation. Since several different physical value and parameters are measured when calibrating radiometric equipment, a detailed analysis of the resultant accuracy of the measurements can be made only with due consideration for all the components of any errors: electrical, energy, geometric, temperature and so on.

We have made a detailed analysis of the errors that arise during the use of calibration techniques based on the use of light-measuring lamps with energy characteristics calculated by some method or another. It turned out that the root-mean-square deviation of the results of measurements made by these techniques is 15 percent, while the magnitude of the uneliminated systematic error (NSP) is 30 percent.

The radiometric equipment calibration technique realized with the "Poisk" installation is free from a number of errors inherent in the previously used measurement methods. This is explained by the fact that this technique is based on direct comparison of the emissions of the sources used during the calibration with the emissions of a standard source. In addition to this, it makes it possible to interconnect the separate calibration stages with each other methodologically.

Let us discuss the basic sources of calibration errors in the "Poisk" installation, as well as several measures that are used to reduce them. The following errors play a definite role.

1. Errors arising during the transmission of the SPEYa unit from the standards to the standard measuring facilities. These errors are defined by GOST [All-Union State Standard] 8.196-76 [5].

2. Instability of the brightness of the radiation sources that are used.

3. Inaccuracy in the setting of the value of the radiation sources' operating current. The lamp current is set with an accuracy of 0.005 Å and is kept at a constant level during measurements. Highly stable MTKS-35M and SIP-35M power sources are used to power the lamps.

4. Nonlinearity of the comparator, which leads to a situation where the ratio of the comparator's signals is not equal to the ratio of the flows from the sources being measured. In order to reduce this error, the OSI is calibrated in several modes, so that it is possible to choose the one of them for which the signals from the OSI and the emitter being measured are as close together as possible. Besides this, measurements of the comparator's amplitude response are made in order to evaluate the possible nonlinearity.

5. Errors caused by a change in the comparator's sensitivity (by photomultiplier fatigue, for example). In order to reduce this error, before the beginning of the measurements the photomultiplier is held under a constant illumination until its sensitivity stabilizes. In addition, a comparator sensitivity monitoring system, which makes it possible to introduce the appropriate correction factors if its sensitivity changes, is provided.

6. The error caused by nonconformity of the section of the OSI's luminous body cut off by the comparator's entrance slit to the section of the luminous body, the SPEYa of which was determined according to the standard.

In order to reduce this error, the lamp is selected beforehand for uniformity of the brightness of its luminous body. In addition, the OSI is aligned relative to the monochromator with a laser beam, utilizing a mark on the bulb that was made during calibration.

7. Errors determined by the difference between the brightness of the section of the diffuse emitter cut off by the comparator and the diffuse emitter's brightness as averaged within the limits of the viewing field of the instrument being calibrated. The brightness distribution over the emitter's area is investigated in order to allow for this phenomenon.

8. Errors caused by nonconformity of the wavelength set in the monochromator to the true one. In order to establish the dependence of the wavelength of the radiation leaving the monochromator on the readings on the monochromator's scale, multiple calibration of the monochromator with respect to wavelengths is carried out. Using the obtained results and the method of least squares, the relationship connecting the drum reading with the wavelength of the radiation leaving the monochromator is calculated.

9. Errors caused by the finite nature of the spectral interval delineated by the monochromator. The mechanism of the appearance of these errors is as follows. Since the dependence of the brightness of the radiation sources used in the installation on the wavelength is a smooth function, it is the case that, by selecting sufficiently narrow monochromator slits, the width of which determines the delineated spectral interval, it can be assumed that within the limits of this interval, the brightness's dependence on the wavelength is linear in nature. In this case,

Table 3. Basic Components of "Poisk" Measuring Installation Error

Source of Error	Magnitude of Error
Installation reproducibility of the monochromators' wavelengths	±0.3 pm [translation unknown]
Areal uniformity of diffuse emitter's brightness	0.5 %
Angular uniformity of diffuse emitter's brightness	0.3 % within limits of 5° angle
Comparator linearity	0.3 %
Comparator stability	0.4 %
Reproducibility of the monochromatic emitter's relative spectral characteristic	1.5 %
Reproducibility of the diffuse emitter's relative spectral characteristic	1.5 %
Reproducibility of the diffuse emitter's absolute spectral characteristic	1.8 %
Effect of scattered light	0.5 % on wavelength of 0.35 μm

the measured spectral density of the brightness will correspond to the brightness on the wavelength lying in the middle of the delineated interval. If the radiation source's spectral characteristic deviates from linearity within the delineated spectral interval, errors appear in the determination of the brightness.

10. Errors arising because of long-term instability in the lamps' brightness caused by irreversible processes taking place in a lamp as it is being used.

11. Errors caused by the presence of scatter light in the monochromators.

12. Errors determined by aberrations in the optical systems.

During the metrological certification of the "Poisk" measuring system, the errors making the basic contribution to the resulting measurement error were investigated. The results that were obtained are presented in Table 3.

In view of the special features of spectroradiometric measurements, it is impossible to guarantee identical accuracy on all wavelengths in the spectral band that is being used. This is explained by a number of reasons, such as subsidence of the radiation sources' brightness into the ultraviolet and near-infrared bands of the spectrum, selectivity in the sensitivity of the photoreceivers that are used, differing degrees of accuracy in setting the wavelengths in different areas of the spectrum, and selectivity of the spectral characteristics of the optical elements that are part of the measuring device.

In view of the total effect of these causes, the resultant error in the reproduction of energy values in the "Poisk" device is lowest in the 0.8-1 μm band and increases in the area of the ultraviolet and near-infrared bands of the spectrum.

The results obtained during the metrological certification of the "Poisk" device, which characterize its resultant accuracy parameters on different wavelengths, are presented in Table 4.

In conclusion let us mention that the "Poisk" installation was put into service in 1978. Since then it has been used to calibrate and certify, in the appropriate

Table 4. Resultant Accuracy of Reproduction of Energy Values on the "Poisk" Installation

Длина волны, мкм (1)	Монохроматический излучатель (2)	Диффузный излучатель (4)	
	Среднеквадратичное отклонение, % (3)	среднеквадратичное отклонение, % (3)	неисключенная систематическая погрешность, % (5)
0,35	4,0	4,5	1,2
0,80	2,0	2,8	0,7
1,20	2,5	3,2	0,7
1,60	2,5	3,2	0,9
2,40	3,0	3,5	1,2

Key:
1. Wavelength, μm
2. Monochromatic emitter
3. Root-mean-square deviation, %
4. Diffuse emitter
5. Uneliminated systematic error, %

manner, a photometric model and a flight version of the "Fragment" multispectral scanning system [6], one of the MKF-6 multispectral camera complexes, and the S-500 airborne scanning system. At the present time, the "Poisk" installation is located at the USSR Academy of Sciences' Institute of Space Research and is being used to certify new generations of scanning systems.

BIBLIOGRAPHY

1. Sychev, A.G., and Tarnopol'skiy, V.I., "On Spectroradiometric Characteristics of Multispectral Surveying Systems," in "Mnogozonal'nyye aerokosmicheskiye s"yemki Zemli" [Multispectral Aerospace Surveys of the Earth], Moscow, Izdatel'stvo "Nauka", 1981, pp 87-93.

2. Bogdanov, V.I., Sapritskiy, V.I., Sychev, A.G., and Tarnopol'skiy, V.I., "Energy Calibration of Surveying Systems Used in Remote Investigations of the Earth," ibid., pp 93-99.

3. Balaban, V.S., Bogdanov, A.A., Koval'skiy, V.Ya., et al., "Technique for Calibrating Teleradiometers in Absolute Energy Units," in "Metrologicheskoye obespecheniye energeticheskoy fotometrii nekogerentnogo izlucheniya" [Metrological Support for Energy Photometry of Noncoherent Radiation], Moscow, VNIIFTRI [All-Union Scientific Research Institute of Physicotechnical and Radiotechnical Measurements], 1979, pp 79-87.

4. Bogdanov, A.A., Koval'skiy, V.Ya., Kolesnikov, A.A., et al., "Basic Varieties of Radiometers Used for Remote Investigations of the Earth, and Their Calibration in Energy Units," in "Problemy energeticheskoy fotometrii" [Problems in Energy Photometry], Moscow, Izdatel'stvo "Atomizdat", 1979, pp 86-94.

5. "Gosudarstvennyy spetsial'nyy etalon i obshchesoyuznaya poverochnaya skhema dlya sredstv izmereniy spektral'noy plotnosti energeticheskoy yarkosti nepreryvnogo opticheskogo izlucheniya sploshnogo spektra v diapazone dlin voln 0.25-2.5 mkm. GOST 8.196.76" [State Special Standard and All-Union Testing Method for Facilities for Measuring the Spectral Density of the Energy Brightness of Uninterrupted Continuous-Spectrum Optical Radiation in the 0.25-2.5 μm Band. GOST 8.196.76].

6. Avanesov, G.A., Ziman, Ya.L., Sychev, A.G., and Tarnopol'skiy, V.I., "Metrological Support for Measurements of the Brightness of the Earth's Surface by the 'Fragment' Multispectral Scanning System," ISSLED. ZEMLI IZ KOSMOSA, No 5, 1981, pp 65-77.

7. Bogdanov, A.A., Nalimov, V.N., Sychev, A.G., Tarnopol'skiy, V.I., and Tolstykh, G.N., "On a Possible Improvement in Radiometric Accuracy During Remote Investigations of the Earth With Multispectral Surveying Systems," ISSLED. ZEMLI IZ KOSMOSA, No 3, 1981, pp 77-84.

11746
CSO: 1866/36

SPACE APPLICATIONS

UDC 551.46:629.7

OBSERVATION OF VISIBLE MANIFESTATIONS OF OCEAN DYNAMICS FROM 'SALYUT-6' ORBITAL STATION

Moscow ISSLEDOVANIYE ZEMLI IZ KOSMOSA in Russian No 4, Jul-Aug 81 (manuscript received 7 Jul 80) pp 5-9

[Article by G.M. Grechko, USSR pilot-cosmonaut, G.A. Grishin and G.A. Tolkachenko, Marine Hydrophysical Institute, Ukrainian SSR Academy of Sciences, Sevastopol']

[Text] The possibility of directly observing and photographing the processes that characterize the dynamic state of the ocean first appeared with the development of satellite systems. With due consideration for the importance of this type of research, sections of oceanographic observations were included in the program for the study of the Earth's natural resources from artificial Earth satellites. As a result, such important features of oceanic circulation as the merging of currents, upwellings, large-scale vortices, water exchange between boundary seas and the ocean and many other phenomena that reflect the complex dynamics of the processes taking place in the ocean were first noted and photographed by the crews of spacecraft and long-term orbital stations (DOS) [1].

Automatic measurement complexes installed in unmanned artificial Earth satellites and making measurements over a broad band in the spectrum of electromagnetic waves, including the visible, infrared and superhigh-frequency bands, have unarguably been called upon to play an important role in space oceanography. The prototype of such complexes is the equipment installed in the specialized "Cosmos-1076" and "Cosmos-1151" satellites. At the same time, at the present stage of ocean and atmosphere investigation, an exceptionally important role is continuing to be played by visual observations and photographic surveying conducted directly by man from on board a manned spacecraft or a DOS. The most important advantages of such research are the possibility of the operational selection of the most interesting objects, the efficient utilization of favorable meteorological conditions, and the possibility of monitoring the dynamics of the process or phenomenon being investigated, which is very important from the viewpoint of the integral perception of an object.

In the process of carrying out the program of investigation of the Earth's resources from the "Salyut-6" DOS, a series of photographs of the South Atlantic Ocean in the area of the Falkland Islands was obtained. This region is interesting because a branch of the circumpolar current, which diverges to the north after passing Cape Horn, flows past the extensive Burdwood Bank and the Falkland Islands and then goes far to the north, under the name of the Falkland Current, where it encounters the water masses of the Brazil Current. According to the observations from space,

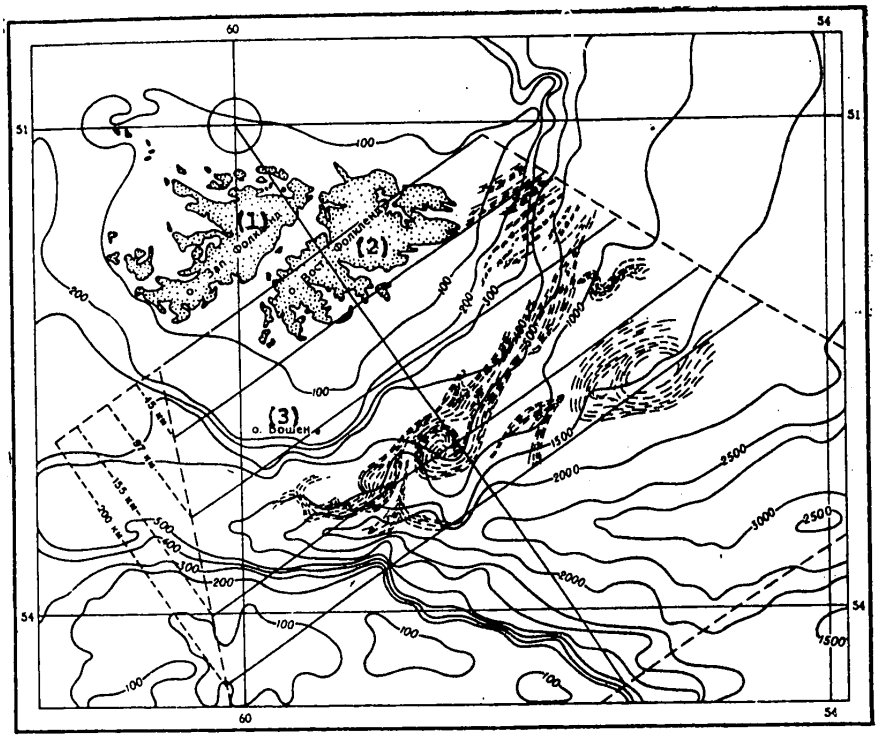

Figure 2. Schematic representation of photographic image, allowing for distortions in perspective and coordinate correlation to the area, with depth and bottom relief marks.

Key: 1. West Falkland
2. East Falkland
3. Beauchene Island

greenish hues caused by the presence of phytoplankton are typical of the Falkland Current's waters. The boundaries of these currents, which are easily distinguishable from a great altitude, are frequently traced for distances on the order of thousands of kilometers. For example, observational data gathered by the "Skylab" DOS in December 1974 [2] were used to trace the frontal zone between the Brazil and Falkland Currents visually, in the form of a thin serpentine strip, for more than 3,500 km without a break. However, the series of photographs made from the "Salyut-6" DOS on approximately a daily basis from 27 December 1977 to 5 January 1978 showed the overall instability of the system of currents and revealed the formation of a whole series of variable-sign large-scale vortices.

The color insert (Figure 1 [omitted]) is a fragment of the survey of the oceanic area to the southeast of the Falkland Islands. This same photograph is reproduced in Figure 2, taking coordinate correlation to the area into consideration, by graphic plotting; on the left are distances illustrating the change in scale in separate sections of the photograph because of distortions in perspective.

The flow of the East Falkland Current is quite visible in Figure 1. Basically, it follows the isolines of the bottom topography, and after it rejoins the western branch the current also moves to the north along the 400-600 m isobath. As is

known, to the east of the Falkland Current there is a countercurrent flowing to the south that can be traced quite easily to a depth of ≈500 m [3]. A characteristic feature of the photograph is the presence of two clearly expressed vortex-shaped structures. A cyclonic vortex that has formed almost completely is quite distinguishable in the center of the photograph because of its greenish shading. To the northeast of it can be seen a vortex rotating in the opposite direction, with a water mass that is deep blue in color as the result of molecular scattering in the biologically pure, low-productivity waters of the open ocean. The vortices are about 50 km long and the distance between them is about 200 km.

It is possible only to formulate hypotheses about the mechanisms involved in the generation of these features. The cyclonic vortex is apparently generated by an unstable barotropic flow over an abrupt sval [possibly dropoff] at depths of 500 to 1,000 m. This is also indicated by the fact that in the summer (for the Southern Hemisphere) period, intensification of the entire system of currents is seen in this region [3]. With respect to the anticyclonic vortex, however, such a conclusion is evidently not entirely correct. Actually, as is obvious from Figure 2, this vortex is located in an area of deeper water and is considerably to the right of the main flow of the East Falkland Current. Therefore, it can be assumed that the vortex is generated by an unstable system of two currents: the East Falkland Current and the countercurrent. For this hypothesis, let us attempt to evaluate a number of characteristics of the anticyclonic formation. For a displacement zone width of 200-300 km and a flow rate of 60-70 cm/s [3], the characteristic period of the most unstable waves is 4-6 days. The rate of movement of such a vortex proves to be quite significant: 17-25 km/day. Unfortunately, the absence of direct measurement data does not enable us to compare these theoretical characteristics with the actual values for the speed and period of movement of anticyclones observed from space in this region.

Another important feature of Figures 1 and 2 is the presence of "short-period" regular waves to the northeast of East Falkland Island. The curvilinearity of the fronts of the wave trains is clearly noticeable in the photograph. The wave field's phase orientation is apparently distorted because of refraction, so a definite angle is formed between the edge of the shelf and the direction of wave propagation. It is interesting to note that closer to the shore, we see greater distances between the wave trains and greater lengths of the trains themselves than on the side toward the sea. These features of wave action on the continental shelf, as observed from space, are also typical of other regions of the ocean, particularly New York Bay [4]. On the average, the width of a wave train is about 1-2 km, while the distance between the trains is 6-10 km. As is known, these features are typical for a field of internal gravitational waves. If the periodic features under discussion are represented in the form of surface waves, for wavelength λ = 1-2 km their periods will be ≈25-35 s, which exceeds significantly the known appraisals of the analogous characteristic of a field of wind-caused waves and ocean swell.

Let us examine the observed features from the viewpoint of the classical concepts of the theory of internal waves. Within the framework of a two-layer approximation of the ocean, the phase velocity of wave propagation is described by the well-known formula

$$c=\left[(g/k)\frac{\Delta\rho/\rho_1}{\operatorname{cth} kh_1+\operatorname{cth} kh_2}\right]^{1/2} \quad (1)$$

where g = gravitational acceleration; $k = 2\pi/\lambda$ = wave number; $\Delta\rho/\rho_1$ = density gradient; h_1, h_2 = thickness of the layers. In January in the investigated region, $\Delta\rho/\rho_1 \approx (2\text{-}4)\cdot 10^{-4}$ and the upper layer's characteristic thickness is $h_1 \approx 50$ m. For a general ocean depth in the shelf zone of 200-300 m and λ = 1-2 km, formula (1) yields the value $c = 0.25\text{-}0.40\ m^{-1}$. For such a velocity and an average distance between the trains of 10 km, the wave trains' period is 7-11 h. The second evaluation corresponds most closely to the half-day period of the internal tide in this region. Thus, it can be assumed that the "short-period" waves observed in the photograph are a manifestation on the ocean's surface of internal wave action formed by the scattering of the barotropic tide's under the effect of bottom topography or the edge of the continental shelf. The orthogonal nature of the wave and current propagation directions can also serve as confirmation for what has been said. Otherwise--during the generation of internal waves by a shear current, for example--the wave and current movement directions do, as a rule, coincide.

The theoretical models of gravitational wave propagation in the ocean that are known at the present time make it possible to describe the dependence of the basic characteristics of wave action on the stratification of the medium, Coriolis force, bottom topography, special features of the generation mechanisms and so on. On the other hand, laboratory and (in particular) full-scale measurements basically confirm only individual fragments of the evolution of a field of internal waves that fit in the framework of the normal classical concepts. In particular, manifestations of internal waves on the sea's surface can be caused only by those mechanisms that allow for the features of the transformation of a wave field's energy near the surface. Several such mechanisms are known at the present time [5]. One of them, for example, indicates that the divergence and convergence of current speeds in a field of internal waves causes transformation of the capillary surface waves under the influence of Reynolds stresses. This leads to an increase in the roughness of the ocean's surface above internal wave crests. Such a picture was seen, in particular, on the 29th voyage of the scientific research ship "Mikhail Lomonosov," at 10°48' S.Lat., 20°48' W.Long., when bands of ripples 30-50 m wide and moving with a period of about 8 min were observed on a mirrorlike sea surface. The results of measurements showed that the range of the fluctuations of the layer of maximum hydrological parameter gradients was 20-25 m, while the rate of change of the water temperature from the minimum to the maximum value at the fixed level of 27 m was 2.5° C/min. According to another mechanism, a high tangential velocity of a water current near the surface, caused by large internal wave amplitudes, results in an increase in the thickness of the film of surface-active substances in the convergence zone, which causes smoothing of the high-frequency components of surface wave action and the appearance of sliki [possibly slicks]. The presence on the surface of bands of ripples or sliki results in local changes in the sea's reflection factor. When observed at large angles to the nadir from a satellite, such sections should show up as dark or light-colored bands that are tens to hundreds of meters wide and hundreds of meters to tens of kilometers long. When observed at the nadir these bands are practically invisible, except for instances when the Sun is at the zenith and sliki located in the area of flashes of sun light are manifested as dark bands on the glittering surface of the sea.

In order to identify bands in photographic images taken from space with internal waves, experimental investigations were made of sliki in the northwestern part of the Black Sea, using an airplane. As in the case of observations from an artificial Earth satellite, the sliki were observed visually as individual bands grouped into

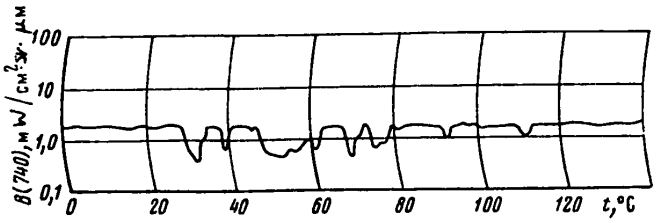

Figure 3. Example of recording, made from an airplane, of a group of internal wave sliki in the Black Sea (Sun at the zenith, sighting at the nadir).

packets. An example of the instrument measurements of the sea surface's brightness in the area of sliki is shown in Figure 3. The number of bands in the packets ranged from 4 to 12, the bands were 50-300 m wide, the distance between the bands in a packet was 0.4-1.5 km, and the average distance between the packets was 5-10 km.

Thus, in principle, the variegated manifestations of internal waves on the ocean's surface give us the opportunity to make mass remote measurements of internal wave action in different regions of the world ocean. Actually, aerospace equipment has repeatedly registered traces of internal waves on the western and eastern shelves of North America, the Florida, California and Somali currents, on the shelf of Southwest Africa, in the central part of the Pacific Ocean, in the South China, Black and Okhotsk Seas and so forth. The particular value of these observations is that they yield rich material for the study of the phenomenon itself and, in addition, make it possible to determine such an important energy characteristic of the ocean-atmosphere system as the thermal reserve of the upper quasihomogeneous layer [6].

Actually, assuming that the lower layer's thickness is much greater than h and that wavelength $\lambda >> h_1$, equation (1) takes on the form $c^2 = gh(\Delta\rho/\rho_1)$. In connection with this, if the water density ρ is basically the result of a change in temperature T, then $\Delta\rho/\rho_1 = \alpha\Delta T$, where α = coefficient of thermal expansion of sea water. Consequently, the expression for determining the thermal reserve, $Q = \rho c_p h_1 \Delta T$, allowing for the formula for c^2, can be rewritten as

$$Q = \rho c_p c^2/g\alpha, \qquad (2)$$

where c_p = thermal capacity of water under a constant pressure. By substituting into (2) the characteristic values ρc_p = 1 cal/deg, $\alpha = 2\cdot10^{-4}\cdot c^{-1}$ and the phase velocity value c = (0.25-0.40) m/s (as determined from the observations), we find that the value of Q in the area of the Falkland Islands in 3-8 kcal/cm^2. On the other hand, for the values h_1 = 50 m and ΔT = 1-2° C, which are typical of the observed region in January, Q = 5-10 kcal/cm^2. By comparing these evaluations and taking into consideration the fact that the value of Q is proportional to the square of the phase velocity of internal waves, it follows that the heat reserve appraisal made with formula (2) is sufficiently realistic in the presence of statistically guaranteed data.

Thus, the results of observations of internal waves from space indicate that the present level of development of satellite oceanography makes it possible to obtain important information about the variability of the ocean's upper layer. Despite the fact that a number of problems have not yet been solved (determining the amplitudes of internal waves, for example, which is a matter of interest for underwater

navigation), in principle the data from remote measurements can be used to evaluate phase velocities, direction of propagation and length of internal waves, and the thermal reserve of the upper quasihomogeneous layer. The value of such information is that it makes it possible to evaluate, on an operational basis, the mechanism of mixing of the upper layer in models of the dynamic interaction of the ocean-atmosphere system.

BIBLIOGRAPHY

1. Lazarev, A.I., Nikolayev, A.G., and Khrunov, Ye.V., "Opticheskiye issledovaniya v kosmose" [Optical Investigations in Space], Leningrad, Izdatel'stvo "Gidrometeoizdat", 1979, 253 pp.

2. Maul, G.A., and McCaslin, M., "An Assessment of the Potential Contributions to Oceanography From Skylab Visual Observations and Handheld Camera Photographs," NOAA ATL. OCEANOGR. MET. LAB. COLLECTED REPRINTS, 1977, p 432.

3. Zyryanov, V.I., and Severov, D.K., "Water Circulation in the Falkland-Patagonia Region and Its Seasonal Variability," OKEANOLOGIYA, Vol 19, No 5, 1979, pp 782-791.

4. Apel, J.R., et al., "Observations of Oceanic Internal and Surface Waves From ERTS," J. GEOPH. RES., Vol 80, No 6, 1975, pp 865-881.

5. Novogrudskiy, B.V., et al., "Issledovaniye okeana iz kosmosa" [Investigation of the Ocean From Space], Leningrad, Izdatel'stvo "Gidrometeoizdat", 1978, 53 pp.

6. Mollo-Christensen, E., "Heat Storage in the Oceanic Upper Mixed Layer Infrared From Landsat Data," SCIENCE, Vol 203, No 4381, 1979, pp 653-654.

11746
CSO: 1866/10

UDC 551.46.0:629.78:528.7

METHOD OF INTEGRATED INVESTIGATIONS OF OCEAN AND ATMOSPHERE FROM SPACE

Moscow ISSLEDOVANIYE ZEMLI IZ KOSMOSA in Russian No 4, Jul-Aug 81 (manuscript received 9 Oct 80) pp 45-53

[Article by M.S. Malkevich and V.V. Badayev, Institute of Oceanology imeni P.P. Shirshov, USSR Academy of Sciences, Moscow]

[Text] Introduction. Remote investigations, from space, of the ocean and the atmosphere above it are based on the rules of the physical mechanism governing the generation and transfer of reflected and intrinsic radiation in the ocean-atmosphere system, the characteristics of which (in different bands of the spectrum) serve as the initial information for the investigations. The necessity of deriving these principles is related to the following special features of problems of determining the parameters of the ocean and the atmosphere that require an integrated approach to their solution.

1. The characteristics of the ocean-atmosphere system are functions of several parameters of these mediums and their interface. Therefore, even when the sections of the spectrum that are most informative with respect to an object being studied are selected, we should expect the appearance of errors caused by other parameters that affect variations in radiation characteristics and create interference. If this interference goes beyond the limits of the allowable errors in determining a given variable, it is necessary to develop techniques that allow for and eliminate it. From this there inevitably arises the problem of determining the entire complex of unknown and interference-causing parameters, it being the case that their relationship can change, depending on the specific goals that have been formulated for the remote sounding that is being conducted.

2. The requirement of an integrated approach to these problems is also related to the fact that most of them are incorrectly formulated (in the mathematical sense) and require the development of regularization methods, using quite specific prior information about the unknown and interference-causing parameters.

The obtaining of such information is an important part of the above-mentioned integrated approach, which includes a combination of space and traditional methods of investigating the radiation fields and physical parameters of natural mediums for the purpose of studying the relationships between radiation characteristics and these parameters.

3. Finally, the requirements for accuracy and reliability of remote methods serve as a substantial argument in favor of the integrated approach, since from them there

follows the necessity of determining the same parameter by at least two independent methods, utilizing radiation characteristics in different bands of the spectrum.

The rules governing the generation and transfer of radiation in natural mediums (the ocean-atmosphere system, in particular), in combination with physically and mathematically rigorous methods for the remote determination of these mediums' parameters from space, are the physical basis for geospace investigations. The study of these rules and the development of remote methods create possibilities for determining substantiated requirements for measuring-equipment complexes that insure the obtaining of the initial complex of characteristics of the Earth's radiation, as well as information-processing systems and methods that make it possible to extract the unknown parameters of the natural mediums from this complex.

Ways of creating the physical bases for remote investigations of the ocean-atmosphere system are discussed below, in examples of the solution of two complexes of problems that were formulated with due consideration for the results of numerous theoretical and experimental projects:

1. A complex of problems in determining the temperature of the ocean's surface and the atmosphere's vertical temperature, moisture and aerosol attenuation profiles, as well as characteristics of cloudiness and the radiative capacity of the ocean's surface on the basis of measurements of the ocean-atmosphere system's intrinsic radiation in the infrared and ultrahigh-frequency bands of the spectrum.

2. A complex of problems in determining the ocean's coefficient of brightness and the atmosphere's optical parameters (optical thickness, scattering indicatrix and vertical profile of the scattering coefficient) on the basis of measurements of the solar radiation reflected by the ocean-atmosphere system in the visible band of the spectrum.

Determining the Temperature of the Ocean and the Atmosphere. The problem of the remote determination of the ocean's temperature T_0 is based on measurements of the intrinsic radiation I_ν of the ocean-atmosphere system in the atmosphere's "transparency windows" in the infrared and ultrahigh-frequency bands (3.5-4 and 10-12 μm, and 3.5 and 8 cm, respectively [1-3]).

For cloudless conditions, the variable $I_\nu(x,y,r)$, which--generally speaking--is a function of frequency ν, spatial coordinates x,y, and direction of radiation propagation r, is related to T_0 by the relationship

$$I_\nu=\delta_\nu B_\nu(T_0)P_\nu(1,r)-\int_0^1 B_\nu[T(\zeta)]\frac{\partial P_\nu(\zeta,r)}{\partial\zeta}d\zeta-2(1-\delta_\nu)P_\nu(1,r)\int_0^1 B_\nu[T(\zeta)]\frac{\partial \bar{P}_\nu(\zeta)}{\partial\zeta}d\zeta, \qquad (1)$$

where $B_\nu[T]=\frac{2h\nu^3}{c^2}\cdot\frac{1}{\exp\left(\frac{h\nu}{kT}\right)-1}$ = a Planck function (h, k = Planck and Boltzmann constants, respectively, and c = the speed of light); δ_ν = radiative capacity of the ocean; $T(\zeta)$ = vertical temperature profile (ζ = altitude in relative units of pressure); $P_\nu(\zeta,r)$ = the atmosphere's transmission function in direction r; $\bar{P}_\nu(\zeta)$ = = transmission function, as averaged for the upper hemisphere of directions.

Under real conditions, all of the enumerated functions of ζ can also depend on coordinates x,y. In addition to this, $P_\nu(\zeta,r)$ depends on the concentration of substances that absorb radiation. In the infrared-band windows, for example, P_ν depends on the water vapor's mass $w(\zeta)$ and the aerosol's optical thickness $\tau_\nu^a(\zeta)$:

$$P_\nu(\zeta, \theta)=\exp[-k_\nu w(\zeta)\sec\theta]\exp[-\tau_\nu^a(\zeta)\sec\theta], \quad (2)$$

where θ = angle between direction r and the vertical axis ζ; k_ν = absorption coefficient of water vapor.

Thus, I_ν in (1) is a functional not only of the unknown value T_0, but also of parameters δ_ν, $T(\zeta)$, $w(\zeta)$ and $\tau_\nu^a(\zeta)$, which it is necessary to determine simultaneously by independent measurements of I_ν for the purpose of allowing for atmospheric radiation in (1). As is known (see, for example, [1,2]), the vertical profiles $T(\zeta)$ and $w(\zeta)$ can be determined from measurements of I_ν in the absorption bands of CO_2 (4.3 and 15 μm) or O_2 (0.5 cm) and, correspondingly, of water vapor (6.3 and 20-25 μm or 1.35 cm).

Relationships of the type of (1) that are used for this purpose and written for the indicated absorption bands are integral equations of the Friedholm Type I variety relative to $T(\zeta)$ or $w(\zeta)$. Methods for regularizing corresponding inverse problems that were formulated incorrectly (in the mathematical sense) have now been worked out. In particular, an effective method for statistical regularization that uses the empirical characteristics of the vertical structure of the $T(\zeta)$ and $w(\zeta)$ fields as prior information about the solution has been proposed (see [1]). As far as $\tau_\nu^a(\zeta)$ is concerned, there still exist contradictory opinions about the aerosol's contribution to the attenuation of infrared radiation. This question is closely related to the classical problem of the physical nature of the continuum in the atmosphere's "transparency windows" in the infrared band.

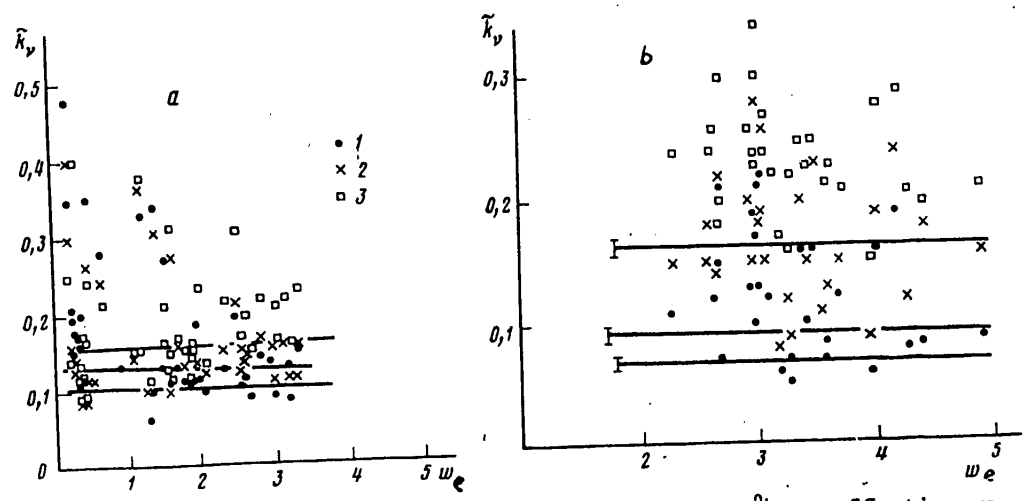

Figure 1. Dependence of effective attenuation factors $\tilde{k}_\nu$ on effective water vapor mass w_e, according to measurements of atmospheric transmission (a) and radiation (b): 1. λ = 10.2 μm; 2. λ = 11.2 μm; 3. λ = 12 μm.

Aerosol Attenuation of Infrared Radiation. Numerous laboratory and full-scale measurements make it possible to evaluate reliably and distinguish the contribution to

the continuum of the wings of the absorption bands of water vapor and the aerosol component [3]. This division is illustrated quite well by the results of measurements of the effective absorption factor in the "windows":

$$\hat{k}_\nu = \frac{\tau_\nu^*}{w_e}, \tag{3}$$

which was derived in [3] for a broad range of changes in the total optical thickness τ^* and moisture content w_e of the entire column of the atmosphere (see Figure 1). Thus, $\hat{k}_{\nu,\,min}$ can be regarded as the coefficients of continual absorption of water vapor, while any excess above $\hat{k}_{\nu,\,min}$ is the contribution of aerosol attenuation.

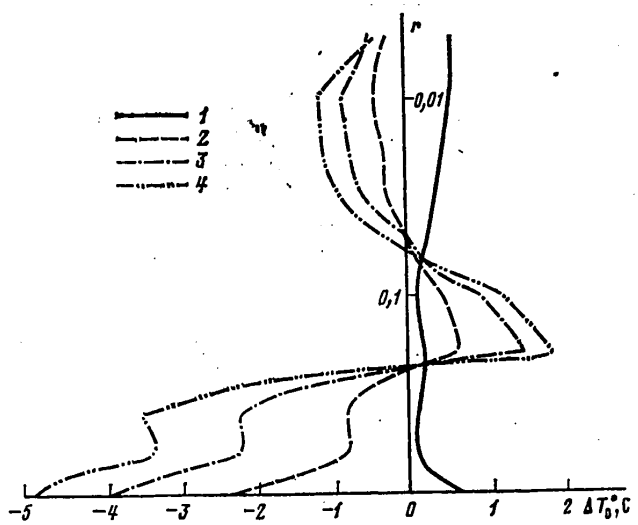

Figure 2. Errors in determining $T(\zeta)$ in the presence of a layer with optical thickness $\tau^a = 0.1$ at different levels in the atmosphere: 1. $\zeta < 0.8$; 2. $\zeta = 0.5$-0.65; 3. $\zeta = 0.3$-0.4; 4. $\zeta = 0.1$-0.2.

Evaluations of the effect of aerosol layers located at different levels in the atmosphere on errors in determining T_0 were made in [4]. As is obvious from Figure 2, the existence of such layers with optical thickness $\tau_\nu^a \approx 0.1$ can lead to errors on the order of 5-8° C. In order to determine the vertical profiles $\tau_\nu^a(\zeta)$ it is possible to use measurements of the angular distributions of radiation $I_\nu(\theta)$ in the atmosphere's "transparency windows," which are related to $\tau_\nu^a(\zeta)$ by relationships of the type of (1) and (2), with $m = \sec\theta$.

The possibilities of solving the corresponding inverse problem were illustrated in [5], using measurements of the angular distributions of incident radiation $I_\nu(m)$ (Figure 3) in the tropical region of the Atlantic Ocean. As is obvious from Figure 4, the $I_\nu(m)$ curves in Figure 3 correspond to two types of layered distribution of the aerosol attenuation factor. These layers, which were observed during direct airborne sounding of the atmosphere in that area of the Atlantic [6], are created by dust coming from the African continent.

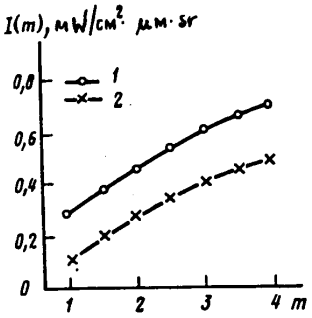

Figure 3. Angular distributions of radiation of the tropical atmosphere $I_\nu(m)$ over the Atlantic Ocean for different degrees of turbidity m = = sec θ: 1. turbid atmosphere; 2. transparent atmosphere.

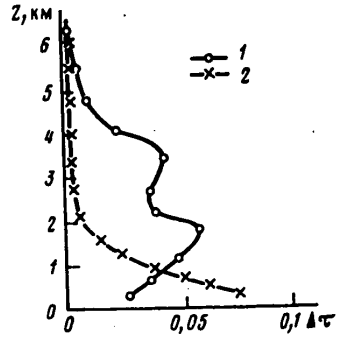

Figure 4. Determination of vertical distributions of aerosol attenuation factor according to measurements of $I_\nu(m)$ (profiles 1 and 2 correspond to curves 1 and 2 in Figure 3).

However, it should be mentioned that when the angular distributions of $I_\nu(m)$ are used to determine $\tau_\nu^a(\zeta)$, there arises the complicated problem of allowing for the horizontal nonuniformity of the aerosol substance.

Thus, the determination of $T(\zeta)$, $w(\zeta)$ and $\tau_\nu^a(\zeta)$ will make it possible to allow for atmospheric distortions during the remote determination of T_0 with the help of relationship (1) under cloudless conditions, as well as in the case of semitransparent and broken cloudiness.

Under solid cloud cover conditions, it is necessary to make joint use of radiation measurements in the infrared and ultrahigh-frequency bands of the spectrum. In the first place, this makes it possible to identify unambiguously the cloud and surface effects in the ultrahigh-frequency radiation's characteristics. In the second place, measurements in the infrared band make it possible to determine the cloud cover's characteristics (altitude, temperature and phase state of the water). Thirdly, joint measurements in the "windows" of the infrared and ultrahigh-frequency bands of the spectrum will make it possible to determine variations in the ocean surface's radiative capacity.

Finally, the most important advantage of the use of a complex of measurements is an improvement in the reliability of the determination of T_0 and the atmospheric parameters, since each parameter will be determined on the basis of independent information at least twice.

This last fact is of exceptional importance when using the mass of information about the oceanic surface's temperature fields (or the vertical distributions of temperature in the atmosphere) that is being obtained at the present time. Recent analyses of the fields (see, for example, [7]) indicate that errors and uncertainties in the determination of T_0 make this information practically useless. The authors of [7] are completely correct in pointing out the necessity of developing more refined remote techniques. This same conclusion follows from an analysis of the results published in [8].

Let us mention here that the problem under discussion was formulated clearly after the processing and analysis of materials gathered during measurements of the ocean-atmosphere system's radiation in the visible, infrared and ultrahigh-frequency bands

of the spectrum by the "Cosmos-149, -243, -320, -384" satellites [1,2,9]. On the basis of the integrated approach explained above, we have now developed a technique for obtaining and processing the appropriate complex of initial information about the characteristics of the field of intrinsic radiation, using the characteristics of the ocean-atmosphere system's brightness field.

Determining the Ocean's Brightness and the Atmosphere's Optical Parameters. In connection with the remote determination of the ocean's brightness on the basis of measurements of solar radiation reflected by the ocean-atmosphere system, it is necessary to allow for the contribution of the atmosphere's brightness, which can exceed the unknown quantity by an order of magnitude [6]. In order to do this, it is necessary to determine the following atmospheric parameters: optical thickness, scattering indicatrix γ_ν and the vertical distribution of the aerosol scattering factor.

The method for solving this problem that is presented in [10] is based on the utilization of measurements of the intensity of the reflected solar radiation I_ν, from a satellite, in several sections of the molecular oxygen absorption band (0.76 μm). The physical basis of the method is the fact that solar radiation reflected by the ocean-atmosphere system is generated by different layers in the atmosphere, the contribution of which to the brightness, as measured from the satellite, is determined by the oxygen transmission function $P_\nu(\zeta,m)$ ($m = 1 + \sec\theta_0$, θ_0 = zenith angle of the Sun). This function is known with a sufficient degree of accuracy, since the relative concentration of oxygen is constant to very high altitudes in the atmosphere and varies little around the Earth, while the 0.76-μm abosrption band has been studied quite thoroughly [1].

The relationship between the intensity of the outgoing radiation I_ν (in percentages of the solar constant $\pi S\nu$) for measurements at the nadir and the atmosphere's optical parameters in the 0.76 μm area of the spectrum (it is assumed that the indicatrix and the optical thickness do not depend on ν within the limits of the absorption band) is established by the formula

$$I_\nu = \frac{1}{4m}\int_1^0 P_\nu(\zeta, m)\frac{\partial\varphi_m(\zeta)}{\partial\zeta}d\zeta, \qquad (4)$$

which was obtained on the basis of the solution of the radiation transfer equation for a plane-parallel medium with a non-light-reflecting underlying surface (the surface's albedo is A = 0), where $\phi_m(\zeta) = \mu \exp[-m\tau(\zeta)]$, μ = brightness indicatrix for the realized scattering angle ψ, as related to the entire stratum of the atmosphere. Here, in the equation for single scattering we have formally introduced brightness indicatrix μ, which is a scattering function aggravated by multiple effects, in place of scattering indicatrix γ. This is done for the purpose of making an approximate allowance in this formulation of the problem of the effects of multiple scattering and is in accordance with the recommendations made in [11].

When allowing for the reflection of light from the underlying surface in the right side of formula (4), in general there must be present the term $AP_\nu(1,m)\phi_m(1)\cdot(\cos\theta_0/\mu)$, which describes the contribution to I_ν of the light coming from the surface. In this case, the solution of the inverse problem (4)--$\tilde{\phi}_m(\zeta)$--will differ from the true solution $\phi_m(\zeta)$ by an arbitrary constant in layers of the atmosphere where $\zeta < 1$ and will have a discontinuity at the surface at the point $\zeta = 1$.

Actually, in the case under discussion functions of the type

$$\tilde{\varphi}_m(\zeta)=\varphi_m(\zeta)+8Am\cos\theta_0\varphi_m(1)\frac{V_1(\zeta)}{\mu},$$

where

$$V_1(\zeta)=\begin{cases} c, & \zeta<1 \\ c_0, & \zeta=1 \end{cases}$$

is a step function with arbitrarily determined constants c and c_0 (for monotonically increasing functions, $c \geqslant c_0$), will satisfy measurements of I_ν with the given degree of accuracy (let us remember that the derivative of step function $V_1(\zeta)$ is delta-function $\delta(1-\zeta)$). Thus, the effects of reflection can be manifested in the solution of equation (4) only in the form of a discontinuity in the solution at the surface and are eliminated easily when determining the atmosphere's optical parameters $\tau(\zeta) = (1/m)\ln(\phi_m(0)/\phi_m(\zeta))$ and $\zeta = \phi_m(0)$ with (for example) the help of numerical interpolation of function $\tilde{\phi}_m(\zeta)$ from the area of altitudes $\zeta < 1$ to the level of the surface $\zeta = 1$.

However, the indeterminacy of component c of function $V_1(\zeta)$ makes problem (4) indeterminate and compels us to resort to the use of additional information about the unknown parameters, without taking into consideration that which is required in order to use the method for the regularization of the solution of the incorrect inverse problem (4) (we use the method of the provisional gradient of minimization of the nonbinding functional in the set of monotonic, bounded functions $\phi_m(\zeta)$). As such information it is possible to use (for example) empirical correlational relationships between the optical parameters μ and τ^*, as obtained by ground measurements in the 0.74-μm area of the spectrum. Such data [11] indicate the presence of a rather high correlational relationship between the brightness indicatrix μ and attenuation factor τ^* that can be expressed by the appropriate regression equation. Another coupling equation for μ and τ^* can be obtained directly from the solution of inverse problem (4) (after the appropriate interpolation of $\tilde{\phi}_m(\zeta)$ to level $\zeta = 1$ if a discontinuity in the solution at the surface is seen):

$$\tilde{\varphi}_m(0)-\tilde{\varphi}_m(1)=\mu(1-e^{-m\tau^*}). \tag{5}$$

The equation for finding parameter τ^* is determined from this last expression and the regression equation. Further, using the value found for τ^* and the coupling equations for the parameters, all the other optical characteristics of the problem are determined sequentially, including the vertical distribution of attenuation factor $\tau(\zeta)$, which makes it possible to discover the layers in the atmosphere with an increased aerosol concentration. After the appropriate elimination of the effects of atmospheric haze, the characteristics of the water surface's brightness are determined from the measurements of I_ν in the 0.74 μm "transparency window."

For an error level of the measurements of I_ν in the 0.76-μm absorption band area of 3 percent, the error in determining τ^* with the help of the approach under discussion is estimated to be 20-25 percent.

The value of $\tau^*_{\nu_0}$ in the λ_0 = 0.74 μm area of the spectrum that has been obtained in this manner can be used as an input parameter for determining the degree of turbidity of the atmosphere in other sections of the visible band of the spectrum. As is known [1], for this purpose it is advisable to use the method of optimal extrapolation of result $\tau^*_{\nu_0}$ to τ^*_ν, because in nature we see a quite close spectral

correlation (the coefficient of correlation is more than 0.9) for aerosol attenuation. The error in such an extrapolation does not exceed 7-10 percent. The use of analogous relationships between the scattering indicatrix and the optical thickness makes it possible, in the same manner, to determine the form of the scattering function, which, along with optical thickness, are the basic parameters used to allow for atmospheric effects when studying the ocean's resources from space.

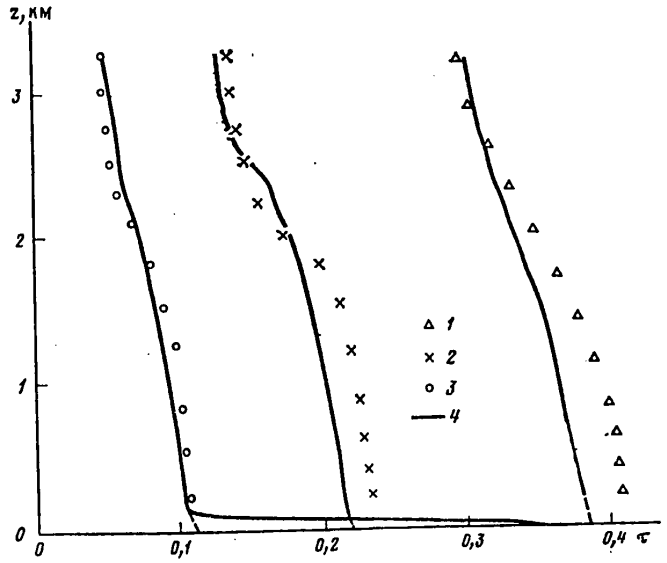

Figure 5. Comparison of airborne measurements of vertical profiles of aerosol optical thickness $\tau_\nu^a(z)$ (curves 1-3) with results of a remote determination of $\tau_\nu^a(z)$ on the basis of measurements of the brightness of the surface-atmosphere system in the 0.76 μm band (curves 4): 1. λ = 0.45 μm; 2. λ = 0.55 μm; 3. λ = 0.74 μm.

A more detailed explanation of the method and the results of its experimental testing are presented in [10,12], from which we took Figure 5, in which the results of airborne measurements of $\tau_\nu(\zeta)$ are compared with the results of the determination of $\tau_{\nu 0}(\zeta)$ with the help of this method. From Figure 5 it is obvious that the method insures the determination of the vertical $\tau_{\nu 0}(\zeta)$ profiles with adequate accuracy. The accuracy of the optimal extrapolation of $\tau_\nu(\zeta)$ into the short-wave area of the spectrum is completely satisfactory. Besides this, in the case under discussion of measurements made over a relatively intensively light-reflecting water surface, the delta-shaped component of the $\tau_{\nu 0}(\zeta)$ profile near the surface is distinguished quite clearly. This component describes the radiation that is reflected directly from the aqueous medium, and makes it possible to differentiate the brightness of the atmospheric haze and the brightness of the surface in the total measured brightness of the surface-atmosphere system.

On the basis of this method of allowing for atmospheric effects in the visible band of the spectrum, technical requirements were formulated for the MKS complex of measuring equipment, which was developed by specialists in the GDR and installed in the "Intercosmos-20" and "Intercosmos-21" satellites. Processed materials from the

satellite measurements confirmed the validity of this approach to the solution of the problem under discussion.

BIBLIOGRAPHY

1. Malkevich, M.S., "Opticheskiye issledovaniya atmosfery so sputnikov" [Optical Investigations of the Atmosphere From Satellites], Moscow, Izdatel'stvo "Nauka", 1973, 205 pp.

2. Basharinov, A.Ye., Gurvich, A.S., and Yegorov, S.G., "Radioizlucheniye Zemli kak planety" [Radio-Frequency Emissions of the Earth as a Planet], Moscow, Izdatel'stvo "Nauka", 1974, 188 pp.

3. Malkevich, M.S., Gorodetskiy, A.K., Orlov, A.P., Chavro, A.I., and Shukurov, A.Kh., "Integrated Method for Investigating Water Vapor's Contribution to Atmospheric Transmission in the 8-13 μm Transparency Windows," TR. GGO, No 369, 1976, pp 143-156.

4. Malkevich, M.S., and Petrenko, B.Z., "On the Effect of Aerosol Attenuation on the Accuracy of the Determination of the Ocean's and Atmosphere's Temperature by Remote Methods," IZV. AN SSSR. FIZIKA ATM. I OKEANA, Vol 14, No 7, 1978, pp 723-732.

5. Orlov, A.P., Badayev, V.V., Gorodetskiy, A.K., and Malkevich, M.S., "Airborne Investigations of Vertical Infrared Radiation Profiles in the 10-12 μm 'Window'," IZV. AN SSSR. FIZIKA ATM. I OKEANA, Vol 12, No 7, 1976, pp 711-719.

6. Malkevich, M.S., Istomina, L.G., and Khovis, V., "On the Transformation in the Atmosphere of Solar Radiation Reflected From the Ocean," IZV. AN SSSR, FIZIKA ATM. I OKEANA, Vol 13, No 1, 1977, pp 21-34.

7. Barnett, T.P., Patzert, W.C., Webb, S.C., and Bean, B.R., "Climatological Usefulness of Satellite-Determined Sea Surface Temperatures in the Tropical Pacific," BULL. AMER. METEOROL. SOC., Vol 60, No 3, 1979, pp 197-205.

8. Malkevich, M.S., "Some Estimates of the Accuracy and Reliability of the Remote Determination of the Ocean Surface's Temperature From Space," INFORM. BYULLETEN' SEMINARA "ATMOSFERA-OKEAN-KOSMOS" PRI GKNT SSSR, No 1, 1980, pp 47-69.

9. Gorodetskiy, A.K., "Method, Results and Error in Determining the Underlying Surface's Temperature From Measurements of Outgoing Radiation in the 10.5-11.5 μm Area of the Spectrum by the 'Kosmos-320' Satellite," in "Kosmicheskaya strela" [Space Arrow], Moscow, Izdatel'stvo "Nauka", 1974, pp 198-208.

10. Badayev, V.V., and Malkevich, M.S., "On the Possibility of Determining Vertical Aerosol Attenuation Profiles From Satellite Measurements of Reflected Radiation in the 0.76 μm Oxygen Band," IZV. AN SSSR. FIZIKA ATM. I OKEANA, Vol 14, No 10, 1978, pp 1022-1029.

11. Glushko, V.N., Ivanov, A.I., Livshits, G.Sh., and Fedulin, I.A., "Rasseyaniye infrakrasnogo izlucheniya v bezoblachnoy atmosfere" [Scattering of Infrared

Radiation in a Cloudless Atmosphere], Alma-Ata, Izdatel'stvo "Nauka", 1974, 210 pp.

12. Badayev, V.V., and Kozlov, Ye.M., "On Determining the Atmosphere's Optical Parameters From Measurements of Reflected Radiation in the 0.76 μm Oxygen Absorption Band," IZV. AN SSSR. FIZIKA ATM. I OKEANA, Vol 16, No 5, 1980, pp 542-545.

11746
CSO: 1866/10

UDC 551.46:629.7

ANALYSIS OF DATA FROM SYNCHRONOUS MEASUREMENTS MADE BY 'METEOR' ARTIFICIAL EARTH SATELLITE AND SHIPS NEAR EASTERN SHORE OF CASPIAN SEA

Moscow ISSLEDOVANIYE ZEMLI IZ KOSMOSA in Russian No 4, Jul-Aug 81 (manuscript received 25 Dec 80) pp 54-60

[Article by G.P. Vanyushin, V.N. Dyadyunov and S.M. Sazhin, All-Union Scientific Research Institute of Marine Fishing and Oceanography, Moscow, and State Scientific Research Center for the Study of Natural Resources, Moscow]

[Text] Along the eastern shore of the Caspian Sea in the area of the Mangyshlak Peninsula, a satellite experiment was conducted in September 1978 for the purpose of further refining the relationships between the distribution of hydrological and biological characteristics and the aqueous medium's brightness fields, as measured by a "Meteor" artificial Earth satellite. Satellite surveying of the range's water area was carried out on 22 September 1978, in four bands of the spectrum (0.5-0.6, 0.6-0.7, 0.7-0.8 and 0.8-1.1 μm), by an MSU-M scanning unit. Seagoing range measurements were made at the same time, by scientific groups from VNIRO [All-Union Scientific Research Institute of Marine Fishing and Oceanography] on two ships belonging to KaspNIRKh [probably Caspian Scientific Research Institute of Marine Fishing] (Astrakhan'); 26 hydrological stations were set up (Figure 1). The observation program included, in particular, the determination of: water temperature at the surface, relative transparency (in meters, using a (Sekki) disk), concentrations of chlorophyll A and inorganic matter suspended at the 0 meter level and a depth equal to half the relative transparency value for a given station. The basis for the selection of an unfixed depth for the second level was as follows:
the aqueous medium brightness values, as measured by the artificial Earth satellite, must be compared to shipboard measurement data obtained for a surface layer of the sea with approximately the same illumination level;
all other conditions being equal, the location of the upper maximum of the phytoplankton concentration depends on the distribution of the illumination levels with respect to depth [1,2], while a given distribution is closely related to the relative transparency value [3].

Thus, a second unfixed level makes it possible to obtain more reliable chlorophyll and phytoplankton concentration values for the layer of the aqueous medium that makes the decisive contribution to the formation of the water area image's brightness fields in the 0.5-0.8 μm section of the spectrum.

Processing of the multizonal data obtained by the "Meteor" satellite was carried out by a specialized, experimental computer complex at GosNITs IPR [State Scientific

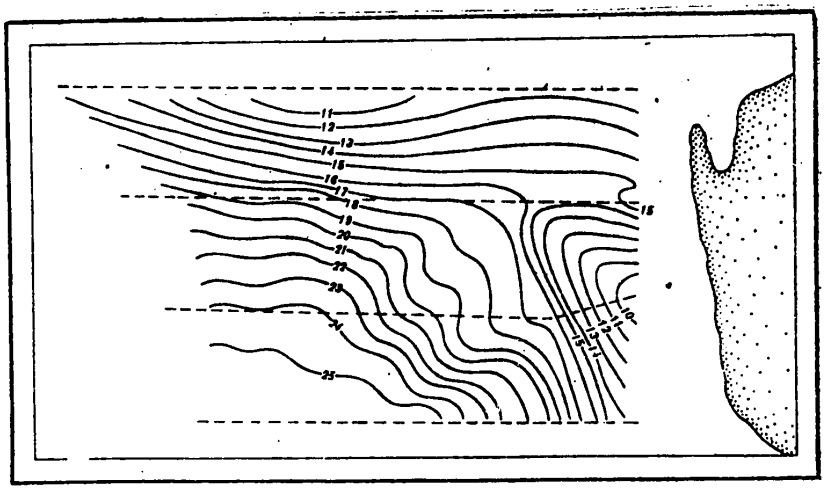

Figure 1. Bathymetric map of range, in meters (broken lines = hydrological profiles).

Research Center for the Study of Natural Resources]. The results of this processing were used to compile brightness distribution maps, using relative values (levels 0 to 255), in three spectral bands λ_1 (0.5-0.6 μm), λ_2 (0.6-0.7 μm) and λ_3 (0.7-0.8 μm) (Figure 2). The accuracy of the determination of the hydrological stations' locations on them was $\approx \pm 3.5$-5 km, allowing for errors in the map compilation technology and the ships' observations. Laboratory processing of samples for inorganic suspended matter and chlorophyll A was conducted with standard techniques, with the results for the two levels being averaged.

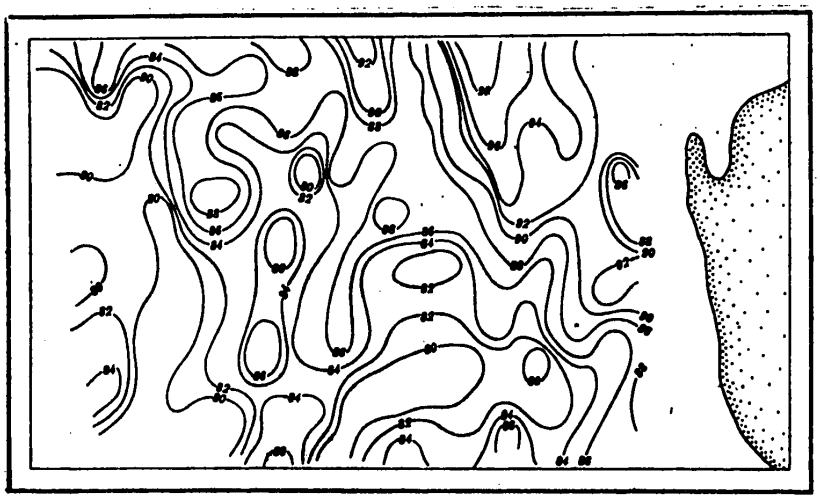

Figure 2. Map of distribution of aqueous medium brightness, in relative values, in the 0.5-0.6 μm spectral band.

The region where the experiment was conducted is a highly productive area of the Caspian Sea, which fact is related to the upwelling of rich biogenic elements from

the subsurface waters near the eastern shore [4]. Seagoing measurements of the water's surface temperature confirmed this. For instance, a drop in temperature from 20.4 to 19.4° C over a distance of about 8 km was registered in the coastal area of the range. The average concentrations of chlorophyll in the surface layer were 2.0-2.5 μg/ℓ. The water depth in the area where the work was done ranged from 10 to 26 m, while the bottom consisted of yellow-gray sand. with an admixture of shell, covered by a thin layer of dark gray silt. The distribution of relative transparency within the borders of the range turned out not to be related to depth. For example, values of 4-5 m were registered repeatedly at depths of 10, 14, 20, 24 and 26 m, while at the same time, relative transparency values of 7-11 m were noted at depths ranging from 10 to 20 m. The distribution of the aqueous medium's spectral brightness B_λ, as measured from the satellite, was also not directly related to bathymetric characteristics, as can be demonstrated for several areas in the range. Calculations made with data published in [3,5] show that the part of the light flow reflected from the bottom is less than 0.2 percent of the total flow actually reflected by the aqueous medium for the given relative transparency values, and for only two stations was the calculated effect of the bottom somewhat greater (0.7 percent). Therefore, any change in the aqueous medium's B_λ value can be regarded as being related to the distribution of the concentration of phytoplankton, inorganic suspended matter and other elements, the more so since the height of the waves during the experiment did not exceed 0.2-0.4 m for the shallow areas and 0.6-0.8 m for the deeper regions, while their length did not exceed 5 and 10 m, respectively, which (according to the data in [6]) does not cause vertical mixing down to the bottom.

During the comparison of the relative values of the aqueous medium's spectral brightness B_λ with the corresponding values of its relative transparency $Y_{rel\ tr}$ for the purpose of reducing the effect of random errors in the measurements of this characteristic, which can reach values of 10-15 percent of the registered value, grouping of the relative transparency's measured values was carried out and the average values of the aqueous medium's spectral brightness $\overline{B}_\lambda$ were computed for the separate groups; the results of these calculations are presented in Table 1.

Table 1. Average Values of $\overline{B}_\lambda$ of the Aqueous Medium in the Region of the Experiment for Different Relative Transparency Values

Границы значений относительной прозрачности в группе, м (1)	Среднее значение в группе, м (2)	$\overline{B}_\lambda$ в спектральных диапазонах (3)		
		λ_1	λ_2	λ_3
<3	2,5	93,3	83,7	40,3
3–5	4,0	87,1	63,0	38,7
5–7	5,4	85,3	59,9	40,8
7–11	10,2	84,0	59,0	42,5

Key:
1. Limits of relative transparency values in a group, m
2. Average value in group, m
3. B_λ in spectral bands

In connection with this, the correlation coefficient r of the average values of the aqueous medium's spectral brightness and the relative transparency's average values for spectral band λ_1 is $r_{\lambda_1} = 0.83$ and for band λ_2 it is $r_{\lambda_2} = 0.57$, while the corresponding regression equations have the form

$$Y_{rel\,tr.} = \overline{B}_{\lambda_1}/(2{,}98\,\overline{B}_{\lambda_1} - 240{,}07),\quad Y_{rel.\,tr.} = \overline{B}_{\lambda_2}/(1{,}03\,\overline{B}_{\lambda_2} - 51{,}8).$$

The results of the comparison are presented graphically in Figure 3.

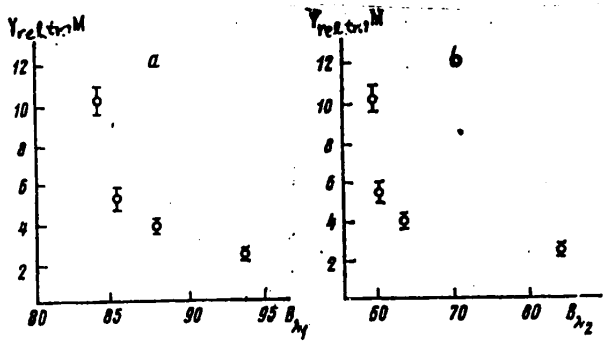

Figure 3. Relationship between values of aqueous medium's brightness in 0.5-0.6 μm (a) and 0.6-0.7 μm (b) spectral bands and relative transparency values.

As is obvious from the results of the comparison, for the region of the experiment the determination of the relative transparency values is more reliable when it is done with the data on the distribution of the aqueous medium's brightness in the λ_1 (0.5-0.6 μm) spectral band.

The next stage of the analysis of the results was a comparison of the values of B_{λ_1} and B_{λ_2} with the corresponding values for the concentration of inorganic suspended matter C_{ism}. In order to reduce the effect of random errors in C_{ism} on the results of the analysis, which can reach a level of 20 percent of the obtained value, analogous grouping of the data gathered on board the ships was carried out. The results of the comparison are presented in Table 2 and Figure 4.

Table 2. Average Values of $\overline{B}_\lambda$ of the Aqueous Medium in the Region of the Experiment for Different Concentrations of Inorganic Suspended Matter

Границы концентрации неорганической взвеси в группе, мг/л (1)	Среднее значение в группе, мг/л (2)	$\overline{B}_\lambda$ в спектральных диапазонах (3)	
		λ_1	λ_2
<1,0	0,8	87,4	60,6
1,0–2,5	1,6	85,4	63,0
2,5–5,0	4,4	89,0	83,0
>5,0	5,7	95,0	90,0

Key:
1. Limits of inorganic suspended matter concentration in group, mg/ℓ
2. Average value in group, mg/ℓ
3. $\overline{B}_\lambda$ in spectral bands

In connection with this, the following regression equations and correlation coefficients were obtained for spectral bands λ_1 and λ_2:

$$C_{ism}=-40{,}50+0{,}49\,B_{\lambda_1},\quad r_{\lambda_1}=0{,}77,\quad C_{ism}=-8{,}55+0{,}16\,B_{\lambda_2},\quad r_{\lambda_2}=0{,}99.$$

The results of the analysis show that the determination of the concentrations of inorganic suspended matter in the surface layer of the aqueous medium for the area of the experiment is more representative when it is done according to the data on the distribution of brightness in the 0.6-0.7 μm spectral band.

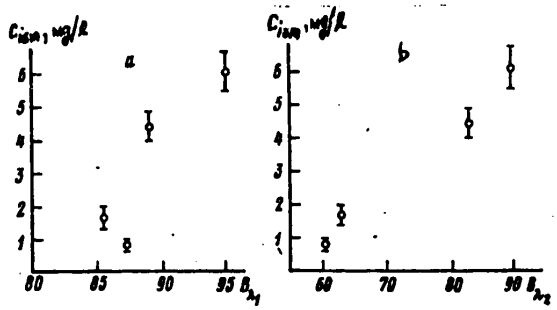

Figure 4. Relationship between values of aqueous medium's brightness in the 0.5-0.6 μm (a) and 0.6-0.7 μm (b) spectral bands and values of concentration of inorganic suspended matter.

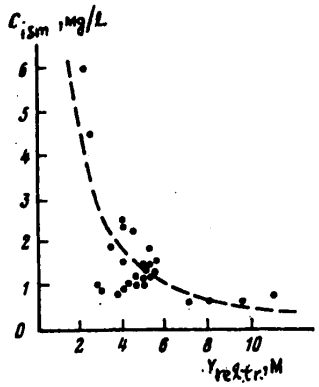

Figure 5. Dependence of values of inorganic suspended matter concentrations on relative transparency values, according to experimental data (points) and data from [10] (broken curve).

The results of the analysis showed that the brightness of the aqueous medium's image in the 0.5-0.6 μm spectral band correlates better with the relative transparency distribution, while in the 0.6-0.7 μm band it correlates better with the concentration of inorganic suspended matter. It is a well-known fact [7,8] that phytoplankton possesses greater reflectivity in the green area of the spectrum (0.5-0.6 μm) in comparison with the red area (0.6-0.7 μm), since the chlorophyll (A, B, C) and related compounds contained in it have several energy absorption maximums in this band of wavelengths. At the same time, the reflectivity of particles of inorganic suspended matter changes insignificantly in the 0.5-0.7 μm spectral band and its graph is in the form of a "plateau" [8,9]. On the average, for the region of the experiment the concentration of chlorophyll A in the water's surface layer is quite high ($\sim$ 2 μg/ℓ), so that the relative transparency values, which depend on both the concentration of inorganic suspended matter and the phytoplankton concentration are determined more reliably on the basis of space surveying data in the 0.5-0.6 μm spectral band, while the concentration of inorganic suspended matter is determined more reliably in the 0.6-0.7 μm band. Finally, the penetration of solar radiation into ocean waters (types I-III) is weaker in the 0.6-0.7 μm spectral band than in the 0.5-0.6 μm, although for highly productive coastal waters this difference is essentially smoothed out.

In the practice of interpreting space surveying materials, prior information about both of the parameters mentioned above is not always available, although a relationship between them has been established experimentally [10]. The results of the verification of the dependence of the values of the concentration of inorganic suspended matter on the relative transparency values that was obtained in [10] demonstrated the possibility of using it in the analysis of space data for the region of the experiment (Figure 5) when one of the parameters was not measured during the seagoing observations made beneath the satellite.

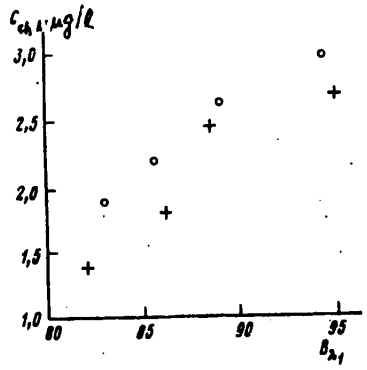

Figure 6. Relationship between values of the aqueous medium's brightness in the 0.5-0.6 μm spectral band and values of chlorophyll A concentrations in the surface layer, for regions with approximately identical concentrations of inorganic suspended matter: o represents $C_{ism} < 1.5$ mg/ℓ; + represents $C_{ism} \geq 1.5$ mg/ℓ.

A search for connections between an aqueous medium's B_λ value and the concentration of chlorophyll A ($C_{ch\ A}$) has been made by many investigators ([8,9,11-13], for example), but most of the results obtained from data gathered during airborne or helicopter measurements of an aqueous medium's B_λ value are, as a rule, for narrow bands of the spectrum. The authors set themselves the task of attempting to use for this purpose the ordinary satellite information received from the "Meteor" satellite for relatively broad bands of the spectrum ($\Delta\lambda = 0.1$ μm). For the given characteristics of the MSU-M scanning device's spectral surveying channels, in order to determine $C_{ch\ A}$ it is possible to use the 0.5-0.6 μm spectral band, in which the reflective properties of phytoplankton cells are most clearly manifested [8,9], while between the phytoplankton and chlorophyll A concentrations there exists a stable relationship [14]. However, a comparison of the aqueous medium's B_{λ_1} and $C_{ch\ A}$ values leads to positive results only when there is no inorganic suspended matter in the water or its concentration is low, as well as when the C_{ism} values in the surface layer are identical and the matter is distributed uniformly. In connection with this, the seagoing measurement data were used to divide the water area under investigation into two parts: the first with a suspended matter concentration $C_{ism} < 1.5$ mg/ℓ, the second with $C_{ism} \geq 1.5$ mg/ℓ. When this was done it was assumed that a change in B_{λ_1} in the segregated sections takes place because of differences in $C_{ch\ A}$.

Table 3. Dependence of Aqueous Medium's Spectral Brightness B_{λ_1} on Values of $C_{ch\ A}$ in Water Areas With Narrow Limits of Changes in C_{ism}

Границы осреднения относительных значений B_{λ_1} (1)	$C_{ism} < 1{,}5$ mg/ℓ		$C_{ism} \geq 1{,}5$ mg/ℓ	
	$\bar{B}_{\lambda_1}$	$\bar{C}_{ch\ A}$, μg/ℓ	$\bar{B}_{\lambda_1}$	$\bar{C}_{ch\ A}$, μg/ℓ
<84	82,8	1,90	82,0	1,40
85–87	85,5	2,20	86,2	1,80
88–90	89,0	2,65	88,5	2,50
>90	94,5	2,94	95,0	2,77

Key: 1. Limits of averaging of relative values of B_{λ_1}

The different areas were distinguished by four gradations, according to the measured values of B_{λ_1} (since the amount of initial data for each area was limited) and the average values of $C_{ch\ A}$ were computed for these gradations (here it is necessary to keep in mind the fact that the instrument accuracy alone in the determinations of $C_{ch\ A}$ is about ±15 percent of the measured value). The results of this analysis are presented in Table 3 and Figure 6.

The regression equation calculated from these data has the form

$$C_{ch\ A}=a+bB_{\lambda_1},$$

in connection with which r = 0.96, a = -33.3, b = 7.98 for C_{ism} < 1.5 mg/ℓ; r = = 0.91, a = -41.2, b = 9.67 for C_{ism} ⩾ 1.5 mg/ℓ.

For identical aqueous medium B_{λ_1} values, the points in the graph (Figure 6) with suspended matter concentration C_{ism} < 1.5 mg/ℓ have higher $C_{ch\ A}$ values, which indicates the correctness of the chosen methodological approach for processing data gathered by space surveying and synchronous seagoing observations.

The calculations that have been made are correct only for the area where the experiment was conducted. However, the proposed methodological approach to the analysis of materials from ship and satellite measurements can be used to process the results of analogous experiments. We should also mention here the possibility of using the 0.5-0.6 μm spectral band to detect highly productive regions in the ocean, utilizing available satellite information and allowing for the fact that changes in an aqueous medium's B_λ values in this band are more closely related (for open ocean waters) to changes in the concentration of biological elements, since the presence of particles of inorganic suspended matter in these waters is limited in comparison with coastal waters.

Finally, in connection with this it is also necessary to allow for the effect of the atmosphere on the radiation leaving the ocean [15,16], although for bodies of water that are small in area it can, in most cases, be provisionally assumed to be uniform and, consequently, all the changes in B_λ recorded for a given area can be attributed to the distributions of the oceanological and commercial biological characteristics of the aqueous medium.

BIBLIOGRAPHY

1. Moiseyev, P.A., "Biologicheskiye resursy Mirovogo okeana" [Biological Resources of the World Ocean], Moscow, 1969, 338 pp.

2. "Biologiya okeana" [Biology of the Ocean], Moscow, Izdatel'stvo "Nauka", Vol 1, 1977, 398 pp.

3. Yerlov, N.G., "Optika morya" [Optics of the Sea], Leningrad, Izdatel'stvo "Gidrometeoizdat", 1980, 247 pp.

4. Kosarev, A.N., "Gidrologiya Kaspiyskogo i Aral'skogo morey" [Hydrology of the Caspian and Aral Seas], Moscow, Izdatel'stvo MGU [Moscow State University], 1975, 273 pp.

5. Man'kovskiy, V.I., "The Relationship Between the Depth of Visibility of a White Disk and the Radiation Attenuation Factor for Ocean Waters," in "Opticheskiye metody izucheniya okeanov i vnutrennikh vodoyemov" [Optical Methods for Studying Oceans and Inland Water Areas], Novosibirsk, Izdatel'stvo "Nauka", 1979, pp 100-106.

6. Zhukov, L.A., "Obshchaya okeanologiya" [General Oceanography], Leningrad, Izdatel'stvo "Gidrometeoizdat", 1976, 376 pp.

7. Gurinovich, G.P., Sevchenko, A.N., and Solov'yev, K.N., "Spektroskopiya khlorofilla i rodstvennykh soyedineniy [Spectroscopy of Chlorophyll and Related Compounds], Minsk, Izdatel'stvo "Nauka i Tekhnika", 1968, 520 pp.

8. "Manual of Remote Sensing," Washington, American Society of Photogrammetry, Vol 2, 1975, 1,756 pp.

9. Pelevin, V.N., "Evaluating the Concentration of Suspended Matter and Chlorophyll in the Sea on the Basis of the Spectrum of Outgoing Radiation as Measured From a Helicopter," OKEANOLOGIYA, Vol 18, No 3, 1978, pp 428-434.

10. Skopintsev, B.A., "On the Coagulation of a Fluvial Discharge's Terrigenous Suspended Particles in Sea Water," IZV. AN SSSR. GEOGRAF. I GEOFIZ., Vol 10, No 4, 1946, pp 357-371.

11. Clarke, G.L., Ewing, G.C., and Lorenzen, C.L., "Spectra of Back-Scattered Light From the Sea, Obtained With an Aircraft, as a Measure of Chlorophyll Concentration," SCIENCE, Vol 167, No 3921, 1970, pp 1119-1121.

12. Szekielda, K.H., "Observations of Suspended Material From Spacecraft Altitudes," Hamburg, Deutsches Hydrographisches Institut, Heft 4, 1974, pp 159-170.

13. Viollier, M., Deschamps, P.Y., and Lecomte, P., "Airborne Remote Sensing of Chlorophyll Content Under Cloudy Sky as Applied to the Tropical Waters in the Gulf of Guinea," REMOTE SENSING OF ENVIRONMENT, Vol 7, No 3, 1978, pp 235-248.

14. Koblents-Mishke, O.I., and Vedernikov, V.I., "Primary Production," in "Biologiya okeana" [Biology of the Ocean], Moscow, Izdatel'stvo "Nauka", Vol 2, 1977, pp 183-208.

15. Malkevich, M.S., "Allowing for the Atmosphere When Studying the Earth's Natural Resources From Space," in "Kosmicheskiye issledovaniya zemnykh resursov" [Space Investigations of the Earth's Resources], Moscow, Izdatel'stvo "Nauka", 1976, pp 110-130.

16. Burenkov, V.I., Gurevich, I.Ya., Kopelevich, O.V., and Shifrin, K.S., "Brightness Spectra of Outgoing Radiation and Changes in Them as the Observation Altitude Changes," in "Opticheskiye metody izucheniya okeanov i vnutrennikh vodoyemov", Novosibirsk, Izdatel'stvo "Nauka", 1979, pp 41-58.

11746
CSO: 1866/10

UDC 551.46.0:629.78

EXPERIMENT IN USING VIDEOINFORMATION FROM 'METEOR' SATELLITES TO INVESTIGATE OCEANIC PHENOMENA

Moscow ISSLEDOVANIYE ZEMLI IZ KOSMOSA in Russian No 6, Nov-Dec 81 (manuscript received 21 Apr 81) pp 48-57

[Article by A.S. Kaz'min and V.Ye. Sklyarov, Institute of Oceanology imeni P.P. Shirshov, USSR Academy of Sciences, Moscow]

[Text] In recent years, the quality of the space information received from satellites in the "Meteor" series has improved considerably. The scanning equipment installed in them (MSU-S [multispectral scanning unit with medium resolution]) makes it possible to obtain images in the visible (0.5-0.7 μm) and near-infrared (0.7-1.1 μm) bands of the spectrum with spatial resolution that is sufficiently high for the solution of a number of problems related to the investigation of the ocean (about 250 m). An analysis of images obtained with the MSU-S scanner in 1980 confirmed the possibility of using such information in the practice of oceanological research. However, limitations related to the observation conditions do not always make it possible to obtain informative images in the visible band. Our analysis of a large number of images obtained with the MSU-S and MSU-M [multispectral scanning unit with low resolution] (with lower spatial resolution) scanners, photographs of the ocean's surface taken by cosmonauts on the "Salyut-6" station, and images and photographs taken from American space vehicles ("Skylab," the "Landsat" ISZ [artificial Earth satellite]) enabled us to reach the following conclusions: 1. As a rule, the depiction in space images of dynamic processes in the ocean (fronts, eddies, current boundaries and meanders, traces of internal waves and so on) takes place under rigorously defined conditions that are related to sighting angles, Sun height and the hydrometeorological situation. 2. Features of the ocean surface's dynamics are seen most clearly in areas where sunlight is reflected; that is, under conditions of a mirror (or close to it) reflection of solar rays. 3. The effect of "visibility" of dynamic processes is caused by modulation of the high-frequency component of wind-caused wave action in a field of currents, which creates contrasts in the roughness of the water surface and corresponding contrasts in the field of reflected solar radiation registered in photographs and images.

Below we discuss specific examples of the investigation of oceanological phenomena in the western part of the Pacific Ocean and in the Mediterranean Sea, using images from "Meteor" ISZ's and other types of space information.

Eddies in Currents. At the present time, remote methods are being used extensively to investigate eddy formations in the ocean, with the primary emphasis being on

synoptic eddies and current rings. Images obtained with the help of ISZ's also make it possible to investigate smaller eddies (20-50 km) that exist in current flows near their frontal limits [1]. This type of eddy (only cyclonic ones have been detected so far) apparently plays an important role in the formation of the thermohaline structure of frontal zones, although their structure and generation mechanism have not yet been studied thoroughly enough. In our opinion, each new case of the discovery of such phenomena deserves attention. The study of the processes of eddy formation in the regions of the most intensive energy exchange between the ocean and the atmosphere--particularly in the zone of convergence of the (Oyyasio) and (Kurosio) Currents--is especially important. Remote monitoring of the location of meanders and eddies in this region can create a real basis for predicting heat advection in the northwest part of the Pacific Ocean and, as a consequence, for predicting ice formation in the Sea of Okhotsk and weather in the eastern regions of the USSR.

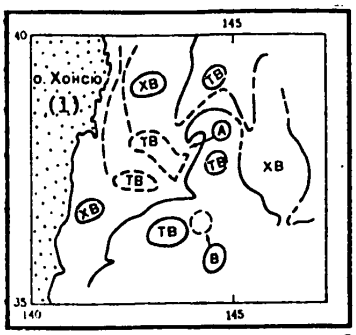

Figure 2. Thermal structure of the ocean's surface in the zone of convergence of the Kurosio and Oyyasio Currents, based on data gathered by the NOAA-6 ISZ on 5-6 June 1980: TB = warm waters of the Kurosio Current; XB = cold waters of the Oyyasio Current; solid lines = location of sharp temperature gradients; dotted lines = location of weak temperature gradients; A, B = location of cyclonic eddies.
Key: 1. Honshu Island

In June 1980, an MSU-S sensor ("Meteor" ISZ, 0.7-1.1 μm band) was used to obtain an image of a section of the Pacific Ocean's surface to the east of the island of Honshu in the zone of convergence of the Kurosio and Oyyasio Currents (Figure 1 [not included]). In it are clearly visible two eddy formations of a cyclonic nature, designated in Figure 1 as eddies "A" and "B." The central part of eddy "A" has approximate coordinates of 37.5-38° N.Lat. and 144.5° E.Long. The center of eddy "B," which is partially obscured by clouds, is 150-200 km to the south (36-36.5° N.Lat.) and is located at 144° E.Long. Our experience in analyzing space images in the visible band of the spectrum enables us to categorize these eddy formations as oceanic rather than atmospheric phenomena. The central part of eddy "A" is 40-50 km in diameter and the nucleus of eddy "B" is also about 50 km in diameter. The diameter of the entire area of water involved in the eddy motion is about 80-100 km for both eddies. Here it is appropriate to point out that images in the visible band of the spectrum reflect the surface manifestations of dynamic processes, whereas infrared data record temperature irregularities on the surface (which are, as a rule, a result of the dynamic processes), so that evaluations of the eddies' parameters on the basis of these two sources do not have to coincide. Moreover, in the case of weak temperature gradients or the absence of them, eddy formations (particularly small-scale ones) may possibly not appear in infrared images.

In order to obtain additional information on the location of the frontal limits in the convergence zone of the Kurosio and Oyyasio Currents, we utilized infrared images (in the 10.5-11.5 μm band) that were obtained with the NOAA-6 and "Tiros" satellites in the time period under discussion. An analysis of the thermal structure

of a section of the surface to the east of Honshu Island, based on data gathered by the NOAA-6 ISZ on 5-6 June 1980 (Figure 2), shows that cyclonic eddy "A" is also manifested quite clearly on the infrared image. This is a boundary eddy ("bridge," according to the terminology used in [1]) that is located at the frontal limit formed by a quasistationary, anticyclonic meander of the Kurosio that exists in this area and the Oyyasio's cold waters. Eddy "B" cannot be identified unambiguously on the basis of infrared data. Its central part, as follows from a comparison of Figures 1 and 2, is displaced somewhat to the southeast of the frontal limit. Thus, eddy "B" is located directly in the flow of the Kurosio Current, in thermally more homogeneous waters, which may be the cause of its absence in the infrared image. However, the question of whether eddy "B" formed on the frontal limit and was then displaced into the Kurosio's flow where it lost its thermal nonuniformity or formed directly in the current flow remains open. The high quality of the image produced by the MSU-S scanner (Figure 1) makes it possible to establish that there are substantial differences in the structures of eddies "A" and "B" that are presumably related to their different locations relative to the frontal limit. Eddy "A" consists of two separate and clearly distinguishable (by tone) spiral-shaped elements, with one being curled cylonically relative to the other. The light-colored spiral, which is 2-10 km wide in the eddy's nucleus and then expands fanwise in the area of the Oyyasio's waters, apparently consists of the Oyyasio's cold waters that have been drawn into eddy-type motion. The dark section of the eddy can be interpreted as warm waters of the Kurosio that have been cut off from the main flow. Eddy "B" is considerably more isotropic in structure, and appears as a set of spiral, threadlike white bands, about 1 km wide, that are curled toward the center.

In the image under discussion (Figure 1), the characteristic shape of the cloud cover, in the form of thin (1-3 km wide) bands of cumulus clouds, draws attention to itself. A comparison of these strips of cloud with the location of the Kurosio's anticyclonic meander (Figure 2) makes it possible to conclude that they formed and are located along the front separating the Kurosio's warm waters (the meander) from the Oyyasio's cold ones. Thus, bands of clouds of this type (which are also seen in other regions) can serve as an additional identifying feature for fronts in the ocean when data in the visible band of the spectrum are being used.

At the present time there is evidence that eddy formations such as the ones discussed above are a typical and permanent feature of the zone of convergence of the Kurosio and Oyyasio Currents [2]. In particular, in [2]--based on infrared data from NOAA satellites--it is mentioned that such eddies (friction eddies, as they are called in [2]) are seen very frequently to the east of Capes Inubo, Kurosaki and Erimo, and it is also pointed out that they are frequently situated one behind another as a pair of eddies on one "slope" of a meander. We, however, do not know of any examples of the analysis of this phenomenon utilizing information in the visible band of the spectrum.

Local Fronts. Above we discussed an example of the interpretation of space images of the front zone of large oceanic currents. Using remote methods it is also possible to investigate fronts in coastal areas and inland seas. The infrared images used for this purpose make it possible to obtain detailed pictures of the location of thermal fronts. A successful example of an investigation of this type is the map of thermal fronts and related phenomena in the Mediterranean Sea that was constructed in [3] from VHRR radiometer data (ISZ NOAA-5) for a period of 2 years (1977-1979). Fronts of this type can also appear in images in the visible band, since along the

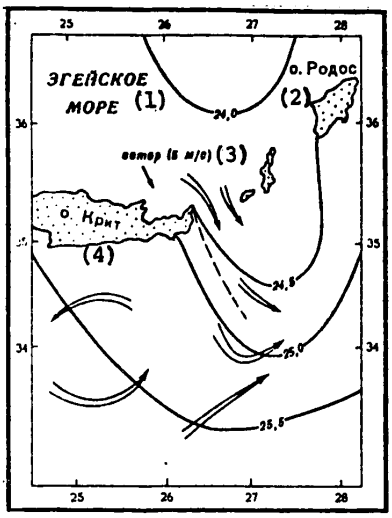

Figure 4. Hydrological conditions in the area depicted in Figure 3: solid lines = isotherms; arrows = direction of currents; dotted line = average location of front, according to infrared data from the "Tiros" ISZ on 22-25 June 1980.

Key: 1. Aegean Sea
2. Rhodes
3. Wind (5 m/s)
4. Crete

front there is usually an accumulation of surface-active films that damp the high-frequency components of the wave action, which results in the appearance of contrasts in the roughness and corresponding contrasts in the field of reflected solar radiation. An example of this is the image of the Aegean Sea and the region around the islands in the Cretan arc that was obtained on 26 June 1980 with an MSU-S scanner ("Meteor" ISZ, 0.5-0.7 μm band) (Figure 3 [not included]). A white band stretching to the southeast from the eastern end of Crete is quite visible in the picture. It represents the frontal boundary between the relatively cold waters of the Aegean Sea, flowing out of the Kasos Strait, and the warmer waters in the central part of the Mediterranean Sea. The Aegean Sea's colder waters flow into the Levantine Sea during the summer under the influence of the prevailing northwest winds; this shows up quite clearly in the average multiyear distribution of surface temperature during the summer period [4] (Figure 4). As additional information confirming that the observed phenomenon is a thermal front, we used infrared images of this region that were obtained with the "Tiros" satellite during the period under discussion. The contrast between the colder waters of the Aegean Sea, flowing out of the Kasos Strait, and the warm waters along the southern coast of Crete is quite noticeable. According to "Tiros" data gathered on 22-25 June 1980, the average location of the front was as shown in Figure 4. The existence of a Cretan front during the warm part of the year is also confirmed by the results of work [3], which has already been mentioned. Observations made on board ships also show that thermal fronts are encountered frequently in the eastern part of the Mediterranean Sea during the summer, and that they have the following characteristics: width--2-10 km; temperature gradient--2-5.8° [5]. In the image under discussion (Figure 3), by its structure and contrasts (a narrow, long band of white against a dark-gray background) we easily distinguish the front from the bright white elongated spots that are adjacent to it and that represent the screening effect of the island of Crete (see below). The front is 1-5 km wide and it reaches 80-100 km in length.

Screening Effect of Islands ("Wind Shadows"). Islands located in the path of a wind current reduce wind velocity and acceleration distance, which leads to the formation on the leeward side of relatively calm areas with low wind altitudes. The contrasts that appear in the mean-square slope of the ocean surface create contrasts in the field of reflected solar radiation and can be recorded by remote methods. In [6] the authors investigate the "wind shadows" of the Antilles Islands (Caribbean Sea) on the basis of data gathered with a VHRR radiometer (NOAA-2 ISZ, 0.6-0.7 μm band).

In the images they observed light-colored bands corresponding to calm areas with a high reflection factor that reach from the leeward side of the islands, in the direction of the wind flow, to distances of up to 200 km. An analogous phenomenon is seen in images of the Aegean Sea (Figures 3 and 5 [not included]) obtained with the MSU-S equipment on a "Meteor" satellite. Particularly clear "wind shadows" from the numerous islands in the Aegean Sea, in the form of bright wide bands elongated in the direction of the wind, appear on the image obtained on 26 June 1980 (Figure 3). It should be mentioned here that these zones of relatively quiet surface appear to be brighter than the surrounding background in the central part of the flashing area. On the edges of the patch of sunlight, however, they are darker than the background. This effect is quite visible in Figure 5. The phenomenon of a change in the contrast sign of calm sections of the sea's surface relative to the background as the distance from the central part of the flashing zone increases was also noted in [6]. It is necessary to keep in mind the fact that in Figures 3 and 5 only the general direction of the wind is indicated (from meteorological data), whereas the "wind shadows" reflect the local wind field structure, which has considerable spatial variability in a region with such a nonuniform underlying surface. In connection with this, noncorrespondence of the directions of "wind shadows" to the prevailing wind direction is seen in some cases. Thus, space images such as this make it possible to study the detailed structure of the wind field in contrast to meteorological maps, which give only the general direction of wind flows. The wind velocity during the periods of the surveys was 5-7 m/s. The extent of the zones of the islands' screening effect varies from 20 to 80 km and is apparently related to the height the islands reach above sea level and their width, which is confirmed by the irregular structure of Crete's "wind shadow" (Figure 3): the longest and most contrasting sections correspond to the highest points on the island, while the breaks between them are explained by the penetration of wind flows through depressions in the relief.

Internal Waves. Visible manifestations of internal waves on the ocean's surface (alternating bands with different degrees of roughness that are seen when winds are weak or moderate) can be caused by two different mechanisms [7,8], the essence of which is periodic modulation of the short-wave component of wind-caused wave action in a field of currents excited by progressive internal waves. Different reflection conditions in the bands create contrasts in the field of reflected solar radiation, which is also the physical basis for the remote registration of internal waves that was carried out successfully by the "Skylab" space laboratory [9], the "Landsat-1" and "Landsat-2" ISZ's [10-12], the DMSP [15] [sic] and airplanes [11]. The results of multispectral surveying from the "Soyuz-22" spacecraft and the "Salyut-6" orbital station, as well as images obtained with the "Meteor" ISZ's, also confirm that, under certain conditions, internal waves are observed on the ocean's surface. Data in the literature and materials available to us show that traces of internal waves are manifested most clearly in areas where there are patches of sunlight, it being the case that the sign of the contrast in the bands relative to the background changes from the center of the patch to its edges. In a number of works, space images have been used to investigate internal waves. We will only point out the most detailed of these investigations [10-12], in which a number of conclusions are reached about the basic parameters and reasons for the generation of internal waves, observable from space, near the Atlantic coast of the United States, the eastern and western shores of Africa, and the Gulf of Mexico and the Caribbean Sea.

Information about internal waves that is obtained in space can be used to investigate the spatial variability of their parameters. As an example, we analyzed images

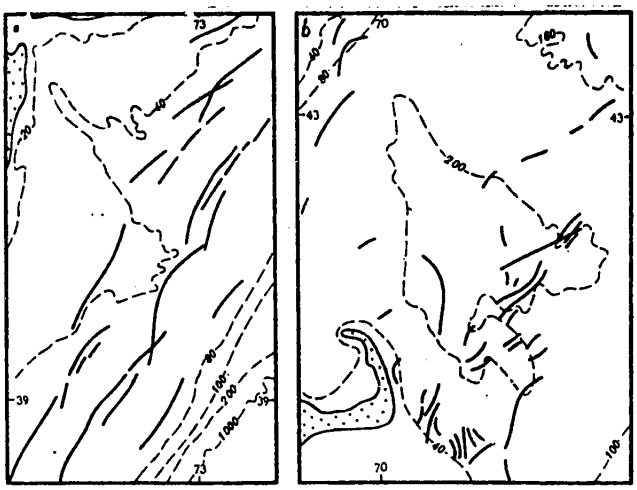

Figure 6. Traces of internal waves on a section of the open shelf (a) and in the Gulf of Maine (b), based on data gathered by the ERTS-1 ISZ in July 1973 and July 1974, respectively. The location of frontal waves, in packets, is noted.

of the traces of internal waves (54 packets) along the eastern coast of the United States during the period 1972-1974, as published in atlas [12]. Two regions are singled out, according to the nature of the relationship of the traces of internal waves with the morphometric conditions: 1) a section of open shelf from Cape Hatteras to Cape Cod, with an average bottom slope of 0.001 (in this section almost all the internal waves propagate in the direction toward the wind and their tracks are parallel to the depth contours (Figure 6a)); 2) the Gulf of Maine, which is a water area with depths of about 200 m, enclosed by slopes with a bottom slope of 0.01-0.02 and separated from the open ocean by the shallow-water Georges and Browns Banks (the basic tidal influx enters the gulf through the narrow Eastern Channel, where a considerably more complicated pattern of internal wave orientation is seen (Figure 6b)). The results of calculations (generalized in the table on the next page) indicate that the internal waves in these two areas have substantially different parameters. This example shows that in the future, remote data can be used to find relationships between the parameters of internal waves and the background conditions and to carry out the corresponding zoning of the ocean.

The investigations mentioned above are concerned primarily with internal waves in the ocean and boundary seas, the generation of which is related to the interaction between the tidal wave and irregularities in the bottom. Considerably more rarely do we see reports on the registration of traces of internal waves in closed seas, where their origin is not related to tides, but to other (and nonperiodic) causes. In this respect, the image obtained on 1 July 1980 with an MSU-S scanner (Figure 5) is of considerable interest. In it we can see a complex pattern of internal wave tracks in the central part of the Mediterranean Sea, in the region of the islands in the Cretan arc. Internal waves were recorded on images in both bands, but the pattern can be seen more clearly in the near-infrared band (0.7-1.1 μm). The interpretation of the observed phenomena and the hydrometeorological situation are presented in Figure 7. Judging by the curvature of the bands in the area most remote from the islands, we are observing propagation of progressive internal waves from the

Average Parameters of Internal Waves in an Area of Open Shelf (From Cape Hatteras to Cape Cod) and the Gulf of Maine

Parameters	Open Shelf From Cape Hatteras to Cape Cod	Gulf of Maine
Length of Frontal Wave	780 m	1,070 m
	350-1,500 m	400-2,500 m
Average Length of Wave in a Packet	685 m	865 m
	350-1,500 m	250-2,000 m
Distance Between Packets	16 km	43 km
	10-40 km	40-60 km
Width of Packet	5 km	6.3 km
	2-12 km	2-12 km

Note: Upper figures = average value; lower figures = limits of change of the parameter.

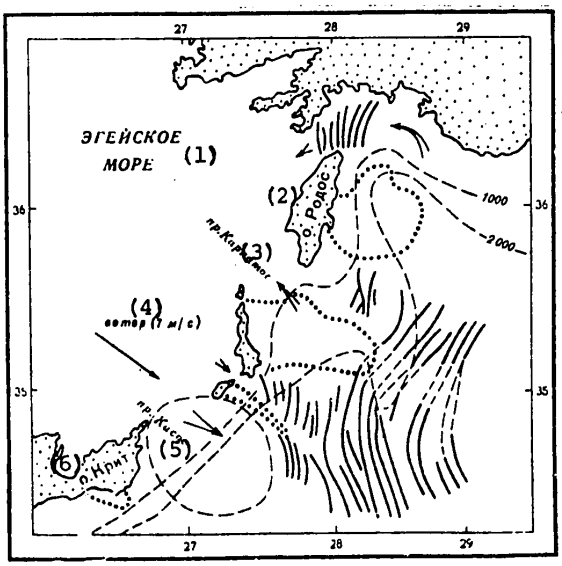

Figure 7. Interpretation of phenomena observed on the image obtained on 1 July 1980 (Figure 5): solid lines = = location of internal wave tracks; broken lines = depth contours; points = boundaries of "wind shadows"; 1. [sic] area of disruption of internal waves; arrows = direction of currents in straits.
Key: 1. Aegean Sea
2. Rhodes
3. Karpathos Strait
4. Wind (7 m/s)
5. Kasos Strait
6. Crete

southeast--the central part of the Mediterranean Sea--in the direction of the islands in the Cretan Arc. The absence in this part of the sea of strong tidal currents, as well as the fact that a large part of the observed waves are found above depths of more than 2,000 m, indicates that in this case their generation is not related to interaction between the tidal flow and irregularities in the bottom. In contrast to an ocean shelf, where internal waves are propagated as packets that are 3-5 km wide and 15-30 km apart (the result of periodicity of the tidal flow) [10-11] (see Figure 6a), in this region we do not see separate packets, but a field of internal wave tracks up to 250 km wide (from the Rhodes Strait to Kasos Strait) that stretch for 100-150 km in the southeasterly direction, into the open part of the sea. The waves are 5-6 km long in the area most remote from the islands; but diminish to 2-2.5 km in length as they near the islands, which may be related to the lessening of the depths near the islands. The internal waves are about 3 km long in the Rhodes Strait. In the image under discussion we observe an interesting example of a change in the form of the tracks of internal waves acted upon by a surface current moving from Kasos Strait into the Levantine Sea, the existence of which current is confirmed by both average multiyear hydrological data [4] and meteorological data on the wind's direction during the period of the survey (see Figure 7). In the image (Figure 5) it is clearly obvious that in the zone of action of the current moving in the direction

opposite to that of internal wave propagation the bands are convex and turned toward the direction of the current, in contrast to the rear part of the wave field where the internal waves' tracks are curved in the direction of their propagation; that is, in the direction opposite to that of the current. Along the current's boundary, which can be determined from the boundary of the area of Kasos Island's screening effect (the light-colored band leading away from the island on its leeward side), there is compression of the internal waves' traces; that is, their length is reduced. In the central part of the Kasos Strait, where the counterflow is maximal, the bands lose their orderly structure and it can be assumed that this is an area of dissipation of the internal waves.

Conclusions. 1. In a number of examples that are also of independent interest, we have demonstrated the possibility of the successful utilization of images in the visible and near-infrared bands of the spectrum, as obtained with the help of ISZ's of the "Meteor" series, in oceanological research. 2. The high spatial resolution of the MSU-S equipment makes it possible, in a number of cases, to obtain more detailed information about the structure of dynamic formations in the ocean than can be derived from infrared data. 3. In order to increase the effectiveness of the utilization of videoinformation from the "Meteor" ISZ's in oceanological practice, the choice of orbits and the planning of the surveys should be done in such a manner as to cover sections of the sea's surface with patches of sunlight as frequently as possible (and this is fully realizable). In order to record surface manifestations of dynamic processes in the ocean that appear in these patches, channels in the spectral band from 0.6 to 1 μm are the most effective. When surveying outside a patch of sunlight, the choice of the optimum bands depends to a considerable degree on the specific problem and requires special consideration.

BIBLIOGRAPHY

1. Sklyarov, V.Ye., and Fedorov, K.N., "Three-Dimensional Structure of the Gulf Stream's Frontal Zone, as Determined From Synchronous Ship and Satellite Data," ISSLEDOVANIYE ZEMLI IZ KOSMOSA, No 3, 1980, pp 5-13.

2. Bulatov, N.V., "Eddy Structure of a Sub-Arctic Front in the Northwestern Part of the Pacific Ocean," UCH. ZAP. LGU. SER. GEOGR. NAUK, No 27, 1980, pp 61-72.

3. Philippe, Michele, "Fronts thèrmiques en Mèdeterraneè d'aprés les donnèes du radiomeytre du satellite NOAA5 (Septembre 1977-Fevrier 1979)," C. R. ACAD. SCI. PARIS, Series B, No 291, 1980, pp 43-46.

4. Ovchinnikov, I.M., et al., "Gidrologiya Sredizemnogo morya" [Hydrology of the Mediterranean Sea], edited by V.A. Burkov, Leningrad, Izdatel'stvo "Gidrometeoizdat", 1976, 376 pp.

5. Levine, E.R., and White, W.B., "Thermal Frontal Zones in the Eastern Mediterranean Sea," J. GEOPHYS. RES., Vol 77, No 6, 1972, pp 1081-1086.

6. Strong, A.E., DeRycke, R.J., and Stumpf, H.G., "Extensive Areas of Reduced Waves Leeward of the Lesser Antilles," GEOPHYS. RES. LETT., Vol 1, No 1, 1974, pp 47-49.

7. Ewing, G., "Slicks, Surface Films and Internal Waves," J. MAR. RES., Vol 9, 1950, p 161.

8. Gargett, A.E., and Hughes, B.A., "On the Interaction of Surface and Internal Waves," J. FLUID MECH., Vol 52, No 1, 1972, pp 179-191.

9. Diets, R.S., "The Oceans From the Skylab-4," SEA FRONTIERS, Vol 20, No 6, 1974, pp 359-363.

10. Apel, J.R., et al., "Observations of Oceanic Internal Waves From the Earth Resources Technology Satellite," J. GEOPHYS. RES., Vol 80, No 6, 1975, pp 865-881.

11. Apel, J.R., et al., "A Study of Oceanic Internal Waves Using Satellite Imagery and Ship Data," REMOTE SENS. ENVIRON., Vol 5, 1976, pp 125-135.

12. Sawyer, C., and Apel, J.R., "Satellite Images of Internal Wave Signatures," Miami, Florida, Atlantic Oceanographic and Meteorological Lab., 1976.

13. Fett, R., and Rabe, K., "Satellite Observation of Internal Wave Refraction in the South China Sea," GEOPHYS. RES. LETT., Vol 4, No 5, 1977, pp 189-191.

11746
CSO: 1866/36

UDC 528.727

GEOMETRIC CORRECTION OF SCANNER PHOTOGRAPHS OF THE EARTH'S SURFACE

Moscow ISSLEDOVANIYE ZEMLI IZ KOSMOSA in Russian No 4, Jul-Aug 81 (manuscript received 31 Jul 80) pp 96-103

[Article by V.I. Khizhnichenko]

[Text] Space television systems installed in artificial Earth satellites produce multispectral photographs of the Earth's surface that make it possible to solve a number of important national economic problems related to the study of natural resources, it being the case that systems of the scanning type are some of the most promising ones [1]. The solution of these problems at the level required by modern consumers is possible only if there is a substantial improvement in the accuracy characteristics of space photographs, particularly their geometric accuracy. However, a number of factors that affect different parts of a system [2] prevent this, which results in the necessity of special ground processing of these photographs with the help of analog or digital computer facilities.

The digital processing of space photographs [3] is being done on an ever broader scale because of its inherent flexibility and high accuracy. In order to solve the problems that have been formulated, a high degree of practicality in obtaining, processing and recording the video information photographically is another extremely important condition. Therefore, the problem of developing special geometric correction algorithms that would be optimal from the viewpoint of minimum time consumption has acquired a particular degree of urgency. Such algorithms realize the recalculation of the coordinates of an image's elements on the basis of special mathematical expressions, with subsequent forwarding (or more complex processing) of the brightness codes. Temporal optimization is possible primarily through simplification of the mathematical expressions for recalculating the coordinates.

Two approaches are possible in this matter. The first of them is widely used in the United States [3], the FRG [4] and other countries to process "Landsat" system photographs, and consists of a polynomial approximation (usually of no higher than the fifth order) of the expressions mentioned above. The polynomials' coefficients are found on the basis of processing the results of the measurement of the locations of identified objects (reference points). In order to look for and identify references points it is necessary to have special templates and precision optico-mechanical devices. The time expended on searching for and identifying reference points in a photograph depends to a considerable degree on the qualifications of the people doing it. For these reasons, processing of the photographs on an operational basis may not be achievable.

The second approach consists of constructing a mathematical model of the scanner survey that takes into consideration only the effect of the weightiest distorting factors. Even in the case of simplified models ([4-6], for example), however, the set of equations of motion of the scanning and recording beams gives inexplicit relationships for recalculating coordinates, which leads to the necessity of looking for a solution iteratively, with the help of a computer [6]. Substantial time consumption, which can have a negative effect on the operational nature of the processing, is possible in connection with this approach.

However, within the framework of the second approach it is possible to construct a special type of survey model in which the distorting factors that have been distinguished are small, which is typical of the existing and more promising systems for studying natural resources. The author of [2] proposes such a model that makes it possible to find the desired relationships, in explicit form, as an exponential series expansion with respect to small distorting factors and subsequent truncation of the series. He also demonstrates that a linear approximation is frequently sufficient for existing and prospective systems. The explicit nature of the relationships that are obtained eliminates the need for the utilization of iterative methods, which saves substantial amounts of time. Further saving of time is possible if the proposed technique is used only to calculate the nodal points of some rectangular network, while the intermediate coordinates are obtained with the help of algorithms of the bilinear interpolation type as the photographs are being processed.

In this article, on the basis of an approximate solution of the system of equations for the special scanner survey model mentioned above, we have derived expressions for recalculating the coordinates of an image's elements for a scanner with plane scanning. These expressions were used to calculate the coordinate networks for nodal points that are needed in the processing of photographs with the help of the correction algorithm explained in [6], and are oriented toward the storage of the information about an interpreted photograph on a magnetic disk, which makes it possible to realize two-dimensional correction of distortions. Further, there is a description of the processing of two photographs of the Earth obtained by one of the "Meteor"-series satellites in 1977 and 1978, as well as an analysis of the improvement in the accuracy characteristics of the photographs that has been achieved.

Expressions for Converting Image Element Line and Column Numbers. As was pointed out above, in [2] the author presents a geometric model of a scanner survey. The equations of motion presented for the scanning and photographic recording beams were solved in a linear approximation of relatively small distorting factors of a deterministic and random nature, for the purpose of finding the dependences of the distorted geocentric coordinates α' and β', as measured in a photograph, on the true coordinates, as read from the ox_0 axis of the orbital system of coordinates $ox_0y_0z_0$ (Figure 1), which is fixed at the moment t_c of scanning of the middle of some line that is assumed to be central, as it applies to the problem of evaluating geometric distortions. The pole formed at the intersection of the ox_0 axis and the Earth's surface is assumed to be the center of the frame. Coordinates α and β are convenient for the purposes of this discussion, since (for example) for photographs covering an area of 600 x 600 km they do not exceed a value of 0.047 in radian measure, regardless of their dependence on the geographic latitude. However, these equations can also be solved in a linear approximation and relative to the scanner coordinates: the scanning angle ξ, also read from the ox_0 axis, and the time interval Δt between the middle of the current line and the moment t_c ($\Delta t = t - t_c$), depending

on the corresponding parameters of the photographic recorder: ξ' = angle of rotation of the recorder's drum, $\Delta t'$ = interval of time between the recording of the current line and the moment t'_c of the recording of the central line ($\Delta t' = t' - t'_c$). This results in the obtaining of relationships that can be used to recalculate the coordinates of an image's elements for the purpose of compensating for geometric distortions.

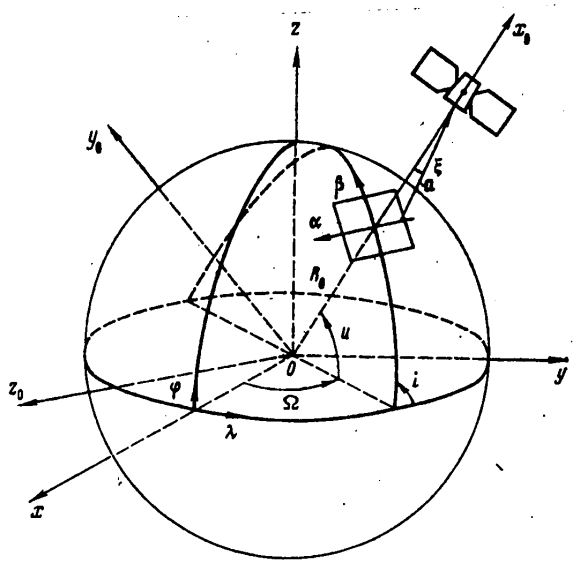

Figure 1. General geometry of scanner surveying.

We will assume that for surveying we are using a scanner with plane scanning, the incident beam vector a of which (Figure 1) has the components (cos ξ, 0 - sin ξ) in the orbital system of coordinates $ox_0y_0z_0$ (we will assume the scanner's intrinsic distorting factors to be equal to zero). Further assuming that the recording is done with a drum-type photographic recorder, we obtain the interrelationship of the photograph's coordinates x,y and the photorecorder's coordinates ξ' and $\Delta t'$ in the form

$$x' = v'\Delta t', \quad y = \rho \frac{\omega_d}{\omega_b} \xi', \tag{1}$$

where ρ = radius of the drum; ω_d, ω_b = angular velocities of rotation of the drum and the scanning beam, respectively; v' = rate of drum feed along the axis.

As a standard, we will use an oblique, cylindrical, equidistant projection oriented along the satellite's orbit. The formulas for this projection can be represented in the form

$$x = M_m R_0 \beta', \quad y = M_m R_0 \alpha', \tag{2}$$

where R_0 = average radius of curvature of the reference ellipsoid in the center of the frame; M_m = a coefficient reflecting the main scale of the photograph. From (1) and (2) we obtain the interrelationship between coordinates α', β' and ξ', η' (η' is an additional dimensionless variable) in the form

$$\alpha' = \frac{\rho \omega_d}{M_m R_0 \omega_b} \xi' \quad \beta' = \frac{v' \Delta t'}{M_m R_0} = \frac{\eta'}{M_m R_0}. \tag{3}$$

By making use of the surveying model equations from [2] and the method for their approximate solution relative to small distorting factors that is explained there, it is possible to find functions $\xi(\alpha,\beta)$ and $\eta(\alpha,\beta) = \nu\Delta t$ (η = angular position of the satellite relative to the center of the frame). Omitting the quite cumbersome intermediate computations, we obtain

$$\begin{aligned}
\xi=&\operatorname{arctg}\left(\frac{\sin\alpha}{k-\cos\alpha}\right)-\frac{k\sin\alpha}{k^2-2k\cos\alpha+1}\left[\frac{\Delta p}{p}+\frac{e_\bullet^2}{2}\sin^2\varphi-\right.\\
&\left.-e(\cos(u-\omega)-\beta\sin(u-\omega))\right]+\frac{k\cos\alpha-1}{k^2-2k\cos\alpha+1}\times\\
&\times\left[(\Delta\Omega-\frac{\omega_\bullet}{\nu}\beta)\sin i\cos(u+\beta)-\Delta i\sin(u+\beta)\right]-\gamma-\frac{\dot\gamma}{\nu}\beta,\\
\eta=&\beta-2e\beta\cos(u-\omega)+\frac{k-\cos\alpha}{\cos\alpha}\left(\theta+\frac{\dot\theta}{\nu}\beta\right)-\\
&-\operatorname{tg}\alpha\left(\psi+\frac{\dot\psi}{\nu}\beta\right)-\left(\Delta\Omega-\frac{\omega_\bullet}{\nu}\beta\right)[\cos i-\\
&-\sin i\operatorname{tg}\alpha\sin(u+\beta)]+\Delta i\operatorname{tg}\alpha\cos(u+\beta)-\Delta u,
\end{aligned}\tag{4}$$

where $e_\bullet$ = eccentricity of the reference ellipsoid; $\omega_\bullet$ = angular rate of rotation of the Earth; ϕ = geographic latitude for the center of the frame; $k = p/R_0$; p, u, ω, e, i, Ω = standard orbital parameters for the center of the frame; Δp, Δu, Δi, $\Delta\Omega$ = their corresponding measurement errors; γ, θ, ψ, $\dot\gamma$, $\dot\theta$, $\dot\psi$ = bank, pitch and yaw angles of the orientation system; $\nu = \sqrt{\mu(1-e^2)^3/p^3}$ = average motion of the satellite; μ = gravitational constant.

When there are no distortions, the equalities $\alpha = \alpha'$ and $\beta = \beta'$ must be fulfilled. Then, having replaced α' and β' in (3) with α and β and substituting the obtained expressions into (4), we obtain the required functions $\xi(\xi',\eta')$ and $\eta(\xi',\eta')$. These coordinates are easily converted into line and column numbers of elements of the original (n and m) and processed (n' and m') images as

$$m=m_0+\frac{1}{\Delta}\xi(m'\Delta_1,n'\Delta_2),\quad n=n_0+\frac{1}{\Delta_2}\eta(m'\Delta_1,n'\Delta_2),\tag{5}$$

where $\Delta_1 = \nu T/(k-1)$ = value of the desired angular resolution that provides equality of the resulting photograph's scales along the x and y axes; $\Delta_2 = \nu T$ = angle of displacement of the satellite during line frequency period T; n_0, m_0 = coordinates of the center of the frame in element numbers; Δ = angular resolution of the scanner.

Thus, when (4) is taken into consideration, expressions (5) give explicit relationships for converting the coordinates of an image's elements during the geometric correction process.

Geometric Correction of Photographs of the Earth. As our initial material we used the central fragments of photographs taken at different times from a "Meteor" satellite: with a low-resolution scanner on orbit 984 and a medium-resolution scanner on orbit 5,094. The photographs depict the Caucasus and the island of Kyushyu (Japan), respectively. The latter is shown in Figure 2 [omitted].

on the days of the surveys, there were available orbital data in a relative equatorial system of coordinates at moment t_0 of the beginning of the first orbit on the ascending node on the given days. Tuning data on the scanners, which proved to be analogous to some bank (γ_0) and pitch (θ_0) angles, were also available.

Reference objects were identified in the original photographs and the corresponding geographic coordinates were determined. The number of points turned out to be 14 and 12, respectively, for each photograph.

The photographs were then encoded in an image input-output unit and entered, element by element (with 100-μm resolution) in special files in a computer disk memory in the form of masses of image elements measuring 2,048 lines by 1,020 columns. The fragments that were entered depicted segments of the Earth's surface measuring 1,781 x 830 and 514 x 237 km for each photograph. By taking into consideration the terms of the second-order expansion with respect to parameter $\omega_0/v \approx 0.073$, which is the weightiest of all the distorting factors, it can be shown that the accuracy of the linear approximation in expressions (4) for both photographs is less than a single element. After this, both photographs were depicted on a graphic display in half-tone form so that the size of each element was 1 x 1 mm. This made it possible to review and make measurements on the photograph with single-element accuracy.

First, temporal correlation of the centers of the frames with coordinates n_0 = = 1,024, m_0 = 510 was carried out. In order to accomplish this, on the graphic images we determined the line numbers corresponding to the beginning of the minute marks formed by the on-board timer during the scanner's return motion, as well as the dimensions of these marks and the width (in elements) of the frames. These measurements made it possible to determine the equivalent angular resolution Δ and line frequency period T of the scanner for each photograph (these parameters are not equal to the scanner's true resolution and period, since the image was obtained from a photograph). Knowing them and the on-board timer's correction factors for Moscow time, which turned out to be 0.3 and 10 s, respectively, the times of passage of the centers of the frames were established and the sidereal time was determined from an astronomical yearbook. Further, standard techniques were used to calculate the orbital parameters and azimuth ζ, which, together with the date and Moscow time of passage of the center of the frame, sidereal time, tuning data and the equivalent values of Δ and T are presented in Table 1. Coordinates x and y of the reference points in the graphic images were then measured.

In view of the comparatively low operating speed of the computer that was used, precise formulas (5) (with due consideration for (4)) were first used to calculate only the nodal points of the curvilinear coordinate networks corresponding to the original photograph: the coordinates of the intermediate points were computed with the help of bilinear interpolation during the actual processing of the photographs (see below). The result of these calculations was two special files on a disk that contained the x and y coordinates of the nodal points. The dimensions of the cells $\Delta n'$ and $\Delta m'$ (for lines and columns) of the rectangular network corresponding to the image that had been processed were selected on the basis of the condition of smallness of distortions caused by the replacement of segments of the curves forming the sides of the network's cells with segments of straight lines because of the effect of the bilinear interpolation algorithm during the processing of the photographs. A second condition was that the curvilinear network not go beyond the boundaries of the original frame. The values of $\Delta n'$ and $\Delta m'$, as well as the corresponding quantities of nodal points with respect to frame (N) and line (M) are also given in Table 1.

Table 1. Initial Data for Processing of Photographs

Параметры (1)	Снимок 1 (2)	Снимок 2 (2)	Параметры (1)	Снимок 1 (2)	Снимок 2 (2)
Дата съемки (3)	4.IX.1977 г.	9.VI.1978 г.	Ω, deg	269,86	95,11
Звездное время (4)	22 ч. 52 м. 0,09 s	17 ч. 08 м. 02.15 s	Δ, deg	$6{,}42\cdot10^{-2}$	$2{,}00\cdot10^{-2}$
t_c	00 ч. 05 м. 11,53 s	00 ч. 46 м. 05.21 s.	T, s	$1{,}266\cdot10^{-1}$	$3{,}655\cdot10^{-2}$
p, км	7009	7004	γ, deg	$3{,}34\cdot10^{-2}$	$3{,}34\cdot10^{-2}$
e	$4{,}481\cdot10^{-3}$	$4{,}724\cdot10^{-3}$	θ, deg	$-4{,}33\cdot10^{-2}$	$4{,}33\cdot10^{-2}$
i, deg	97,92	97,86	$\Delta n'$	94	100
u, deg	44,79	31,97	$\Delta m'$	72	74
ω, deg	148,85	1,98	N	20	20
ν, 1/s	$1{,}0759\cdot10^{-3}$	$1{,}0771\cdot10^{-3}$	M	12	10
ζ, deg	-11,06	-9,22	M_m	8 685 199	2 506 986

Key:
1. Parameters
2. Photograph No .
3. Date of survey
4. Sidereal time

Finally, the actual processing of the photographs for the purpose of geometric correction according to the algorithm described in [7] was carried out; the result of the processing of the photograph in Figure 2 is shown in Figure 3 [omitted]. After the processing was completed, graphic images were again produced and the coordinates of the reference points were measured. On the basis of knowledge of the equivalent line frequency period for each photograph and the satellite's average motion ν, coefficients M_m were found for the obtained photographs with the formula

$$M_m = \nu T R_0 \cdot 10^7. \tag{6}$$

The corresponding results are also presented in Table 1.

The effectiveness of the proposed photograph correction algorithm was evaluated in the form of the ratio of the line, angle and area measurement errors before processing to the corresponding indicators after processing. As these errors we took, respectively, the values

$$\delta_l = \left|\frac{M_m l_c - l_e}{l_e}\right|, \quad \delta_\gamma = |A_c - A_e|, \quad \delta_n = \left|\frac{M_m^2 S_c - S_e}{S_e}\right| \tag{7}$$

where l_c, A_c, S_c = lengths of sides, angles and areas of triangles on the photograph with vertices at reference points; l_e, A_e, S_e = the same characteristics for spherical triangles on the Earth's surface. Averaged indicators (6) were computed for all possible pairs (during the measurement of lengths) and triplets (during angle and area measurements) of reference points, except for angles greater than 160°. The results of the calculations made before and after the processing of the photographs are given in Table 2 (in the table, a tilde indicates the values of the distortions occurring in the processed photographs, while M(...) designates an averaging operation).

It is now appropriate to look into the methodological errors and then move on to an analysis of the effectiveness of the proposed method for calculating coordinate networks and then correcting photographs. The errors in bilinear interpolation, as calculated on the basis of the data for the values of $\Delta n'$, $\Delta m'$, N and M presented in Table 1, proved to be less than one-third of an element for all the photographs; that is, they can be ignored. A detailed analysis of the mean-square errors caused

Table 2. Evaluations of Distortions of Lengths, Angles and Areas Measured on Photographs Before and After Processing

Искажение до обработки (1) / Искажение после обработки (2)	Снимок 1 (3)	Снимок 2 (3)
$M(\delta_д)$, % / $M(\delta_д)$, %	4,543 / 1,656	6,084 / 2,180
$M(\delta_у)$, min / $M(\delta_у)$, min	2,923 / 1,411	4,760 / 0,876
$M(\delta_п)$, % / $M(\delta_п)$, %	12,683 / 3,287	11,310 / 5,718
Погрешность метода, % (4)	0,39	0,37

Key:
1. Distortion before processing
2. Distortion after processing
3. Photograph No .
4. Method error, %

by the total effect of the plotting of the reference points (pinholes), the extrapolation of the geographic coordinates and the discretization of the photograph, yielded figures of 0.49 and 0.47 percent for the two photographs. Multiplication by the figure $2/\sqrt{2\pi} \approx 0.8$ enables us to make the transition to the mathematical expectations of criteria (6) if we assume that the total errors are distributed according to a law that is close to normal. The data obtained in this manner are presented, as method errors, in Table 2. Errors in area measurements will be approximately equal to the data obtained, while angle measurement errors will apparently be negligibly small.

Considering the data in Table 2 and the methodological errors presented above, it is possible to draw the following conclusions in, for example, the case of measurements of lengths. For the first photograph, this error was able to be reduced to about 1.6 percent, and since the methodological error here is approximately 0.4 percent, the residual error should be attributed to errors in the operation of the satellite's spatial orientation system that were not allowed for.

The values obtained for the residual errors remaining after the processing of the photographs meet the demands made of modern cartographic technology. A visual comparison of the photographs before and after processing with a map of the corresponding scale also shows that processed photographs correspond better to cartographic data than unprocessed ones. All of what has been said makes it possible to conclude that it is possible to use the proposed methods for calculating coordinate networks and processing photographs, for the purpose of correcting them geometrically, to solve problems concerning the mapping of the Earth's surface, as well as a number of problems that arise during the study of natural resources.

BIBLIOGRAPHY

1. Selivanov, A.S., Chemodanov, V.P., Suvorov, B.A., Narayeva, M.K., Sinel'nikova, I.F., Bondarenko, R.S., and Seregin, V.I., "Opticomechanical Scanners for Observation of the Earth," TEKHNIKA KINO I TELEVIDENIYA, No 6, 1978, pp 17-21.

2. Khizhnichenko, V.I., "Technique for Evaluating the Accuracy Characteristics of Scanner-Type Television Systems," GEODEZIYA I KARTOGRAFIYA, No 11, 1979, pp 28-32.

3. Bernstein, "Digital Image Processing of Earth Observation Sensor Data," IBM JOURNAL OF RESEARCH AND DEVELOPMENT, Vol 20, No 1, 1976, pp 40-57.

4. Schur, W., "Digitale Entzerrung multispectraler Bilder," BILDMESSUNG UND LUFTBILDWESEN, Vol 44, No 5, 1976, pp 202-208.

5. Bocharov, V.P., and Sazhin, S.M., "Correction of Geometric Distortions of Space Video Information by Digital Methods," TR. GOSNITS IPR, No 8, 1980, pp 8-16.

6. Kadnichanskiy, S.A., "Photogrammetric Processing of Orbital Television Panoramas, Using Reference Points," TR. TSNIIGAIK [Central Scientific Research Institute of Geodesy, Aerial Surveying and Cartography], No 222, 1979, pp 59-80.

7. Tyuflin, Yu.S., Kadnichanskiy, S.A., and Khizhnichenko, V.I., "Analytical Transformations of Orbital Television Panoramas Into a Cartographic Projection," GEODEZIYA I KARTOGRAFIYA, No 4, 1979, pp 51-57.

11746
CSO: 1866/10

UDC 535.36:528.7

FILMING MOONSETS FROM SPACE AS METHOD OF STUDYING EARTH'S ATMOSPHERE

Moscow ISSLEDOVANIYE ZEMLI IZ KOSMOSA in Russian No 6, Nov-Dec 81 (manuscript received 5 Feb 81) pp 58-62

[Article by A.S. Gurvich, V. Kan, L.I. Popov[1], V.V. Ryumin[1] and S.A. Savchenko, Institute of Physics of the Atmosphere and Institute of Space Research, USSR Academy of Sciences, Moscow]

[Text] When the Sun and the Moon are observed through the Earth's atmosphere, refraction leads to both smooth compression of the images of these heavenly bodies and small-scale deformation of the images' shapes. Light refraction measurements can be used to determine the atmosphere's parameters.

Small-scale deformations of the shape of the Sun's image, in the form of steps, were first observed from space by the crew of the first expedition in the "Salyut-6" orbital scientific station (Yu.V. Romanenko and G.M. Grechko). They took separate photographs of the Sun near the horizon that were used to make approximate calculations of the vertical structure of the temperature field in the Earth's atmosphere [1]. It should be mentioned here that such steps have not yet been mentioned in the observations of American astronauts, as follows from the most recent publications on this question [2]. In [3] the authors present only theoretical calculations for the standard model of the atmosphere and proposes a method for determining the altitude of the tropopause according to the characteristic break as a function of the angle of refraction.

For the purpose of further investigating the Earth's atmosphere from the viewpoint of light refraction, the crew of the lengthy fourth expedition in the "Salyut-6" station filmed risings and settings of the Sun and Moon, thus making it possible to derive the altitudinal pattern of the angle of refraction and investigate in detail the dynamics of the typical small-scale deformations of the shapes of these heavenly bodies. The filming was done with long-focus lenses at a rate of 24 frames per second. In this article we present a brief preliminary analysis of three series of films of the Moon, two of which were made on 29 June and one on 25 August 1980.

The dependence of the magnitude of oblateness $\varkappa$ on frame number N for the survey series made on 29 June 1980 is shown in Figure 1. Here $\varkappa = d_1/d_2$, where d_1 is the vertical and d_2 the horizontal diameter of the Moon's visible disk. The altitude of

---

[1]USSR Pilot-Cosmonaut.

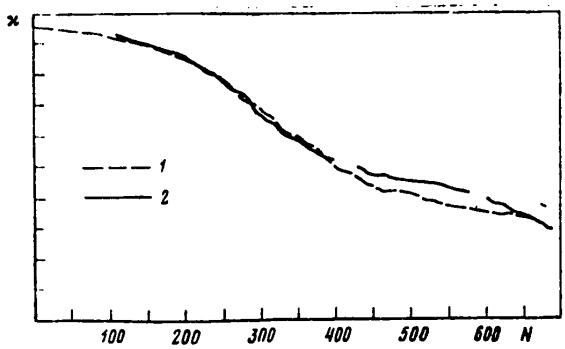

Figure 1. Dependence of oblateness on frame number for observations made on 29 June 1980: 1. Series 1; 2. Series 2.

the perigee of the light ray from the Moon's center corresponding to the most oblate image ($\varkappa$ = 0.30) is approximately 6 km (here and henceforth, altitudes are correlated with values of $\varkappa$ calculated for the standard model of the atmosphere). For the two series under discussion, the angle between the sighting line and the plane of the orbit was 22-25°. The origin of reading of the frames was chosen arbitrarily, with curves 1 and 2 being superimposed according to the maximum values of $\varkappa$ by displacement along the x axis. During Series 2, the Moon's disk passed through a cloud layer about 1 km thick, at an altitude of 13 km, as it was setting. The discontinuities in curve 2 correspond to the passage of the Moon's upper and lower edges through the cloud, when its oblateness could not be measured.

From Figure 1 it is obvious that smooth compression of the Moon's visible disk as it sinks is accompanied by wavelike perturbations of small amplitude that are apparently related to the effects of horizontally layered irregularities in the density of the air. This hypothesis is supported by the fact that these undulatory perturbations correspond approximately to the same frames in which irregularities in density are manifested clearly as deformations (steps) in the shape of the Moon's image. From Figure 1 it is also obvious that although in their upper sections the dependences have approximately the same type of diminution, curves 1 and 2 differ substantially in their lower parts, which corresponds to the passage of the Moon's disk through the cloud for Series 2. This is related to the fact that both above and below the cloud there are temperature gradients differing from those that are observed at the same altitude under cloudless conditions.

In Figure 2 [not included] we see as an example eight frames that were filmed as part of Series 1. Since only the shape and deformation of the Moon's outline are important for quantitative processing, the originals of the moving picture film were copied on contrast film of the "Mikrat-300" type and the photographs were also printed on contrast paper. The photographs in Figure 2 were obtained from sequential frames of the film, separated by a time interval of one-third second; that is, from every eighth frame. The oblateness value for the first frame is $\varkappa$ = 0.67, while for the last it is $\varkappa$ = 0.57; the altitude of the ray's perigee changed from 20 to 18 km, respectively. In the lower part of each photograph, deformations in the form of steps are clearly visible on the right and left sides of the outline, it being the case that the horizontal dimensions of the irregularities that caused these deformations are many times greater than the vertical ones and exceed the visible size of the Moon's disk. The outline deformations in the upper left part of each photograph are not related to the perturbations caused by diffraction, but are connected with the darkening of the lunar seas located there, which was intensified during the process of increasing the contrast. The series of photographs in Figure 2 gives us a graphic picture of the dynamics of the development of the deformations in the Moon's visible disk; that is, of the magnitude and nature of the change in oblateness and the size, shape, location and asymmetry of the step-shaped

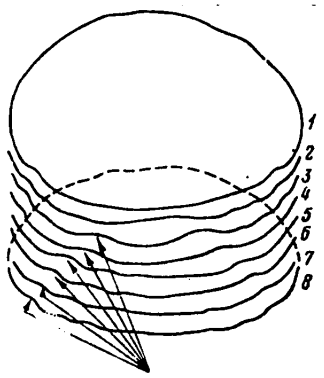

Figure 3. Evolution of deformations of the lower edge of the Moon's outline (numbering of the outlines corresponds to the numbering of the images in Figure 2).

deformations, the change in them as they move across the Moon's disk and so on.

Figure 3 depicts the evolution of the lower edge of the Moon's visible image. The outlines are redrawn from the series of photographs presented in Figure 2. The outline of the Moon's lower edge designated by the number 1 is deformed by steps located on its left and right sides. The shape and location of these steps indicates that they were caused by the same horizontally layered irregularity. On the next outline (2), in addition to this irregularity--which has moved upward on the Moon's disk--there begins to be manifested the effect of the next (and lower) irregularity: the disk's lower edge is severely deformed and flattened. In outline 3 this new irregularity appears in the form of thick, step-type deformations and, in addition, the lower edge of the Moon's disk bulges outward slightly. On outline 3 and further in the series, the disturbances of the Moon's image caused by the effect of this irregularity are indicated in the figure by arrows. In addition, beginning with outline 5, the effect of the next irregularity appears: in outline 5, the Moon's lower edge is deformed and flattened and deformations in the form of steps appear in the following outlines. It is also obvious that this irregularity is substantially weaker than the preceding ones and that its effect on the Moon's visible disk is correspondingly less significant. The slight asymmetry of the outline deformations on the right and left sides indicates that the irregularities have a horizontal structure. Let us mention here that filming of the Sun and Moon from orbit is of substantial assistance in determining the horizontal structure of irregularities, since it produces horizontal "profiles" of the atmosphere; that is, the angle between the sighting line and the plane of the orbit is about $\pi/2$.

Figure 4 [not included] is a sequential series of images of the Moon, taken from moving picture film on which one of the settings of the Moon observed on 25 August 1980 was recorded. This series is noticeable for the fact that in it is depicted the dynamics of the development of an interesting phenomenon: refractive disruption of the Moon's image. The altitude of the perigee of the ray from the lower edge is 14 km. Refractive disruptions are caused by areas with such severe density perturbations that the dependence of the apparent zenith angle on the true one becomes ambiguous. In this case, the lower edge of the disk is depicted three times as the result of this ambiguity. Refractive disruptions of the images of heavenly bodies were also observed by preceding crews in the "Salyut-6" station, although until now such observations were represented only by single photographs, whereas filming has enabled us to register the entire process of the development of these severe refraction deformations with high temporal resolution.

In order to emphasize the typical details of the process, for Figure 4 we selected frames separated by different time intervals: between photographs 1 and 2, the interval is one-third of a second; between 2 and 3--one-half second; between 3 and 7--

one twenty-fourth of a second each (that is, these frames are successive ones); between 7 and 8--one-sixth of a second. Photographs 1 and 2 show the beginning of the process: it is obvious that in addition to deformation of the Moon's disk in the form of steps having a complicated shape, the lower edge of the Moon in photograph 2 in comparison with 1 is flattened noticeably, which is caused by the effect of nonuniformity of the air's density. In photographs 3-7 this nonuniformity is manifested in the form of severe deformations, which are a refraction image of the lower part of the Moon's visible disk. Although the refractive disruption is barely noticeable in photograph 3, as the visible rays sink into the disturbed layer of air, an ever more significant part of the Moon is seen below the line of the refractive disruption. In photograph 7 the line of the disruption is very weak, whereas in photograph 8 the refractive disruption has disappeared and be converted into a step with sharp edges, with the step being deeper and sharper on the right side. This asymmetry, which is related to the horizontal nonuniformity of the disturbed layer of air, is also manifested in preceding photographs 5, 6 and 7 in the nonidentity of the right and left edges of the refraction-affected part of the Moon's image. When the time during which the refractive disruption was observed and the rate of subsidence of the visible ray are known, it is possible to evaluate the thickness Δ of the layer with the anomalous density pattern; for the case depicted in Figure 4, $\Delta \sim 250$ m. The hypothesis of the existence of such thin layers was advanced in [4] on the basis of observations of flickerings of stars and planets.

In conclusion let us mention that, as the derived data indicate, filming of sun- and moonsets with long-focus lenses is a new and promising method for making a quantitative study of the structure of refraction distortions. Filming makes it possible to observe the uninterrupted pattern of the change in oblateness, which can further be used to study variations in the vertical profiles of air density and temperature. In connection with this, the rather high temporal and (consequently) spatial resolution of the irregularities makes it possible to distinguish and identify deformations of the outlines of heavenly bodies caused by disturbances in density after eliminating the random errors in individual frames.

BIBLIOGRAPHY

1. Grechko, G.M., Gurvich, A.S., Romanenko, Yu.V., Savchenko, S.A., and Sokolovskiy, S.V., "Vertical Structure of the Temperature Field in the Atmosphere, Based on Observations of Refraction From the 'Salyut-6' Orbital Station," DOKL. AN SSSR, Vol 248, No 4, 1979, pp 828-831.

2. Garriot, O.K., "Visual Observation From Space," J. OPT. SOC. AMER., Vol 69, No 8, 1979, pp 1064-1067.

3. Shuerman, D.W., Giovane, F., and Greenberg, J.M., "Stellar Refraction: A Tool to Monitor the Height of the Tropopause From Space," J. APPL. METEOROLOGY, Vol 14, No 6, 1975, pp 1182-1186.

4. Grechko, G.M., Gurvich, A.S., and Romanenko, Yu.V., "Structure of Density Irregularities in the Stratosphere, Based on Observations From the 'Salyut-6' Orbital Station," IZV. AN SSSR. FIZIKA ATM. I OKEANA, Vol 16, No 4, 1980, pp 339-344.

11746
CSO: 1866/36

UDC 528.946

USING SPACE PHOTOGRAPHS TO STUDY AND MAP AGRICULTURAL UTILIZATION OF LAND

Moscow ISSLEDOVANIYE ZEMLI IZ KOSMOSA in Russian No 5, Sep-Oct 81 (manuscript received 28 Apr 81) pp 103-110

[Article by L.F. Yanvareva, Department of Geography, Moscow State University imeni M.V. Lomonosov]

[Text] The study of the agricultural utilization of land occupies a central position in economic and geographic investigations of agriculture. It is essentially a multiaspect problem, but in the end its goal is to reveal the interrelationships between natural conditions and systems for carrying out agricultural work and to determine the confinement of different types of agricultural utilization of land to different natural types of soil and local economic conditions [1]. Such a study of land utilization gives a scientific basis for the suitable territorial organization of agriculture.

Until now, the original materials for studying land use were large- and medium-scale land management cartographic materials, data from field investigations of separate key farms, statistical materials on individual agricultural enterprises, and complexes of natural maps. The collection and processing of such detailed materials for large territorial units is extremely difficult.

In this respect, the use of materials gathered by space surveys offers new opportunities. Space surveys not only give a quite detailed image of the land surface over an extensive area, but also make it easier to study the confinement of separate types of agricultural utilization to natural types of soils, since they can be interpreted in the topographical, geomorphological, soil and geobotanical aspects at the same time.

In this article we discuss the possibility of using multizonal scanner photographs taken in space by the "Fragment" system, on a scale of 1:500,000, for these purposes.

The photographs encompass a region located inside two geographical zone--forest-steppe and steppe--that change from the former to the latter from north to south. A large portion of the photograph is occupied by the Kalachskaya upland, which is fragmented severely by a system of gullies and ravines. In the northwest, at the edge of the photograph, lies part of the Khopersko-Buzulukskaya accumulation plain. On the southern edge, along the right bank of the Don River, stretches the Donetskaya ridge, which is also severely dissected by an erosion network.

Practically all of the watershed area and slopes have been tilled (Figure 1 [not included]). The gully and ravine network more or less cuts into a unified arable mass, creating an erosion figure in the land's territorial structure. From a comparison of the space photograph with a topographical map it is obvious that as recently as the 1960's, the very highest sections of the Kalachskaya upland were not being tilled. The grassy virgin steppes were used as pastures and for haymaking. Now, only the natural meadowlands along the gullies and ravines remain untilled. Their agricultural value is not great. A considerable part of the gullies and ravines in the upper reaches have been reforested or planted with bushes in order to prevent the development of water erosion. This shows up quite well on photographs in the orange band (λ = 0.6-0.7 μm), as an abrupt darkening of the tone of the upper reaches of a ravine or gully.

The valleys of the large Don and Khoper Rivers (and their flood plains and terraces), which are clearly visible on photographs taken in any band, make up a complex mosaic of different types of land: open and bush-covered meadows, underbrush, blocks of forest. On the high right original bank of the Don, which is dissected severely by ravines and gullies, the agricultural lands are fragment and represented by small, isolated sections that are impossible to distinguish on a space photograph.

The extensive left bank terraces of the Don and its tributary the Peskovatki are also occupied by a complicated complex of lands. In this area, grassy steppes used to alternate with sections of sand. A large part of the terrace is now occupied by pine forests that were primarily planted by man. The remaining steppe pastures are severely broken up.

Through office interpretation of small-scale photographs taken by the "Fragment" system, this territorial structure of the lands in the region makes it possible to compile small-scale land maps (Figure) with the help of topographic and forestation maps.

The delimitation of tilled fields and the discrimination of the natural meadowlands along the gullies and ravines is the first and most complicated stage in the process of interpreting the land types.

A comparison of the space photograph with a topographic map of about the same scale showed that almost all of the ravine and gully network shown on the map can also be seen in the space photograph. However, from the photographs it is impossible to distinguish ravines from gullies and defiles and thus distinguish the lands and natural meadowlands that are confined to the ravines and gullies and are not used in agriculture.

Plowed lands can be distinguished most reliably from a complex of multizonal photographs that were taken at the same time. Both summer (July) and autumn (October) photographs were used in the interpreting process.

The boundary of the tilled land along the brows of large gullies and ravines is seen most clearly in summer photographs in the near-infrared band (λ = 0.8-1.1 μm), where the network of gullies and ravines has a lightened, whitish tint (Figure 3a [not included]). However, small gullies blend in with the plowed land background. They are more clearly distinguishable in an autumn photograph taken in the same band, where the autumn-plowed fields are distinguished from the gray gully network by their dark, almost black tone (Figure 3b).

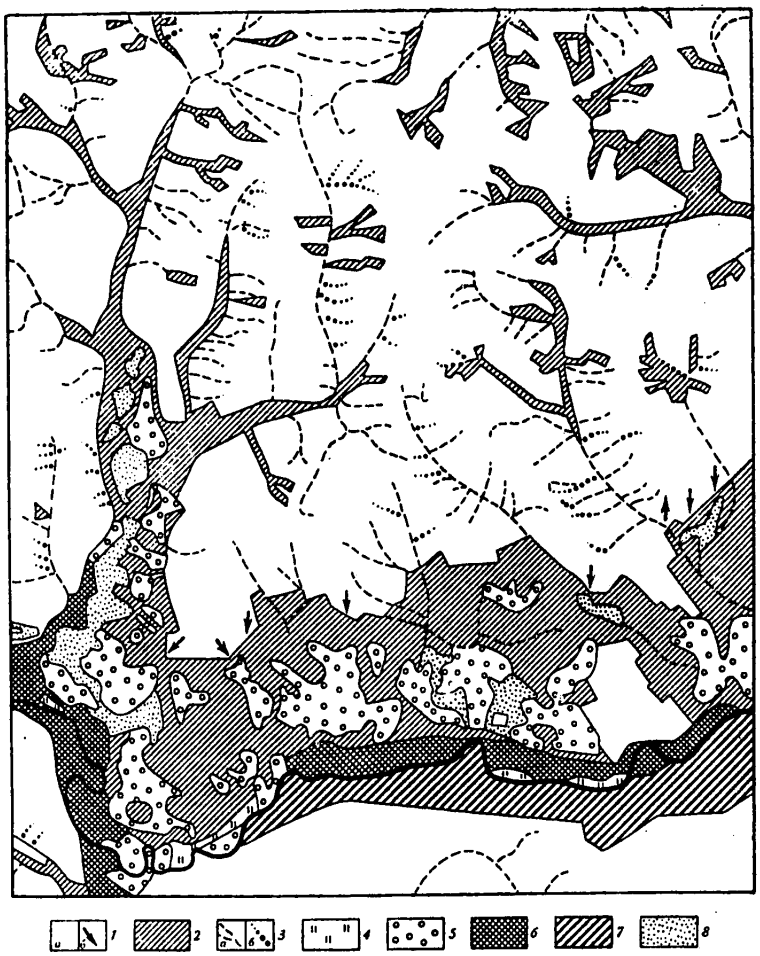

Figure 2. Fragment of land map compiled on the basis of space photographs taken by the "Fragment" system. Lands: 1a. tilled land; 1b. eroded tilled land; 2. pastures and hay-producing areas; 3. pastures and hay-producing areas along ravines and gullies (a. open, b. covered with underbrush); 4. flooded hay-producing areas; 5. forest. Composite lands: 6. forests along river flood plains combined with open and brush-covered ravines; 7. plowed land combined with natural meadowlands and land not used in agriculture. Unused lands: 8. sands.

The reliability with which the outlines of plowed lands are distinguished depends largely on the size of the fields, the clearness of the boundaries between them, and the rectilinearity of their shape. The larger and more rectilinear a field is, the easier it is to distinguish from other types of land. This is why plowed lands can be distinguished most clearly in plains-type steppe regions.

The sizes of the fields in the photograph range from 50-100 to 300-400 ha. Small fields covered with grain plant stubble that are adjacent to or dissected by gullies are difficult to identify, and following the boundary of the plowed land is quite difficult. The observed lack of clarity and the washed-out nature of the boundaries of the tilled lands along the sands of the Don's terraces indicates that the fields have been eroded.

The formation of the pattern of the cutting of the fields depends on a number of factors. The density of the dissection of the relief affects it decisively. On the Kalachskaya upland, the cutting of the fields is irregular: being oriented in different directions, they form a complicated mosaic. Placement of fields at right angles to slopes, with the formation of more or less domelike structures, is typical of the highest part of the Kalachskaya upland. The pattern of fields on the Khopersko-Buzulukskaya plain is distinguished by a high degree of orderliness. The rectangular fields stretch from the northeast to the southwest and form a rectilinear structure that resembles a chessboard. Here the boundaries of the tilled land are distinguished most clearly and reliably.

The network of administrative and farm boundaries has a definite effect on the formation of the field pattern. In the photograph there are boundaries of three oblasts (Voronezhskaya, Rostovskaya and Volgogradskaya) and a number of administrative regions. They can all be traced quite well, either on the basis of the differently oriented cutting of the fields or by the change in the shape of the fields and their elongation along the boundaries. The boundaries of the agricultural enterprises--kolkhozes and sovkhozes--can be interpreted just as easily. Rayon or oblast land utilization plans are used in the identification of the administrative and farm boundaries.

The definition of the boundaries between fields used in the crop rotation system affects the separation of the plowed land from other types. It depends on the diversity of the crops in the planted areas, the proportions of different groups of crops in the crop rotation system, and the special features of their phenological development. In some cases, the sharpness of the fields' boundaries can also depend on the lithological composition of the surface deposits.

As has already been mentioned, in comparison with the watershed areas the river valleys are notable for the high degree of complexity of the structure of their lands. The resolution of the photographs taken with the "Fragment" system does not make it possible to differentiate the lands in the valley complexes. Further enlargement of the photographs' scale or the use of synthesized color images does not produce a positive effect in the identification of the valley land structures. In the summer orange-band photograph, from the structure of the image it was possible to distinguish open meadows from brush-covered ones and underbrush only on the Don's broad flood plain. Forests are identified in the photographs with confidence because of their darker tone. In the valley of the Khoper and along the right bank of the Don it is possible to distinguish only combinations of lands, although the boundaries of these combinations can be traced very reliably in any area in the summer photographs.

The formulation of a plan for identifying lands and determining the boundaries of their outlines is possible only by analyzing all the zonal images for both periods.

Despite the impossibility of obtaining detailed information about the location of the different types of lands (particularly for the valley complexes), space photographs have substantial advantages for studying the confinement of certain types of agricultural usage to natural types of soils. The features of the territory's organization as a function of the relief and the degree of its ruggedness are manifested quite clearly in them.

The interpretation of space photographs offers us great opportunities when studying forms of agriculture as complex methods for the agricultural utilization of land. The territory in the photograph is a typical grain-growing region with a large percentage of grain plantings for the production of marketable grain. Grain growing is combined with the raising of livestock for meat and milk. The insignificant percentage of natural fodder resources in the overall land pattern indicates that the livestock fodder base rests on field fodder production. Only on the flood plains in the Don and Khoper valleys do the flooded meadows have any agricultural value.

The basic indicator of the arable land utilization system on individual farms is the proportion of the groups of crops (cultivated, uncultivated, perennial and annual grasses) that play different roles in crop rotation, as well as fallow and planted pairs of fields. The relationship among these groups of crops makes it possible to obtain an idea of types of crop rotation being used.

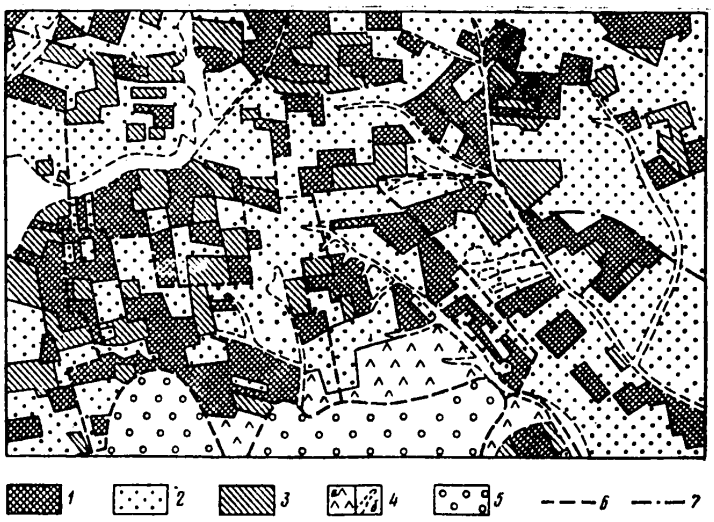

Figure 4. Fragment of land utilization map. Agricultural crops: 1. cultivated (sunflowers and corn); 2. uncultivated (winter and spring grains and others); 3. fallow fields. Natural meadowlands: 4a. steppe-type, on river terraces; 4b. along gullies and ravines; 5. State forest reserve lands; 6. kolkhoz and sovkhoz land utilization boundaries; 7. boundaries of administrative regions.

The analysis and interpretation of the photographs make it possible to obtain such information. In the photographs we first determine the boundaries of the agricultural enterprises (the kolkhozes and sovkhozes) in order to determine the relationships of the groups of crops on specific farms. Of course, the proportions of the different groups of crops in the planted area of a farm do not give a precise picture of the role of the crops in specific crop rotation plans, but are still a quite reliable indicator that make it possible to form an opinion about the forms of agriculture in use. When studying forms of agriculture covering large areas, generalized statistical statistical data on administrative rayons and even oblasts are normally used. A space photograph makes it possible to obtain the required information not only for farms covering considerable areas, but also to see the location of different groups of crops on farms; that is, to come closer to a study of the crop

rotation methods actually in use (Figure 4). From an enlarged, synthesized space photograph it is easy to extract information about agricultural crops; in it it is comparatively easy to distinguish, quite simply, groups of crops, the identification of which on the basis of zonal black-and-white photographs is a complicated procedure.

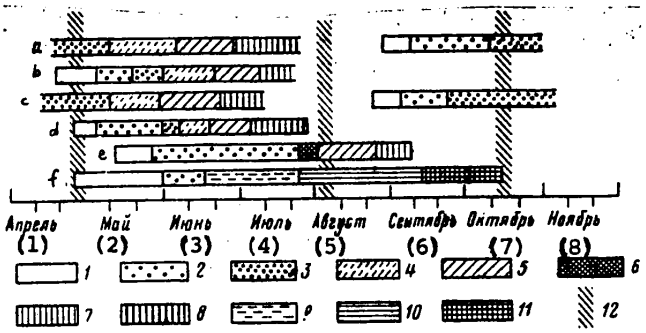

Figure 5. Diagrams of phenological development of agricultural crops: a. winter wheat; b. spring wheat; c. winter rye; d. spring barley; e. corn; f. sunflowers. Stages in organogenesis: 1. seed; 2. sprouting; 3. tillering; 4. leaf-tube formation; 5. heading and flowering; 6. tasseling of panicle; 7. milky ripeness; 8. waxy ripeness; 9. formation of sunflower racemes; 10. browning of sunflower calathide; 11. [omitted]; 12. recommended surveying dates.

Key:

1. April
2. May
3. June
4. July
5. August
6. September
7. October
8. November

In the synthesized photograph taken on 30 July, three types of fields can be distinguished: fields covered with uncultivated grain crops, both winter and spring varieties (gray-blue color); cultivated crops (sunflowers and corn--orange in color); plowed fields (dark blue color). The division of crops into cultivated and uncultivated proved to be possible because of the different dates of onset of the basic stages of these two groups of crops' phenological development[1]. The diagrams that were constructed to show the passage of the agricultural crops through different phenophases and stages of organogenesis (on the basis of average multiyear data and data for the year of the survey) indicated that the spring and winter grains (winter wheat and rye, spring barley) in the southern part of the area surveyed had reached full ripeness and were already harvested (Figure 5). The cultivated crops were in different stages of vegetation: the sunflowers were in the flowering stage and the corn in the panicle-tasseling stage. The plowed fields were open and fallow and were ready for the planting of winter crops. In the autumn photograph, taken on 10 October, they are differentiated from the autumn-plowed fields, since the winter grains planted in them had already reached the tillering stage.

However, from neither the summer nor autumn photographs is it possible to obtain an idea about the location and percentage of winter crops in the crop rotation system.

---

[1]Data on the location of crops on key farms, gathered by M.A. Shepel', were used in the identification of the crops.

For this purpose it is better to use photographs taken in the spring, in the period when the sprouts of the spring crops have not yet appeared and the winter ones have reached the tillering stage.

The necessary surveying dates for different regions can be determined on the basis of diagrams of the vegetative development of agricultural crops that are constructed from average annual data, with corrections for the meteorological conditions of the specific year.

In the end, the analysis of photographs taken at different times makes it possible to determine the proportions of crops in planted areas and the percentage of fallow fields, thus producing information about the utilization of tilled lands and types of crop rotation systems. In the area under discussion, for example, "grain-fallow-cultivated" crop rotation is the one primarily used, with a large percentage of winter and spring uncultivated grains.

The study of forms of agriculture provides for the investigation of the agricultural technology and land reclamation methods used, as well as the systems of measures for preventing wind and water erosion, the use of fertilizers and so on. Normally, when using space photographs to determine the complex of antierosion measures being used in dry steppe regions, we have at our disposal an entire system of external indicators: the presence of forest belts to protect fields, strip siting of agricultural crops and fallow fields, a significant percentage of perennial and annual grasses in the crop rotation, specific strip-type cutting of fields across the direction of the prevailing winds [2].

The study of a system of antierosion measures with space photographs is more difficult. The following agrotechnical measures do not appear in space photographs: contour plowing, working of the soil without plowing, the banking or furrowing of autumn-plowed fields and other forms of antierosion working of fields aimed at reducing the washing away of soil from level fields. The same thing can also be said of hydraulic engineering measures: the building of terrace walls on slopes and the erection of channeling structures. As has already been said, space photographs taken with the "Fragment" system have been used to identify water-control forest plantings on the edges of ravines and gullies, but we have not succeeded in identifying field-shielding windbreaks in them.

It is necessary to mention here that in the laying out of fields, too little attention is given to the susceptibility of soils to water erosion, despite its significant development in the region under discussion.

The thorough study of the agricultural utilization of land with the help of space photographs must be based on field investigations of key types of farms, the choice of which can be made on the basis of preliminary interpretation of the photographs.

In the end, the use of space photographs to study the agricultural utilization of land should facilitate the "geographication" of territorial economic and geographic research and the compilation of maps reflecting the interrelationship of natural conditions and the contemporary agricultural utilization of land.

The experience gained in analyzing space photographs taken with the "Fragment" system has demonstrated their suitability for compiling and revising small-scale land

utilization maps, types of territorial organization, and forms of agriculture in the steppe and forest-steppe zones.

The study of the agricultural utilization of land in all its aspects requires the use of photographs taken at different times. Despite their insufficiently high resolution, therefore, space photographs taken with the "Fragment" system have acquired particular value for agricultural interpretation.

BIBLIOGRAPHY

1. Rakitnikov, A.N., "Geografiya sel'skogo khozyaystva" [Agricultural Geography], Moscow, Izdatel'stvo "Mysl'", 1970, 341 pp.

2. "Issledovaniye prirodnoy sredy kosmicheskimi sredstvami. Geografiya. Metody kosmicheskoy fotos"yemki. T. 4, razdel 'Sel'skoye khozyaystvo'" [Investigating the Environment With Space Facilities. Geography. Space Photosurveying Methods. Volume 4, "Agriculture" Section], Moscow, VINITI [All-Union Institute of Scientific and Technical Information], 1975, pp 57-67.

11746
CSO: 1866/35

UDC 681.3:518

EXPERIMENTAL EVALUATION OF METHODS FOR AUTOMATED INTERPRETATION OF AGRICULTURAL CROPS ON BASIS OF PHOTOGRAPHS OBTAINED WITH 'FRAGMENT' MULTISPECTRAL SCANNING SYSTEM

Moscow ISSLEDOVANIYE ZEMLI IZ KOSMOSA in Russian No 6, Nov-Dec 81 (manuscript received 28 Apr 81) pp 89-92

[Article by I.A. Labutina and I.K. Lur'ye, Department of Geography, Moscow State University imeni M.V. Lomonosov]

[Text] At the present time no one doubts the urgency of the problem of automating the interpretation of aerial and space photographs. A large number of scientific publications devoted to this question have appeared recently. The results presented in them do not yet make it possible to talk about the automatic processing of data received from artificial Earth satellites. Experience has shown that it is necessary to have the participation of an interpretative specialist in the process of interpreting images with a computer, and that the photograph processing system must be interactive. Although the number of available methods for interpreting aerial and space photographs is quite large, it is difficult to give preference to any one of them. The choice of the method depends on the quality of the surveying materials, the demands on the computer that emanate from the desired accuracy of the results, and the type of prior information about the surveyed objects. The purpose of this article is to compare the most widely used automated interpretation methods on the basis of the results obtained.

For our experiments in automated interpretation, we selected a photograph of the territory of the Don and Khoper Rivers' interfluve that was obtained with the "Fragment" multispectral scanning system on 30 July 1980. We used a four-band image that was recorded on magnetic tape and subjected to radiometric correction.

The area depicted in the photographed is almost completely farmed. Despite some slight differences in agricultural practices in Voronezhskaya, Volgogradskaya and Rostovskaya Oblasts, parts of which are seen in the photograph, in general the main features of the structure of the planted areas are similar: typically, winter and spring grain crops--wheat and barley--predominate. Part of the planted areas are occupied by cultivated crops, the main ones of which are sunflowers and corn. Materials[1] on the distribution of agricultural crops by crop rotation fields (and their status) were gathered in the fall of 1980 in an area encompassing the

[1]The materials were gathered by N.A. Shepel' and L.A. Kovrizhnykh.

territory of two sovkhozes in Veshenskiy Rayon, Rostovskaya Oblast. These materials, as well as Hydrometeorological Service data on the phenological phases of crops were used as standards in the evaluation of the results of automated processing that had as its purpose the identification of the composition, by type, of agricultural crops. We also used spectral and color synthesized photographs on a 1:500,000 scale and the results of visual interpretation.

A fragment of the photograph measuring 512 x 300 elements, which contained about 100 agricultural fields (including 38 fields in the standard section) was subjected to automated processing. The fragment was first processed on a YeS [Unified System of Electronic Computers] EVM-1022 at MGU's [Moscow State University imeni M.V. Lomonosov] NIVTs [probably Scientific Research Computer Center] by a program developed in the Laboratory of Aerospace Methods, Cartography Section, Department of Geography, MGU. It was assumed that there was no prior information about the nature of the distribution of probabilities inside the classes of objects and that the only digital recordings on magnetic tape were used as the initial data. The program realizes a cluster analysis algorithm and is based on a single element-by-element survey of all the assigned lines in the photograph. By analyzing the distances between the elements in the photograph in a multidimensional space (in this case its dimensionality is four) and comparing them with a previously given threshold value, the program forms clusters that are identified as homogeneous formations. In connection with this, the centers of the clusters are defined as the average values of the spectral characteristics of the elements in them and the intracluster dispersions and the distances between the centers of the different clusters are determined. The values of the boundaries of the objects for each line in the photograph are plotted in a special table (if the object is not an isolated element). Using an alphanumeric printer, the computer produces a classification map in which each cluster is designated by its own alphanumeric symbol. This classification map is compared with data gathered on the ground or a visualized image, and the standard fields are identified. In the experiment being described, the identification of the fields was made quite easy because of the presence in the photograph fragment being investigated of images of fallow fields; that is, fields with exposed soil. They can be grouped into one cluster very easily because of, in the first place, the substantial difference between their brightness in all surveying bands and the brightness of cultivated fields and, in the second, the relatively high uniformity of their spectral characteristics. Confident identification of fields on the classification map was also facilitated by the fact that their boundaries could be seen clearly in almost all cases.

An analysis of the results revealed the following. Fields planted with grain crops, the harvesting of which had already been completed by the time of the survey, were easily combined into a single cluster. Fields planted with corn and sunflowers and that had a greenish appearance at the moment of surveying could not be distinguished with sufficient confidence. The plantings of these crops in each field was, as a rule, not uniform, as a result of which it was not possible to obtain more or less homogeneous salient features on the classification map even when different threshold values were used. The plantings of these crops were characterized only by their own set of clusters, in which they were combined, since on the classification map the fields corresponding to these crops were designated by two or three symbols of overlapping clusters, although almost everywhere a single predominant symbol could be distinguished. During the first stage of classification, therefore, it turned out to be possible to obtain information about the centers (the average values of the

spectral characteristics) of all the clusters of interest to us; that is, the standard fields planted with different crops.

In the second stage, we set a desired number of clusters and gave several threshold characteristics for combining or separating clusters. As our initial data we used the values of the centers of the clusters (the average values of the spectral characteristics of homogeneous formations) that had been obtained during the first stage of the cluster analysis program's utilization. In an iterative fashion, this program compares the centers in question with standard values. The clusters are combined if the distances between their centers are less than the given threshold value and separated if the intracluster dispersion for any spectral component is greater than the given threshold value. In connection with this, new cluster coordinates are formed.

Such a sequence of procedures has quite substantial advantages: the first stage is quite simple to realize and rapid in execution (in the sense of computer time required) and makes it possible to reduce the quantity of initial information significantly: instead of the characteristics of the 512 x 300 elements of the original photograph, after the first stage we have only characteristics on the order of 60 cluster centers. The second stage is more complicated to realize, but this complexity is offset by the small amount of information to be processed. As a result of this automated interpretation method, the reliability of the classification of the agricultural crops was evaluated at 80 percent.

The same photograph fragment underwent processing in an automated complex in the ONP [expansion unknown] of the USSR Academy of Sciences' Institute of Space Research[1]. Two programs were used: classification by minimum distance and a program that realizes the method of maximum likelihood. In order for these programs to function, it was necessary to obtain the values of the vectors of the average values of the standard fields' spectral characteristics and the values of the covariance matrices. The following procedures were realized for this purpose. The standard fields were identified visually on a display screen and representative sections inside them, measuring 5 x 5 elements, were distinguished. The vectors of the average brightness values for each spectral channel and the covariance matrices were computed for each such section. The minimum-distance classification program was set up to sort the original photograph into five classes: fallow fields (bare soil), winter wheat and barley (stubble), corn and sunflowers. The results of the classification were: 1) the fallow fields were distinguished very clearly (as with the preceding method, they served as the basis for identifying fields on the classification map); 2) plantings of corn and sunflowers were combined into a single class, in connection with which on the fields planted with corn, the symbols representing the class were arranged compactly, almost without spots, while in the sunflower fields there were individual spots combined with designations of unclassified objects; 3) a class containing natural meadowlands along gullies and ravines was distinguished. Thus, we distinguished three of the five classes of fields that can be identified quite confidently during visual interpretation of spectral photographs and that correspond to the three basic colors in a synthesized color photograph because of the fact that they characteristic entirely different states of agricultural fields: plowed soil, vegetative growth and grain stubble after harvesting.

---

[1]The photograph processing programs were developed by V.A. Krasikov and V.A. Shamis.

The maximum-likelihood method is considered to be a much more accurate but also more laborious automated interpretation method. It presupposes that the distribution of probabilities for each class of objects is normal. In order to relate each element in the photograph to some class with the maximum likelihood, a Gaussian decision rule is used. In connection with this, it is necessary to know the number of distinguishable classes of objects, the vector of the average values for each class, and the elements of the covariance matrix.

The first classification variant with this program, when the spectral characteristics of arbitrarily selected fields planted with the crops named above were given as the centers, yielded the same results as the classification with the minimum-distance determination program. In order to distinguish between fields planted with sunflowers and corn, an attempt was made to distinguish 13 classes corresponding to standard fields with crops in different states. Thus, the characteristics of fields with dense and sparse plantings were used. The experiment proved to be unsuccessful: there was a confusion of classes and only one--the fallow fields--could be distinguished clearly.

The next attempt to separate corn and sunflower plantings proceeded as follows. The average values of of the characteristics of two fields planted with each of these crops were introduced into the maximum-likelihood program as the centers instead of the characteristics of a single, arbitrarily chosen field. In connection with this it was assumed that the covariance matrices for these fields are quite similar, so they were not recomputed. The result proved to be positive: corn and sunflower plantings were separated into two classes. True, some fields were relegated immediately to two clusters (that is, they were represented by a combination of designations of both crops), but in almost all cases it was possible to determine the predominant class. All six fields planted in corn that appeared in the fragment that was processed were combined confidently into a single class, while of the five planted with sunflowers, only one could not be placed confidently in one class or another.

This experiment confirmed our supposition that when using classification programs with instruction, it is not possible to assign the spectral characteristic of a single field as the center of a class, since fields with a single crop that belong to a single class can have significant differences in spectral characteristics. The use of the average value of the characteristics of several fields defines the boundaries of a class more accurately.

This experiment in interpretation shows that in addition to objects that differ tangibly in all bands (or most of them), objects differing from each other by an insignificant value in only one band are encountered very frequently (particularly among agricultural crops). During visual interpretation such cases are usually detected. The introduction of a weighting factor in the spectral characteristics of such objects in a single band would make it possible to separate them during automated interpretation.

These experiments showed that the methods used yield quite similar results, at least for small fragments of photographs. The choice of method is affected by the subjective attitude of the user. For large volumes of information it is advisable to use the least laborious and fastest automated interpretation methods, with mandatory participation of an interpretative specialist in the initial stages of the work.

It is reasonable to conduct the business of thematic processing in several stages. The first step, even at the stage of adjusting and instructing the automated satellite information processing systems, should consist of a preliminary visual or photometric (depending on the required degree of accuracy) interpretation of the photographs in separate representative sections, which makes it possible to obtain prior information about the advisable number of classes and special features of the image of an object being identified in spectral photographs.

11746
CSO: 1866/36

UDC 528.946

MAPPING FORESTS FROM SPACE PHOTOGRAPHS

Moscow ISSLEDOVANIYE ZEMLI IZ KOSMOSA in Russian No 5, Sep-Oct 81 (manuscript received 28 Apr 81) pp 111-116

[Article by T.V. Kotova, V.I. Kravtsova and A.K. Makarevich, Department of Geography, Moscow State University imeni M. V. Lomonosov]

[Text] One of the northern regions of the European part of the USSR was used as the example during an investigation of the possibility of studying and mapping forests on the basis of photographs obtained with the experimental "Fragment" system. The analysis of the pictures of forest growth was conducted in the Aerospace Methods Laboratory, Cartography Faculty, and the Problems Laboratory of Integrated Cartography and Atlases, Department of Geography, MGU [Moscow State University] imeni M.V. Lomonosov.

Previous experience in working with multizonal space photographs had shown that scanner photographs from the "Landsat" satellite, taken in 4 spectral bands with 80-m resolution, were suitable for mapping types of forest growth and distinguishing coniferous, broad-leaved and mixed forests, but could not be used to distinguish forests differing in valuation characteristics. That conclusion was reached by Canadian specialists [1]. Very promising, from the viewpoint of mapping forests, proved to be the multizonal photographs obtained with the MKF-6 camera, in which it was possible to distinguish forests not only on the basis of tree type, but also according to several valuation characteristics [2-4]. It is a matter of interest to determine the place in the system of space surveying materials of the photographs obtained with the "Fragment" equipment.

For our analysis of the forest growth pictures, we used photographs taken in the orange (0.6-0.7 μm), red (0.7-0.8 μm) and near-infrared (0.8-1.1 μm) bands on 30 July 1980; the work was done with prints on a 1:500,000 scale.

The photograph that was analyzed (Figure 1 [not included]) encompasses the upper reaches of the Severnaya Dvina River in the area of confluence of its righthand tributary, the Vychegdy River, with the Malaya Severnaya Dvina River. This region is located at the junction of the boundaries of three oblasts: Arkhangel'skaya, Vologodskaya and Kirovskaya.

This area is a slightly hilly plain dissected by river valleys. The black bands of the channels of the Malaya Severnaya Dvina, Vychega, Yug and Luza Rivers, fringed with light-colored sandbars and shallows, are clearly visible in the photographs in

the red (0.7-0.8 μm) and near-infrared (0.8-1.1 μm) bands. On the flood plains of the larger rivers (Malaya Severnaya Dvina, Vychegda) we can see ancient lakes and river-terrace meadows. Another characteristic is the presence of bogs and boggy sections on the high terraces, the crest-and-hollow relief of which is emphasized by vegetation of different types.

A large part of this territory is forested. This is quite obvious in the orange-band (0.6-0.7 μm) photograph, where the unforested sections are represented by a light-gray tone, while the forested areas are indicated by gray and dark-gray tones. The area of the survey belongs to the subzone of midtaiga forests and podsolic and boggy soils. The virgin forests are primarily coniferous (pine and spruce) and have a dark tone in the photographs taken in the red and near-infrared bands. In this region, the birch and birch-aspen forests--represented in these bands by a light-gray tone--are secondary.

The degree of agricultural development of this area is comparatively low. The arable land is concentrated near the rivers; together with the flood-plain meadows, which are the primary fodder base for milk-cattle raising, they form a light-colored "frame" for the valleys in the orange band. In the orange-band photographs, a bright, light-colored tone represents the large cities: Kotlas at the confluence of the Malaya Severnaya Dvina and the Vychegda, Velikiy Ustyug on the left bank of the Malaya Severnaya Dvina, Koryazhma on the left bank of the Vychegda, Luza on the same river's right bank. The light-colored line of a broad clearing extends along the Vychegda. Light-colored rectangular cuttings--indicative of the industrial use of woos--against the dark background of the forests are visible in the orange-band photograph. Sawmills and woodworking and cellulose-paper industry enterprises using this raw material base are operating in Kotlas and Velikiy Ustyug. Further intensive utilization of the forests is indicated by the replacement of coniferous trees with broad-leaf varieties over a considerable part of the territory. With the help of other sources of information about this region, we succeeded in detecting bogginess in some of the cuttings.

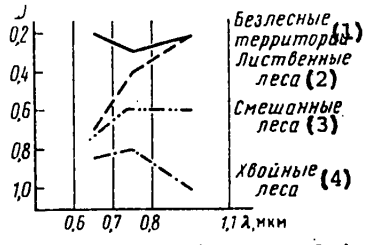

Figure 2. Curves of spectral image of different types of forest growth in photographs obtained with the "Fragment" multizonal scanning system.
Key: 1. Unforested territories
2. Broad-leaf forests
3. Mixed forests
4. Coniferous forests

Photographs taken in different spectral bands give information on different features of the structure of the vegetative cover and should be used to solve various problems.

The boundaries of unforested areas, both along the river valleys (flood plain meadows, bogs, agricultural lands, settled areas) and in the interfluvial spaces (cuttings, bogs that have formed in cuttings) are quite visible in the orange-band photograph. From these photographs it is possible to distinguish unforested sections among forest masses (primarily the outlines of cuttings); the minimum size for these sections is on the order of 2 mm^2 for a photograph with a scale of 1:500,000 (or 0.5 km^2 in actuality). In orange-band photographs, differentiation of tones inside forest masses is very weak. Forest boundaries are more clearly distinguished in

photographs taken in the red and near-infrared bands: unforested territories do not have such a light image tone as in the orange band, but the forest areas are differentiated very clearly by their image tone. A comparison of the photographs with topographic and forest maps shows that the differences in phototone are caused by changes in the types of trees in the forests. On the basis of a comparison of a photograph with forest maps of Arkhangel'skaya (a scale of 1:2,000,000), Kirovskaya (1:1,250,000) and Vologodskaya (1:1,250,000) Oblasts and a geobotanical map of the Non-Black-Earth Zone of the RSFSR (1:1,500,000), we have established identification features of forests with different types of compositions and characteristic changes in the density of the image phototone for transitions from one surveying zone to another; that is, the spectral image of the objects to be identified that are of interest to us. The curves of the basic objects' spectral images are presented in Figure 2. They were obtained by visual measurements of the image's density on positive prints of the photographs, using a standard scale of densities, and characterize the image of these objects not in general, but only for the prints we used.

The spectral image curves give a visual picture of the change in the image density of the basic objects to be identified in the zonal photographs. They confirm that in the orange-band photographs, unforested territories have a brighter image (in comparison with other objects). Therefore, it is easiest to use these photographs to delineate the boundaries of forests, but distinguishing types of trees in them is impossible, since forests of different types are characterized by image density values that are very close to each other in this band. In the photographs taken in the red band, there is an increase in the brightness of the image of broad-leaf forests, which makes it possible to distinguish the outlines of coniferous, mixed and broad-leaf forests, the differences in the image density of which are $\Delta D = 0.2$. In photographs taken in the near-infrared band, these differences are even greater: coniferous forests show up as a dark-gray, almost black, tone ($D = 1.0$), mixed forests as a gray tone ($D = 0.6$), and broad-leaf ones as light gray ($D = 0.2$); the differences in image density of $\Delta D = 0.4$ insure reliable discrimination of these types of forests. In connection with this, however, unforested territories show up as a light-gray tone that is the same as the tone for broad-leaf forests. The combined use of multiband photographs makes it possible to identify all of the required set of objects. In connection with this, it is possible to recommend a definite, most advisable sequence for the utilization of multiband photographs during the identification process. In the first stage, orange-band photographs are used to identify forest boundaries and differentiate between forested and unforested areas. Then, the photographs taken in the near-infrared band are used to differentiate them into coniferous, mixed and broad-leaf forests. After this sensible breakdown of the objects, red-band photographs--which have the best resolution--are used to correct the pattern of their outlines.

The results of the identification of forest growth with space photographs are depicted in Figure 3. The system of forests shown in it was compared with previously published forest and geobotanical maps of about the same scale, such as the "Geobotanical Map of the Non-Black-Earth Zone of the RSFSR," which has a scale of 1:1,500,000. In comparison with this map, the interpretation with the photographs does not yield any additional information. On the contrary: the published map, for example, identifies spruce and pine plantings that cannot be distinguished in the space photographs. However, the detail of the delineation of outlines on the map compiled from the space photographs is considerably better; they are accurately localized and are tied in quite well with the pattern of other natural elements (river

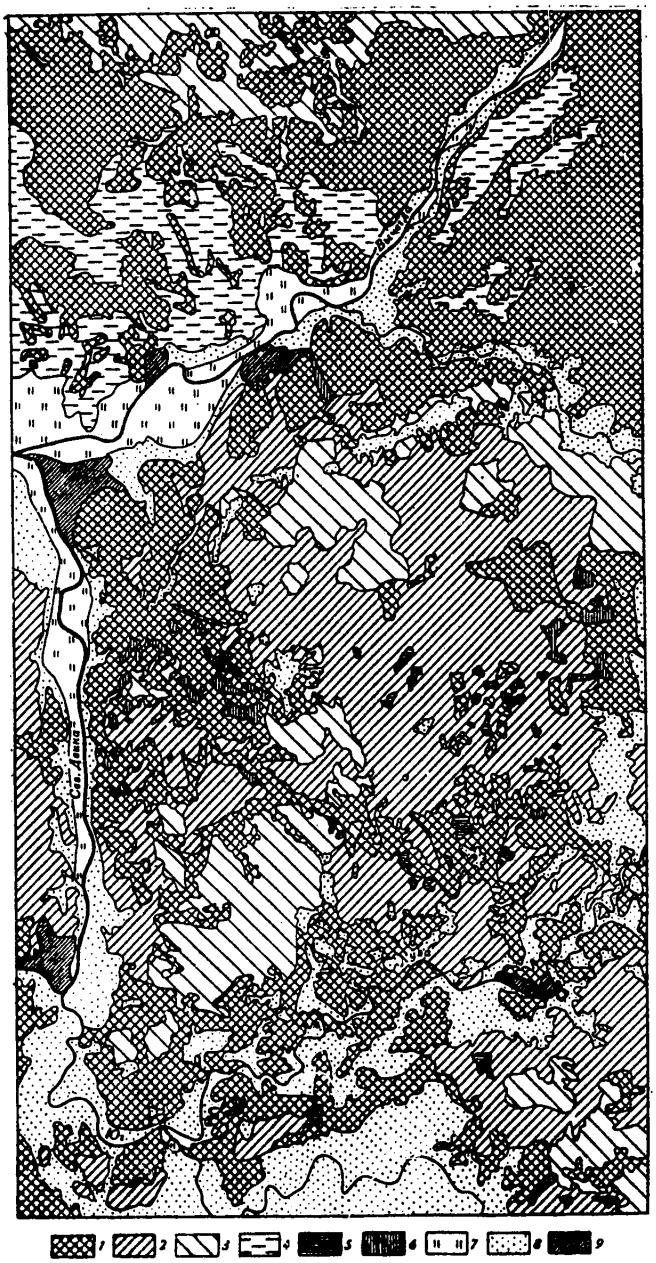

Figure 2. Identification of forests in the area of the upper reaches of the Severanaya Dvina, as compiled from space photographs. Forests: 1. coniferous (spruce, pine); 2. mixed (spruce, pine, birch, aspen); 3. broad leaf (birch, aspen). Unforested areas: 4. bogs along river valleys; 5. boggy areas on cutting sites; 6. cuttings; 7. flood-plain meadows; 8. settled and agricultural lands; 9. urban areas.

valleys and so forth). This indicates that there is a possibility of improving the degree of detail in medium-scale forest maps by using materials from multispectral scanner space surveying.

Thus, photographs obtained with the "Fragment" multispectral scanning system can be used for small- and medium-scale mapping of forests. However, although they can be of assistance in obtaining a detailed and geographically correct pattern of outlines, they do not provide the total content of such maps and much additional material must be used to complement them. Using them to compare forest maps with a detailed description of the types of trees present and valuation indicators is, unfortunately, impossible.

BIBLIOGRAPHY

1. "Manual of Remote Sensing," Washington, Vols 1 and 2, 1976, 2144 pp.

2. Kamyshan, O.L., and Kravtsova, V.I., "Mapping Northern- and Mid-Taiga Forests, Using Central Yakutiya as an Example," in "Kosmicheskiye s"yemka i tematicheskoye kartografirovaniye. Geograficheskiye rezul'taty mnogozonal'nykh kosmicheskikh eksperimentov" [Space Surveying and Thematic Cartography: Geographic Results of Multispectral Space Experiments], Moscow, Izdatel'stvo MGU, 1980, pp 85-96.

3. Kotova, T.V., and Garanina, I.N., "A Study of Mountain-Taiga Forests and Their Anthropogenic Dynamics for the Purpose of Small-Scale Cartography, Using the Pre-Baykal Area as an Example," ibid., pp 96-105.

4. Sukhikh, V.I., and Sinitsyna, S.G., editors, "Aerokosmicheskiye metody v okhrane prirody i v lesnom khozyaystve" [Aerospace Methods in Environmental Conservation and Forest Management], Moscow, Izdatel'stvo "Lesnaya promyshlennost', 1970, 288 pp.

11746
CSO: 1866/35

UDC 711.528.7:629.78

SPACE-BASED RESEARCH FOR URBAN PLANNING

Leningrad KOSMICHESKIYE ISSLEDOVANIYA DLYA GRADOSTROITEL'STVA in Russian 1981 (signed to press 30 Mar 81) pp 6, 9-13, 176

[Annotation, introduction and table of contents from book "Space-Based Research for Urban Planning", by A. Alekseyev, A. Bogdanov, G. Vanyushin, G. Grechko, D. Grnchiar, Yu. Zonov, I. Ivanov, V. Kaznacheyev, I. Kvitkovich, A. Lishevskiy, R. Lobachev, A. Melua, S. Mityagin, V. Modev, V. Mordyuk, A. Peshkov, A. Porubski, M. Reykhshteyn, N. Selivanov, Ya. Feranets, and V. Shidlovskiy, Stroyizdat (Leningrad Division), 3000 copies, 176 pages]

[Text] This book surveys the results of investigation of the Earth's natural resources from space over the twenty-year period of manned space flight. Progress in and prospects for use of satellite imagery in regional and urban planning and investigation of environmental quality in the socialist nations are considered. Scientists and specialists from Bulgaria, the GDR, Poland, the USSR, and Czechoslovakia, the participant nations in the Intercosmos program, were involved in its preparation. The book is intended for scientific workers and personnel involved in land use planning and environmental protection.

Introduction

The Soviet space program is directed primarily at solution of pressing "terrestrial" problems, i.e., at seeking ways for effective utilization of the results of space experimentation for peaceful purposes, including solution of the most important scientific-technical and economic problems confronting the USSR and the socialist nations.

A certain amount of experience has already been amassed in the use of space technology to study the Earth's natural resources and monitor ecological processes, for radio and television, and for meteorology and navigation. A new scientific discipline, space ecology, is rapidly evolving.

The past few decades have been characterized by significant scientific and design achievements in the field of urban and regional planning. In the Soviet Union, the territorial scale of the urbanization of new lands is rapidly expanding, particularly in the North, Siberia, and the Far East. Interlinked systems of population centers are being created and cities are growing to cover extensive areas.

The vigorously developing urbanization in the USSR and its sister socialist nations required that rapid decisions be made in the field of the regulation of urban growth and environmental protection and that changes be made in methods for gathering and processing information on the rapidly shifting status of various urban subsystems, local and regional settlement systems, and the areas occupied by major industrial facilities.

The 1970's in the Soviet Union were marked by a switch to planning forecasts made at the regional level. Thus, the General Plan for Settlement of the USSR and the General Plan for Development of Health Resorts, Recreation Areas, Tourism, and Natural Parks in the USSR were the first documents in the world to reflect the broad opportunities afforded by the socialist system for solution of pressing problems of urban planning and environmental protection on the scale of a nation as vast as the USSR. These general plans are serving as the foundation for compilation of regional planning documents for the major economic regions and Union republics, various district planning programs, and general city plans.

Multipurpose territorial analysis during different stages of the planning process requires the creation and introduction of new technical methods and tools. This has generated an urgent need for the development of automated systems for management of large urban-planning operations and organization of a continuous dynamic planning process that will quickly react to the changing external situation.

Space-based studies have opened up totally new opportunities for gathering information and making design decisions in urban and regional planning and landscape architecture (Table 1). Unique archives of space imagery of the Earth's surface, including images sent to Earth by the participants in experiments carried out under the Intercosmos program, are being created. Utilization of this imagery is having an enormous economic effect. For example, imaging of 5.5 million km^2 of the Soviet Union by cosmonauts P.I. Klimuk and V.I. Sevast'yanov from the long-lived orbital station Salyut-4 produced a savings of 50 million rubles.

What advantages are provided by the introduction of space imagery into the planning of cities and major territorial systems?

First of all, the planner is able to examine all of a very large area simultaneously, something that was previously impossible. The space photographs used for this purpose graphically show the environment of the region to be studied and provide a clear picture of the distribution of features with respect to height as well as area.

Secondly, in contrast to traditional topographic maps, space images give an "instantaneous" representation of features that more accurately and comprehensively reflects the properties of territorial systems during a given period. In planning any major territorial system, especially in regions that are sparsely settled and on which little research has been done (e.g., Tyumen' District), it is often necessary to employ topographic maps from which a significant proportion of current information has been omitted as a consequence of the slow rate at which such maps are updated on the basis of the results of ground surveys.

Table 1

Some Economic Sectors in Which Space Imagery is Utilized in the USSR (from Published Data)

Organization	Problems Being Solved or to Be Solved by Use of Space Imagery
State Committee for Urban Planning	Provision of a technical-economic foundation for the disposition and territorial expansion of population centers Zoning of territories with respect to favorability of conditions for different types of functional utilization Monitoring of the dynamics of population centers and settlement systems Analysis of landscape and recreational conditions Study of environmental conditions in the vicinity of large population centers
Ministry of Geology	Large- and small-scale geological mapping Identification of areas promising in terms of mineral prospecting
State Committee on Forestry	Mapping of forests Prediction of fire danger in forests and of the consequences of forest fires
State Committee on Hydrometeorology and Monitoring of the Environment	Meteorological research and weather forecasting Study of environmental conditions (space monitoring) Hydrological studies
Ministry of Transport Construction	Siting of roads Technical-economic substantiation of the disposition of transport facilities Monitoring of the status of transportation networks and transport equipment
Ministry of Agriculture	Forecasting of harvests Study of land resources Planning of conservation measures
Main Administration for Geodesy and Cartography	Compilation of different types of maps and charts
Ministry of Public Health	Study of public health in relation to exposure to environmental pollution

Table 1 continued

Academy of Sciences of the USSR	Study of the Earth's natural resources from space Development of technical tools and methods for study of natural resources
Ministry of Culture	Archeological research
Ministry of Education	Study of geography and earth science
Ministry of Higher and Midlevel Specialized Education	Study of certain scientific disciplines

The advantages of space imagery are also indisputable from the standpoint of reflection of the current status of the Earth's surface, particularly if one takes into consideration the rapidity with which information can be gathered, its novel character, and the savings over, e.g., aerial photography (Table 2).

Thirdly, the organization within the overall framework of space-based research of regular imaging cycles for definite regions makes it possible to discern trends in the evolution of anthropogenic and natural landscapes and to determine the extent to which changes in the environment have a dynamic character.

The most interesting prospects are for use of space photographs in the planning of cities and large territorial complexes that include settlement systems, areas of intensive industrialization, recreational facilities, tourist attractions, and natural parks and reserves. It is actually possible to establish the precise boundaries of cities and metropolitan areas, the structure of open spaces and built-up areas, degree of forestation, the extent to which man has altered the environment, air and water quality (including the extent of polluted areas), etc.

By using space imagery, architectural planners can see the three-dimensional structure of the landscape viewed from above rather than two-dimensional images of the contour lines for cities and forests. For example, even when photographs are taken on a scale of 1:300,000-1:500,000, the problem of providing a variety of landscape features in laying out tourist routes over large areas can be more easily and quickly solved.

It would be naive to assume that the problem of introducing space imagery into urban planning is limited to the use of images of a specific region. The analysis of information gathered from space and its employment for purposes of planning are directed at solution of a wide variety of complicated research and organizational problems. There are many vague and disputed aspects of the organization of this activity at both the urban-planning and multipurpose levels. It is therefore necessary to conduct a great deal of development work on scientific methodology and to draw up experimental plans based on the use of new information sources, which will make it possible to devise a methodology for use of space imagery in various sectors of the economy.

Table 3

Requirements of Different Users for Information Content of Space Imagery (from Published Data)

Purposes and users of space information	Resolving power of image, m	Image coverage, km^2	Local information need, μm	Periodicity of imaging, days	Thermal resolution, °K	Minimum solar elevation, deg
Synoptic imaging	150,000	-	-	60	1	-
Imaging of coastal waters and major lakes	5000	10^6	-	As required	1	-
Soil moisture content	200	10^5	-	1-30	5	-
Water table	200	-	-	As required	5	-
Status of ocean surface	150,000	-	-	0.25-1	5	-
Oil slick detection*	100	10^4-10^5	-	As required	10	-
Measurement of water surface area	1000	-	-	1-7	10	-
Ice-water boundary	200	-	-	7	20	-
Snow line	200	-	-	7	5	-
Snow temperature	200	-	-	As required	1	-
Snow moisture content	100	10^4-10^5	-	1	1	-
Total content and vertical distribution of gases (both anthropogenic and natural in origin) in atmosphere	10,000	-	-	-	-	-
Mapping of local pollution sources**	100-500	-	-	-	-	30-40
Study of soils	15	10^4	-	-	-	-
Springs	30-100	-	0.51-0.57 0.8-1.3 8-12	30	-	30

Note. This table gives only published figures; additional research is needed in other cases.

*After accidents.
**Within framework of planning programs.

Table 2

Effect Anticipated or Obtained from Use of Space Imagery (from Published Data)

Area of application or problem solved by use of space imagery	Annual effect, millions of pounds sterling
World agriculture and forestry	2-2.4
World geography	Up to 2
World geology and mineral resources	Up to 24
World hydrology and water resources	Up to 4
World oceanography	Up to 36

At the research level, urban-planning criteria intended for evaluation of territory at different planning scales must be clearly defined and it is necessary to establish the feasibility of extracting new information at different scales from space photographs, together with their degree of detail and their reliability. Scientific research must be greatly expanded in the area of space-based methods for urban-planning studies, considering them both separately from and in combination with traditional ground-survey and aerial-photographic techniques (Table 3).

At the organizational level, the proper place for space-based urban-planning studies in the overall structure of space experiments must be determined. It is especially important to concentrate all work on scientific methodology in this area under the State Committee for Construction Affairs, in order to devise a standard methodology, ensure a high scientific-technical level for research, and provide an opportunity for creation of a data bank in which all analysis and application processes are automated. It would obviously be expedient to provide for the training of qualified specialists to work at urban-planning institutes.

The material above does not cover all aspects of space-based research on urban planning, but it does reflect the diversity of the problems involved and the need for solution of a number of interdisciplinary problems and for technical and methodological (particularly programming) innovations. All these factors are evident in the structure of the present book, which considers both the goals of urban planning and the most important technical and organization aspects of the subject.

This book is the first international publication on space research for urban and regional planning; it was prepared in cooperation with specialists from the socialist nations. Its contents are divided into sections intended to provide the reader with general scientific information on the technology and methods of space imaging of Earth and on interpretation methods and sections containing data characterizing the potential applications of space imagery at the theoretical level.

In our opinion, this sort of organization most closely corresponds to the task at hand, i.e., that of familiarizing the reader with a new scientific-technical field and of demonstrating the feasibility of incorporating the achievements of cosmonautics into planning practice.

Contents Page

2478
CSO: 1866/31

UDC 711:528.7 629.78

SATELLITE IMAGING FOR URBAN PLANNING

Moscow KOSMICHESKAYA S"YEMKA DLYA GRADOSTROITEL'STVA in Russian 1981
(signed to press 7 May 81) pp 2-5, 159

[Annotation, introduction and table of contents from book "Satellite Imaging for Urban Planning", by Sergey Ivanovich Krest'yashin, Arkadiy Ivanovich Melua and Tamara Nikolayevna Chistyakova, Stroyizdat, 2000 copies, 160 pages]

[Text] This book examines various aspects of the gathering of reliable and comprehensive information for urban planning by means of satellite technology. Planning requirements with respect to the informational content of satellite images and the principles of their interpretation are discussed. There are examples of the results of satellite-image analyses that reveal features of the terrestrial landscape, urban and regional development, and air and water quality. The use of satellite photographs in urban planning is shown to be cost-effective. This book is intended for architects and specialists working in the field of urban planning. It includes 16 tables, 57 illustrations, and a bibliography of 134 items.

Introduction

The resolution entitled "Basic Directions to be Taken by the Economic and Social Development of the USSR During 1981-1985 and over the Period Through 1990" provides for further study and utilization of space in order to promote further progress in science, technology, and the national economy. This extremely important state document reflects a concern with a new field of technology and science whose effectiveness has been proven within a very short period of time.

It was only about 25 years ago that the first artificial earth satellite was launched from the USSR. Two years later, the first vehicles carrying photographic equipment were sent into space. At the time, many scientists denied the expedience of using satellite imagery of Earth for national-economic purposes.

Satellite photography of Earth is today an effective method for territorial studies and the most important area of the space program. Hundreds of organizations use satellite images for solution of various scientific, planning, and industrial problems. Satellite imaging has revealed new mineral deposits, promising fisheries, etc. Nevertheless, many specialists still cannot see see the prospects afforded by satellite photographs for their particular field, have a skeptical attitude toward the use of satellite images in planning, and deny that populated areas and transportation networks can be studied from space.

The present book is intended to familiarize urban planners with the information-gathering capabilities of satellite imagery. Numerous examples are presented to show that the size of an feature visible in an image depends on the photographic technical conditions specified by the user. A planning problem of definite scale should be matched by photographs having a specific field of view and resolution (referring to the resolution of photographs of a given locality, which is determined by the minimum size of the features visible in the image). Thus, photographs with a resolution of 20-50 m are suitable for regional planning, while the appropriate resolution for suburban areas is 10-20 m and that for general urban planning is less than 10 m. Here one can see two material advantages of satellite imaging, which can be carried out on different scales and with different resolutions. First of all, the less stringent resolution requirements imposed on imagery by a small planning scale produce a considerable savings of time and money. Secondly, a progressive reduction in the resolution of photographs (from several meters to hundreds of meters) leads to progressive generalization of the image, i.e., discrimination of the features that are significant at the scale in use, which makes it possible to improve territorial studies. The appearance of the first satellite photographs resulted in modification of the boundaries of the natural regions of the natural regions of the North American continent, which had for decades been considered immutable; supplemental investigations carried out on the ground confirmed the validity of the conclusions drawn from the satellite images. There are many examples of the redrawing of maps after analysis of satellite photographs. Photographic maps with an information content substantially greater than that of ordinary maps have been compiled from satellite images (a satellite-photographic map of the Aral-Caspian region has been published in the USSR). If the unit of information is assumed to be the smallest territorial area within whose image there is no change in information flow, it is 2-3 orders of magnitude greater for a satellite photograph than for a map of similar scale.

All the features in a satellite image are seen at the same level of generalization and in terms of a uniform field of view, which is especially important in seeking relationships and interdependences among natural features. Satellite imaging has made it possible to carry out systematic investigations of dynamic phenomena, rapid telemetric data transmission, etc. The use of satellite images requires development of methods that take into account the scale and nature of the problem to be solved.

The authors are convinced that satellite photographs should be a standard reference aid and form of documentation for all planners and scientific workers concerned with settlement patterns and regional and urban planning.

This book was based on research conducted by the Leningrad Scientific-Research and Planning Institute for Compilation of General Plans and Programs for Urban Development. The results of work carried out by many Soviet and foreign organizations have been utilized in considering individual problems; the bibliography lists the appropriate publications.

The authors wish to thank Prof. V.N. Belousov, who reviewed the book and whose advice contributed to its improvement during all stages of its preparation.

Chapter I was written by S.I. Krest'yashin (Sections 1 and 3 jointly with T.N. Chistyakova), the introduction, Chapters II and III, and the conclusions were written by A.I. Melua, and Chapter IV was written by T.N. Chistyakova.

Contents Page

2478
CSO: 1866/30

UDC 528.946

USING MATERIALS FROM MULTISPECTRAL SCANNER SURVEY TO STUDY ANTHROPOGENIC EFFECT ON THE ENVIRONMENT

Moscow ISSLEDOVANIYE ZEMLI IZ KOSMOSA in Russian No 5, Sep-Oct 81 (manuscript received 28 Apr 81) pp 117-123

[Article by V.I. Kravtsova and I.S. Nizkaya, Department of Geography, Moscow State University imeni M.V. Lomonosov]

[Text] The goals of rational utilization of nature and protection of the environment require the development of mobile methods for monitoring the anthropogenic effect on the environment, among which space monitoring is becoming the method of primary importance [1-3]. The main space monitoring tool may be good-resolution multispectral scanner surveying, which provides for both operational and long-term tracking of the effect on the environment of human actions. In this connection, it is important to analyze the possibilities of using photographs obtained with the help of the "Fragment" system in order to study the anthropogenic effect on the environment.

In order to analyze the possibility of studying the anthropogenic effect on the environment, we selected regions lying outside the main agricultural zone that differ sharply in both their natural conditions and the nature of their economic development. The two areas selected were the taiga regions in the northern section of the European part of the USSR and desert areas in Central Asia (the central part of the Ustyurt Plateau), for which we analyzed the anthropogenic effect on forest growth and desert landscapes, respectively.

In order to study the anthropogenic effect on forest growth, we used a photograph that depicts part of the territory of three oblasts: Arkhangel'skaya, Vologodskaya and Kirovskaya (Figure 1 [not included]). Rich forest resources are concentrated in this area and are being exploited industrially by enterprises in the cities of Kotlas, Sol'vychegodsk, Koryazhma, Veliki Ustyug and Luza.

Photographs of this area are interesting in that they depict quite well the results of economic development. Cities, agricultural lands and broad clearing are visible as light-colored spots. These are elements of the anthropogenic effect that are related to the development of the territory. An anthropogenic effect of a negative nature is manifested here primarily in the destruction of forest growth and the disruption or alteration of the type of trees to be found. Indirect indicators can be used to determine changes in the soil cover (bog formation on cutting sites). These features of the anthropogenic effect, as identified in the photograph, are depicted in Figure 2.

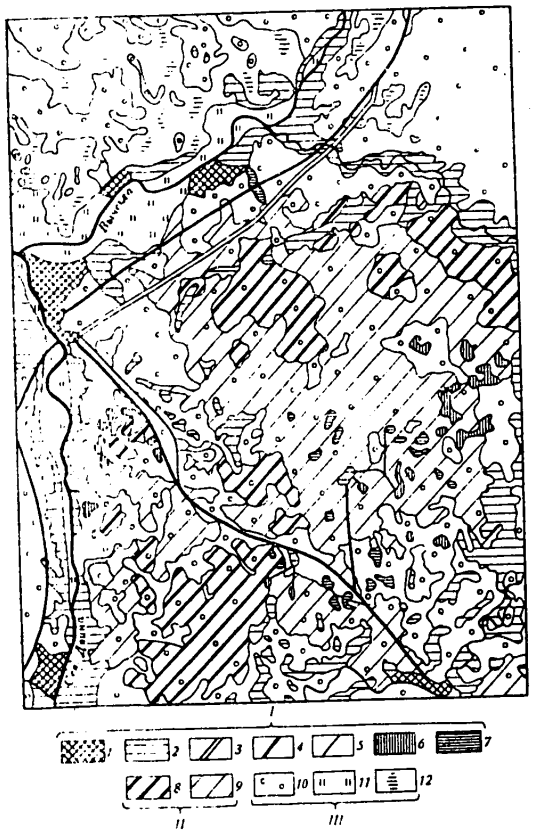

Figure 2. Diagram of the anthropogenic effect on the forest growth near the city of Kotlas. I. Destruction of forest growth as the result anthropogenic action (unforested sections): 1. near urban construction; 2. near settled and agricultural lands; 3-5. along broad clearings; 6. cuttings; 7. boggy cuttings. II. Change in composition of forest growth as the result of anthropogenic activity: 8. total replacement of native coniferous forests by broadleaf forests; 9. partial replacement of native coniferous forests by mixed forests. III. Other designations: 10. forests; 11. flood-plain meadows; 12. bogs.

The interpretation was based on photographs taken in three bands: orange (0.6-0.7 μm), red (0.7-0.8 μm) and near infrared (0.8-1.1 μm). Different spectral photographs were also used to identify various objects. The reason for this was the different information content of the images of the territory in the three bands named above. For instance, for the detection of sections where the anthropogenic effect shows up the brightest, the orange-band photograph proved to be optimal. Unforested territories (of various origins and being used for various purposes) show up in it quite clearly because of their light tone. For example, in this photograph it is easy to identify the unforested sections that are urban areas located along the rivers, since they show up as bright-colored spots with irregular shapes. Settled and agricultural lands (without any further breakdown) are also quite visible in the photograph. Their light-colored outlines, in the form of bands with broken boundaries, stretch along the valleys of the large rivers, as well as along small valley in the forest masses that show up as a dark-gray tone. Broad clearings are distinguished quite clearly, although fragmentarily in places.

Another type of human effect on the forest growth and the soil cover appears as the result of the systematic reduction of coniferous forests for industrial purposes. Cuttings are identified in orange-band photographs. As a rule, they are light-colored spots of small size (no more than 4-5 mm^2 in photograph with a scale of 1:500,000), with rectilinear boundaries, that are located primarily along rivers and near populated points.

We can also point out another, no less important, feature: the cuttings are located primarily in places where coniferous trees grow, because spruce is the most highly valued tree in the cellulose and paper industry. Therefore, as additional material for identifying cuttings it is advisable to use the red-band photograph, in which it is possible to differentiate forests according to the types of trees in them. In the photograph taken in this band, coniferous forests are represented by a dark tone. The orange-band photograph can be

used to distinguish such anthropogenic formations as boggy cuttings, but only if additional cartographic sources are available. This is on aspect of man's effect on nature in this region.

Another type of effect is manifested as a change in the composition of the northern European coniferous forests as a result of their many years of use as a valuable source of wood. These changes are expressed either as a partial replacement of the native coniferous forests by mixed ones or as a total replacement by broad-leaf forests. These changes show up best in photographs taken in the red and near-infrared bands. Mixed forests appear as gray areals with a characteristic grainy image structure and separate dark impregnations. This is caused by the combination of coniferous and broad-leaf trees, which gives the picture a unique character because of the alternation of dark and lighter spots that frequently have the rectilinear shape of overgrown cuttings. These formations are located in the center of the photograph, near the populated points, as well as along the right bank of the Severnaya Dvina River. The broad-leaf forest masses are represented by a light-gray tone and are located, as a rule, near the settled and agricultural lands.

The results of the interpretation give us grounds for reaching the conclusion that it is necessary to institute a complex of measures for the purpose of restoring the coniferous forests in this region. They also make it possible to judge the huge scales of the anthropogenic effect on the forest growth and its utilization. In this region, for example, only about 30-40 percent of the forest areas are still virgin forest composed of the valuable conifers; 40-50 percent of the forests have been affected by partial replacement of the coniferous forests with mixed ones; in 15-20 percent of the area, they have been completely replaced. It is important to call attention to the fact that improper economic activity creates conditions that lower the ability of the forests to resist the unfavorable factors of the anthropogenic effect. For instance, excessive and unfounded reduction of a forest leads to the formation of bogs on cutting sites. About 50 percent of the cuttings existing here are boggy.

In order to avoid such negative consequences of economic activity, it is necessary to develop measures for the rational utilization of forest resources, as well as to carry out a complex of reclamation projects to renew and restore our timber resources (particularly the coniferous types).

The anthropogenic effect on the soil and plant cover in the deserts on the Ustyurt Plateau was studied with the help of a photograph showing the central part of the plateau within the boundaries of the western part of the Uzbek SSR (the Karakalpakskaya ASSR) and the eastern part of Mangyshlakskaya Oblast in the Kazakh SSR (Figure 3 [not included]). Topographically, the flat or gently sloping plateau is a loamy desert with a complex of boyalycheno-biyurgunovaya [translation unknown] vegetation on the grayish-brown desert soils. Karst formation processes are highly developed in this area, it being the case that the entire plateau is mottled with leaching funnels and sinkholes. They show up as dark points about 1 mm in diameter. Wormwood and grasses (primarily feather grass) grow densely in the sinkholes. On the plateau there are also shallow (up to 5 m deep) but very wide (up to several kilometers) and flat "urpa" [translation unknown] depressions. For them the characteristic vegetation is the bright green ittsegeka [translation unknown] bush, which imparts a dark tone to the image of these depressions in the photograph. This system of depressions stretches from the northwest to the southeast. Between the

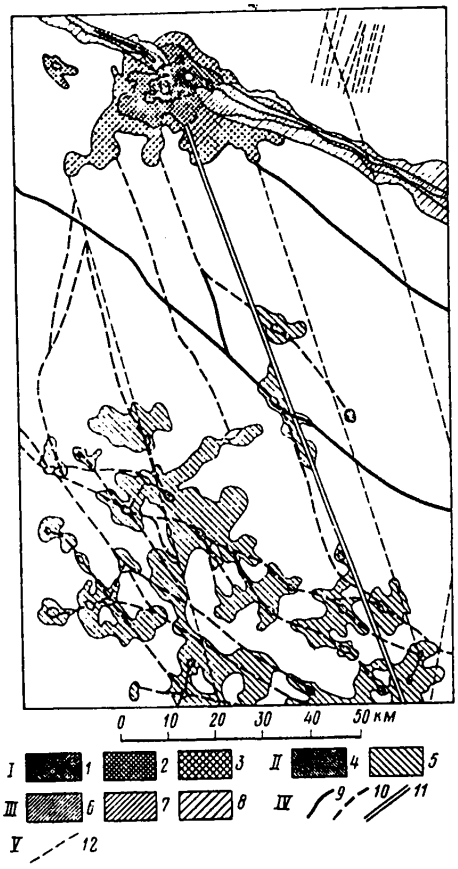

Figure 4. Diagram of anthropogenic effect on desert landscapes, as compiled from a space photograph. I. Disturbance of soil and vegetative cover as the result of industrial activity and pasturing around populated points: 1. total destruction of vegetative cover and serious soil deflation; 2. partial destruction of vegetative cover and significant soil deflation; 3. disturbance of vegetative cover and insignificant soil deflation. II. Disturbance of soil and vegetative cover around wells as the result of pasturing and trampling by cattle: 4. complete destruction; 5. partial destruction. III. Disturbance of soil and vegetative cover as the result of construction and operation of a large transportation line: 6. total destruction of vegetative cover and serious soil deflation; 7. partial destruction of vegetative cover and significant soil deflation; 8. disturbance of vegetative cover and insignificant soil deflation. IV. Disturbance of soil and vegetative cover as the result of the movement of transport vehicles and cattle along roads and cattle trails: 9. total destruction of soil and vegetative cover as the result of cattle movement along cattle trails; 10. partial destruction of soil and vegetative cover as the result of movement of transport vehicles along dirt roads. V. 11. 12. Disturbance of soil and vegetative cover as the result of geological surveying work and other types of activities.

hollows there are weakly delineated elevations (up to 2 m), which are the so-called "bozyngeny" [translation unknown], where the gypsum horizon lies directly on the surface; it is precisely this that causes the light tone of their image in the photograph. Salt bottoms and takyr soil located in depressions in the relief appear in the form of white and light-gray spots with clearcut boundaries.

Until recently, the desert regions of Central Asia and Kazakhstan were little developed and almost untouched by economic activities. The section depicted in the photograph is interesting because in recent years the desert landscapes have been altered considerably as the result of anthropogenic effects on nature [4]. These changes are related to the searches for and development of useful mineral deposits (gas and oil deposits have been discovered); the construction of the Bukhara-Center gas pipeline, the Kungrad-Chardzhou railway line, highways and new settlements serving these transport lines; the increased anthropogenic load on the region that is connected to this. Intensive development of this part of the plateau is also leading to negative consequences that are manifested mainly as disturbances (of various

origins) of the soil and vegetative cover. The degree of their manifestation and the nature of their distribution are depicted in space photographs that have been interpreted, and are shown in a map that has been compiled and is presented in Figure 4.

In the upper part of the photograph, the large light-gray spot that in places has a white tone with unclear boundaries calls attention to itself. This section, which stretches from northwest to southeast, reaches 40 km in length and 15 km in width. In its center, near a railway station, is the settlement of Karakalpakiya. As a result of the construction and utilization of all these objects, as well as the movement of transport and the pasturing of cattle around the settlement, there have been substantial disruptions of the soil and vegetative cover: destruction of the sparse vegetation, such as it is, and related deflation of the soil, the thickness of which does not exceed 15-20 cm. Deflation takes place in the direction of the prevailing winds, from the northeast to the southwest. In the photograph it is easy to see the nature and degree of disturbance of the soil and vegetative cover, which is maximal near the populated point and the transportation line, then decreases gradually as the distance from them increases. The light image tone in the center of the section indicates the exposure of light-colored carbonaceous rocks. Determination of the overall limits and the degree of the effect on the soil and vegetative cover is easier when photographs taken in two surveying bands--red and near infrared--are used.

A number of roads converge on the settlement from the south. The dirt roads' image is characterized by curvilinearity. As a result of the use of the strip along the sides of the roads for the movement of transport, the soil and vegetative cover has been disturbed near them. The roads appear in the photographs, which have 80-m resolution, in the form of noticeable light-colored strips. On both sides of the image of the main transport road, temporary roads--traces of the movement of specialized transport along the geological profiles during the conduct of geological surveying work--appear as rectilinear, parallel light-colored strips. Even a single passage results in disturbance of the vegetative cover and, as is obvious from the image of these profiles, is accompanied by soil deflation and is preserved in the landscape for a long time.

The deserts on the Ustyurt Plateau are used as a fodder base for livestock (Karakul sheep and milk and wool production by free-running sheep). During the spring, summer and autumn period, there is active pasturing of cattle. Numerous wells have been dug in places where the ground-water lenses occur at a shallow depth. As a result of their systematic use, extensive areas with disturbed soil and vegetative cover have formed around them. The intensity of the disturbance around the wells varies. In place, the soil and vegetative cover has been completely destroyed near a well. These sections appear in the photographs as white, sun-shaped spots with rays of roads and tracks leading away from them. As the distance from the wells increases, the extent of the unfavorable effect on the landscape decreases, and there is a corresponding weakening of the light-colored tone's intensity. The pattern of the image of the pasturing areas has a number of characteristic features: it is as if the light-colored spots around the wells and the cattle stands have been strung onto the light-colored lines of the roads.

Thus, the interpretation of scanner-type space photographs makes it possible to detect some anthropogenic effects on the desert's natural landscape--primarily on the soil and vegetative cover--and establish their origin, nature and extent, as well as

compile appropriate maps of the anthropogenic effect on the landscape that can be used to develop recommendations for the rational utilization and protection of nature.

The work that has been done demonstrates that multispectral scanner photographs obtained with the "Fragment" system can be used to detect a quite extensive range of anthropogenic effects on the landscapes of different natural zones. Using additional materials, with the photographs it is possible to establish the origin, nature and degree of these changes, compile special thematic maps, and develop the necessary recommendations for the rational utilization of natural resources and the prevention of unfavorable consequences of intense anthropogenic activities.

BIBLIOGRAPHY

1. Ryabchikov, A.M., and Sayko, T.A., "Study of the Anthropogenic Effect on the Environment," in "Issledovaniye prirodnoy sredy kosmicheskimi sredstvami. T. 4. Geografiya. Metody kosmicheskoy fotos"yemki" [Investigating the Environment With Space Facilities. Volume 4. Geography. Space Photosurveying Methods], Moscow, VINITI [All-Union Institute of Scientific and Technical Information], 1975, pp 80-83.

2. Burov, V.P., Glushko, Ye.V., and Yermakov, Yu.G., "Standardization of the Images of Anthropogenic Formations and Complexes in Space Photographs," in "Kosmicheskaya s"yemka i tematicheskoye kartografirovaniye. Geograficheskoye rezul'taty mnogozonal'nykh kosmicheskikh eksperimentov" [Space Surveying and Thematic Cartography: Geographic Results of Multispectral Space Experiments], Moscow, Izdatel'stvo MGU [Moscow State University imeni M.V. Lomonosov], 1980, pp 247-257.

3. Glushko, Ye.V., "Experiment in Calibrating an Anthropogenic Change in the Environment With the Help of Space Photographs," ISSLEDOVANIYE ZEMLI IZ KOSMOSA, No 4, 1980, pp 35-39.

4. Viktorov, A.S., "On Some Possible Causes of the Complexity of the Ustyurt Plateau," ZEMLEVEDENIYE, Vol 12, 1977, pp 179-183.

11746
CSO: 1866/35

UDC 061.3:502.3:629.78

'INTERCOSMOS' PROGRAM MEETINGS ON ENVIRONMENTAL POLLUTION

Moscow ISSLEDOVANIYE ZEMLI IZ KOSMOSA in Russian No 4, Jul-Aug 81 pp 122-124

[Article by I.M. Gal'perin]

[Text] The first coordinating meeting on the subject "Utilization of Aerospace Information to Determine and Monitor Environmental Pollution" was held in Bratislava in October 1980. The national coordinators of Hungary, the German Democratic Republic, Poland, the USSR and the Czechoslovak Socialist Republic participated in the meeting. The international coordinator in this matter is Yozef Kvitkovich, the deputy director of the Slovakian Academy of Sciences' Institute of Geography.

The particular importance and urgency of the matter of pollution was emphasized during the discussion and it was discovered that the participants had different concepts of the most dangerous pollutants, as a result of which it was not possible to develop a common international program for scientific research in this matter. Those present at the meeting turned to the Soviet delegation with a request for the preparation of a plan for an international program of scientific research in this field.

A second meeting of these national coordinators was held in Moscow in March 1981. Those present discussed and adopted an international program of scientific research for 1981-1985, the plan of which was prepared by workers at the Laboratory for Anthropogenic Monitoring and the Institute of Water Problems of the USSR Academy of Sciences.

This program provides for the development of methods of obtaining and processing information about anthropogenic pollutants and the determination of their effects on the environment, including ecological changes of an anthropogenic origin.

The investigation and determination of types of pollutants must be conducted in the atmosphere, on land and in water areas, seas and oceans. By 1985 we should have techniques for the remote determination of anthropogenic pollutants and the detection of their effects.

A meeting of coordinators concerned with the subject "Development of Methods for Investigating and Monitoring Water Resources and Their Pollution With the Help of Aerospace Information" was held in Budapest in March of this year. The international coordination of work in this subject is the responsibility of (Goda Laslo), director of the Hungarian Hydrological Institute.

Representatives of five countries--Hungary, Poland, Romania, the USSR and the CSSR, who reported on the work that had been done in 1980--attended the conference.

A survey of methods for predicting melt water runoff has been compiled in Hungary, as well as a description of the operational observation network for collecting data on the snow cover. During the joint Soviet-Hungarian spaceflight, Hungarian specialists actively participated in the collection of ground data at the Kishkőre and Balaton monitoring ranges. First attempts were made at the machine processing of space photographs in order to determine the characteristics of closed-drainage waters and soil conditions in the Kishkőre range.

Aerospace information is being used in the CSSR for the following purposes: studying the hydrophysical characteristics of soils subject to erosion; investigating the characteristics of the snow cover; studying the geomorphological development of drainage basins in connection with the formation of alluvial deposits and the silting of reservoirs.

In Romania the primary attention is devoted to investigating the characteristics of soil moisture, which are determined by comparing synchronously gathered ground, aircraft and space data.

Last year in Poland, the basic assignment was to study thermal pollutants in reservoirs and moving water. The characteristics of the thermal regime of water objects was investigated on the basis of synchronous ground observations and aerial photographs.

Soviet specialists used aerospace information to compile hydrographic maps of the deltas of the rivers flowing into the northern Caspian Sea and hydrogeological maps of the Fergana region and the territory of the MPR [Mongolian People's Republic] and are working on a large project for the integrated study of reservoirs.

During the analysis of the results of all this work, those present at the meeting noted a number of difficulties that have arisen because of the insufficient amount of equipment for gathering and processing aerospace information, primarily because of the extremely limited number of aircraft being used to carry out aerial surveying.

At the meeting there was a discussion of a plan for scientific research covering the following areas:
1. The development of methodological principles for evaluating the status and dynamics of water objects and their drainage areas on the basis of data from aerospace surveys.
2. The development of methods for evaluating the spatial distribution of snow cover and its aqueous-physical properties for the purpose of using aerospace information in hydrological prediction of fluvial drainage.
3. The study of the Earth's surface for the purpose of determining subterranean water distribution areas.
4. The development of methods for determining the composition and distribution of pollutants of surface and subterranean waters.

By the end of 1985, the conduct of research in these areas will create a basis for compiling a common methodological manual on the use of aerospace information for the investigation, evaluation and prediction of water resources, which will be the main final result of the work in this field.

11746
CSO: 1866/10

SPACE POLICY AND ADMINISTRATION

INTERNATIONAL MONITORING FROM SPACE

Moscow MEZHDUNARODNYY KONTROL' S ISPOL'ZOVANIYEM KOSMICHESKIKH SREDSTV in Russian
1981 (signed to press 8 Apr 81) pp 2-4, 119

[Annotation and table of contents from book "International Monitoring From Space", by Ivan Ivanovich Kotlyarov, Izdatel'stvo "Mezhdunarodnyye otnosheniya", 1,900 copies, 120 pages]

[Text] This book examines the role of monitoring of the discharge of governmental obligations assumed under international treaties in the areas of disarmament, environmental protection, the use of space, etc. The author considers forms and methods of monitoring and the validity of using space technology for this purpose.

INTRODUCTION

The CPSU and Soviet government are tirelessly and consistently striving to strengthen peace and bring about a relaxation of international tensions, "since there is at present no more significant or important problem for any nation than the preservation of peace and the assurance of the most fundamental right of every human being -- the right to life," as was pointed out in the report of the CPSU Central Committee to the 26th Party Congress.

This policy is reflected in bilateral and multilateral treaties concluded by the Soviet Union with other governments.

Under the influence of the foreign policy of the USSR and other socialist nations, a number of agreements directed at disarmament and environmental protection have been reached during the past decade alone: the treaty of 1971 forbidding the disposition of nuclear weapons and other weapons of mass destruction on the ocean bottom or in the oceans themselves, the Soviet-American agreements of 1972 to limit strategic arms, the convention forbidding the development, production, and stockpiling of bacteriological (biological) and poisonous weapons and providing for their destruction, the agreements between the USSR and USA to limit the underground testing of nuclear weapons (1974), to regulate underground nuclear explosions for peaceful purposes (1976), to limit strategic offensive armaments (1979), and so forth, and the convention forbidding the military or other hostile use of agents affecting the environment.

The future course of international relations depends on the extent to which governments conscientiously fulfill the obligations they have accepted. It is not

fortuitous that the principle of conscientious fulfillment of obligations under international law found legal reinforcement in the final communique of a general European conference. In this connection, the institution of internation monitoring is becoming increasingly common in international law; it is employed in the relations between governments as one guarantee of the fulfillment of the obligations they have assumed. Soviet scholars specializing in international relations have made a significant contribution to work on the legal aspects of international monitoring that have arisen in different areas of intergovernmental relations.

Foreign experts in international law have devoted a great deal of attention to this topic.

As for legal problems pertaining ot the use of space technology for international monitoring, virtually no light has been shed on this subject.

The Soviet and foreign literature do not contain specialized monographs devoted to multifaceted research on formalized international monitoring. At the same time, international experience has shown that a multiplicity of legal problems of scientific and practical interest that require further theoretical investigation arise in the activity of monitoring organizations.

The establishment of international monitoring systems is a complex and difficult problem, in view of the existence of two opposing social-economic orders differing in the attitudes of their governments toward the use of international monitoring.

The Soviet Union and other socialist nations have taken a constructive position with regard to the use of international monitoring, a stand manifested in an unbroken identity between the obligations undertaken by their governments with respect to agreements in different areas of international cooperation and the need to ensure verification of their satisfaction.

It is typical of capitalistic governments to make a fetish of monitoring activity, detaching it from the subject matter and scope of treaty agreements, which essentially can lead to an undermining of the authority of international monitoring. The initiatives of bourgeois governments in regard to the use of international monitoring, e.g., in the field of disarmament reduce not to implementation of actual disarmament measures but to monitoring of weapons, which would promote an arms race and the gathering of intelligence under the pretext of international monitoring.

Soviet diplomats and experts in international law are taking vigorous measures intended to ensure that international monitoring will promote implementation of the measures reached and strengthening of the trust between governments, so as to be a true instrument of peace.

Contents Page

2478
CSO: 1866/29

- END -